Holography for heavy ions collisions

Irina Aref'eva
Steklov Mathematical Institute, RAS

10th MATHEMATICAL PHYSICS MEETING:
School and Conference on Modern Mathematical Physics

9 - 14 September 2019, Belgrade, Serbia

Outlook

Outlook

- **Holography for QCD (AdS/QCD)**
- **Holography for HIC (Heavy-Ions Collisions)**

Outlook

- Holography for QCD (AdS/QCD)
- Holography for HIC (Heavy-Ions Collisions)
- Results from holography for HIC:

Outlook

- **Holography for QCD (AdS/QCD)**

- **Holography for HIC (Heavy-Ions Collisions)**

- **Results from holography for HIC:**

  Fits experimental data

Outlook

- Holography for QCD (AdS/QCD)
- Holography for HIC (Heavy-Ions Collisions)
- Results from holography for HIC:

  Fits experimental data

  Predicts new results

Outlook

- Holography for QCD (AdS/QCD)
- Holography for HIC (Heavy-Ions Collisions)
- Results from holography for HIC:

    Fits experimental data

    Predicts new results

- What is special for NICA

Outlook

- Holography for QCD (AdS/QCD)
- Holography for HIC (Heavy-Ions Collisions)
- Results from holography for HIC:

  Fits experimental data

  Predicts new results
- What is special for NICA

Outlook

- Holography for QCD (AdS/QCD)
- Holography for HIC (Heavy-Ions Collisions)
- Results from holography for HIC:

  Fits experimental data

  Predicts new results

- What is special for NICA

I.A, “Holographic approach to quark–gluon plasma in heavy ion collisions”,
Phys. Usp., 57:6 (2014), 527–555

I.A,``Holography for Heavy Ions Collisions at LHC and NICA”, 1612.08928

Few remarks on holography (AdS/CFT)

Few remarks on holography (AdS/CFT)

Holography is nowadays one of the most effective tools to study quantum non-equilibrium physics of strongly interacting many body systems.

Few remarks on holography (AdS/CFT)

Holography is nowadays one of the most effective tools to study quantum non-equilibrium physics of strongly interacting many body systems.

These systems include ultrarelativistic heavy-ion collisions, cold atom systems, quantum simulators, "ultrafast" techniques in condensed matter physics, etc.

Few remarks on holography (AdS/CFT)

Holography is nowadays one of the most effective tools to study quantum non-equilibrium physics of strongly interacting many body systems.

These systems include ultrarelativistic heavy-ion collisions, cold atom systems, quantum simulators, "ultrafast" techniques in condensed matter physics, etc.

Holography translates the physics of quantum many body systems into a dual classical gravitational problem in a space-time with an extra dimension.

Few remarks on holography (AdS/QCD)

Few remarks on holography (AdS/QCD)

Three important achievements in AdS/QCD

Few remarks on holography (AdS/QCD)

Three important achievements in AdS/QCD

I) **Transport Coefficients in High Temperature Gauge Theories**

Few remarks on holography (AdS/QCD)

Three important achievements in AdS/QCD

I) Transport Coefficients in High Temperature Gauge Theories

Perturbation theory doesn't reproduce experimental value

Arnold, Moore, and Yaffe (2000)

$$\frac{\eta}{s} \sim \frac{1}{g_{\rm YM}^4 \log g_{\rm YM}^{-1}}$$

AdS/CFT

Policastro, Son, Starinets, PRL'01

$$\frac{\eta}{s} = \frac{1}{4\pi}$$

Few remarks on holography (AdS/QCD)

Three important achievements in AdS/QCD

I) Transport Coefficients in High Temperature Gauge Theories

Perturbation theory doesn't reproduce experimental value

Arnold, Moore, and Yaffe (2000)

$$\frac{\eta}{s} \sim \frac{1}{g_{\rm YM}^4 \log g_{\rm YM}^{-1}}$$

AdS/CFT

Policastro, Son, Starinets, PRL'01

$$\frac{\eta}{s} = \frac{1}{4\pi}$$

Karch, et al, '06; White '07; Pirner et al; Gubser et al, Kiritsis et al, Y.Yang et al

Few remarks on holography (AdS/QCD)

Three important achievements in AdS/QCD

I) Transport Coefficients in High Temperature Gauge Theories

Perturbation theory doesn't reproduce experimental value

Arnold, Moore, and Yaffe (2000)

$$\frac{\eta}{s} \sim \frac{1}{g_{\mathrm{YM}}^4 \log g_{\mathrm{YM}}^{-1}}$$

AdS/CFT

Policastro, Son, Starinets, PRL'01

$$\frac{\eta}{s} = \frac{1}{4\pi}$$

II) Cornell Potential **reproduces lattice data for zero chemical potential**

Karch, et al, '06; White '07; Pirner et al; Gubser et al, Kiritsis et al, Y.Yang et al

Few remarks on holography (AdS/QCD)

Three important achievements in AdS/QCD

I) Transport Coefficients in High Temperature Gauge Theories

Perturbation theory doesn't reproduce experimental value

Arnold, Moore, and Yaffe (2000)

$$\frac{\eta}{s} \sim \frac{1}{g_{\rm YM}^4 \log g_{\rm YM}^{-1}}$$

AdS/CFT

Policastro, Son, Starinets, PRL'01

$$\frac{\eta}{s} = \frac{1}{4\pi}$$

II) Cornell Potential **reproduces lattice data for zero chemical potential**

Karch, et al, '06; White '07; Pirner et al; Gubser et al, Kiritsis et al, Y.Yang et al

III) Multiplicity **Landau theory predicts** $\mathcal{M}_L \sim s^{0.25}$

IA, Golubtsova, '15 $\mathcal{M}_{HQCD} \sim \mathcal{M}_{LHC} \sim s^{0.155}$

Outlook

Outlook

- Holographic anizotropic phenomenological model
  - Motivations for the model
  - Physical properties of the model

Outlook

- **Holographic anizotropic phenomenological model**
    - **Motivations for the model**
    - **Physical properties of the model**
    - **What is special for non-zero chemical potential**
    - **What is special for anizotropic case**

Outlook

- Holographic anizotropic phenomenological model
  - Motivations for the model
  - Physical properties of the model
  - What is special for non-zero chemical potential
  - What is special for anizotropic case

I.A., K.Rannu, JHEP 1805 (2018) 206

Outlook

- **Holographic anizotropic phenomenological model**
  - **Motivations for the model**
  - **Physical properties of the model**
  - **What is special for non-zero chemical potential**
  - **What is special for anizotropic case**

I.A., K.Rannu, JHEP 1805 (2018) 206

- **Holographic in strong magnetic field (anizotropic model)**

Our Goal

Our Goal

Our Goal

- **Holography – new type of phenomenology.**

Our Goal

- **Holography – new type of phenomenology.**

Our Goal

- **Holography – new type of phenomenology.**
- **Goal:**

Our Goal

- **Holography – new type of phenomenology.**
- **Goal:**

Our Goal

- **Holography – new type of phenomenology.**
- **Goal:**

  Fit experimental data via holography:

Our Goal

- **Holography – new type of phenomenology.**
- **Goal:**

  Fit experimental data via holography:

Our Goal

- **Holography – new type of phenomenology.**
- **Goal:**

  Fit experimental data via holography:

Our Goal

- Holography – new type of phenomenology.
- Goal:

  Fit experimental data via holography:

  Transport coefficients, eta/s, Thermalization time,

Our Goal

- **Holography – new type of phenomenology.**
- **Goal:**

Fit experimental data via holography:

Transport coefficients, eta/s, Thermalization time,
Multiplicity, Direct-Photon Spectra,

Our Goal

- Holography – new type of phenomenology.
- Goal:

  Fit experimental data via holography:

  Transport coefficients, eta/s, Thermalization time, Multiplicity, Direct-Photon Spectra,

Our Goal

- **Holography – new type of phenomenology.**
- **Goal:**

  Fit experimental data via holography:

Transport coefficients, eta/s, Thermalization time,
Multiplicity, Direct-Photon Spectra,

Our Goal

- Holography – new type of phenomenology.
- Goal:

Fit experimental data via holography:

Transport coefficients, eta/s, Thermalization time,
Multiplicity, Direct-Photon Spectra,

Predict new data (the form of QCD Phase Diagram)

Our Goal

- Holography – new type of phenomenology.
- Goal:

Fit experimental data via holography:

Transport coefficients, eta/s, Thermalization time,
Multiplicity, Direct-Photon Spectra,

Predict new data (the form of QCD Phase Diagram)

Our Goal

- Holography – new type of phenomenology.
- Goal:

  Fit experimental data via holography:

  Transport coefficients, eta/s, Thermalization time, Multiplicity, Direct-Photon Spectra,

  Predict new data (the form of QCD Phase Diagram)

- What is special for NICA

Starting point - 5-dim background

Starting point - 5-dim background

1) A solution to classical Einstein eqs (with matter) that has the form of deformed AdS

Starting point - 5-dim background

1) A solution to classical Einstein eqs (with matter) that has the form of deformed AdS

2) Holographic renormgroup flow has to reproduce RG in QCD

Starting point - 5-dim background

1) A solution to classical Einstein eqs (with matter) that has the form of deformed AdS

2) Holographic renormgroup flow has to reproduce RG in QCD

3) The Cornell potential at zero chemical potential has to be reproduced lattice data

Starting point - 5-dim background

1) A solution to classical Einstein eqs (with matter) that has the form of deformed AdS

2) Holographic renormgroup flow has to reproduce RG in QCD

3) The Cornell potential at zero chemical potential has to be reproduced lattice data

4) The action has to be found by «trial and error method»

Starting point - 5-dim background

1) A solution to classical Einstein eqs (with matter) that has the form of deformed AdS

2) Holographic renormgroup flow has to reproduce RG in QCD

3) The Cornell potential at zero chemical potential has to be reproduced lattice data

4) The action has to be found by «trial and error method»

5) What is a «best> 5-dim background?

5-dim Anisotropic Background

5-dim Anisotropic Background

Einstein-dilaton-two-Maxwell

I.A., K. Rannu, JHEP' 18

$$S = \int \frac{d^5x}{16\pi G_5} \sqrt{-\det(g_{\mu\nu})} \left[R - \frac{f_1(\phi)}{4} F_{(1)}^2 - \frac{f_2(\phi)}{4} F_{(2)}^2 - \frac{1}{2} \partial_\mu \phi \partial^\mu \phi - V(\phi) \right]$$

5-dim Anisotropic Background

Einstein-dilaton-two-Maxwell

I.A., K. Rannu, JHEP' 18

$$S = \int \frac{d^5x}{16\pi G_5} \sqrt{-\det(g_{\mu\nu})} \left[R - \frac{f_1(\phi)}{4} F_{(1)}^2 - \frac{f_2(\phi)}{4} F_{(2)}^2 - \frac{1}{2} \partial_\mu \phi \partial^\mu \phi - V(\phi) \right]$$

$$ds^2 = \frac{Lb(z)}{z^2} \left[-g(z)dt^2 + dx^2 + R(z)(dy_1^2 + dy_2^2) + \frac{1}{g(z)} dz^2 \right]$$

$$\phi = \phi(z), \qquad A_\mu^{(1)} = A_t(z)\delta_\mu^0, \qquad F_{\mu\nu}^{(2)} = q \; dy^1 \wedge dy^2$$

5-dim Anisotropic Background

Einstein-dilaton-two-Maxwell

I.A., K. Rannu, JHEP' 18

$$S=\int\frac{d^5x}{16\pi G_5}\sqrt{-\det(g_{\mu\nu})}\left[R-\frac{f_1(\phi)}{4}F_{(1)}^2-\frac{f_2(\phi)}{4}F_{(2)}^2-\frac{1}{2}\partial_\mu\phi\partial^\mu\phi-V(\phi)\right]$$

$$ds^2=\frac{Lb(z)}{z^2}\left[-g(z)dt^2+dx^2+R(z)(dy_1^2+dy_2^2)+\frac{1}{g(z)}dz^2\right]$$

$$\phi=\phi(z),\qquad A_\mu^{(1)}=A_t(z)\delta_\mu^0,\qquad F_{\mu\nu}^{(2)}=q\;dy^1\wedge dy^2$$

Schematic picture of central HIC

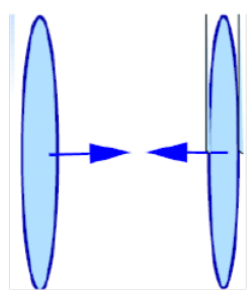

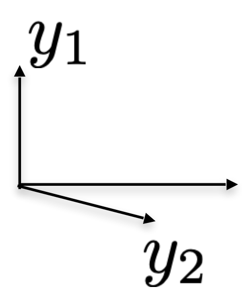

$\vec{y}=(y_1,y_2)$

x − beamer line

Anisotropic thermalization

QGP is created after very short time after the collision $\tau_{therm} \sim 0.1 fm/c$ and it is anisotropic for a short time $0 < \tau_{therm} < \tau < \tau_{iso}$

The time of locally isotropization is about $\tau_{iso} \sim 2 fm/c$

M. Strickland, 1312.2285 [hep-ph]

Heavy Ions Collisions in Holographic Approach: shock waves collisions in 5-dimension

Heavy Ions Collisions in Holographic Approach: shock waves collisions in 5-dimension

$$S=\int d^5x\sqrt{|g|}\left(R[g]+\Lambda-\frac{1}{2}\partial_M\phi\partial^M\phi-\frac{1}{4}e^{\lambda\phi}F^2_{(2)}\right)$$

$$ds^2=\frac{1}{z^2}\left(-dt^2+dx^2+z^{2-2/\nu}(dy_1^2+dy_2^2)+dz^2\right)$$

IA, Golubtsova, JHEP'15

Shock domain walls/planar shocks collision:
ENTROPY

$$\mathcal{M}=\frac{\nu}{2G_5}(8\pi G_5)^{1/(1+\nu)}s^{\frac{1}{2+\nu}}$$

Heavy Ions Collisions in Holographic Approach: shock waves collisions in 5-dimension

$$S = \int d^5x\sqrt{|g|}\left(R[g] + \Lambda - \frac{1}{2}\partial_M\phi\partial^M\phi - \frac{1}{4}e^{\lambda\phi}F^2_{(2)}\right)$$

$$ds^2 = \frac{1}{z^2}\left(-dt^2 + dx^2 + z^{2-2/\nu}(dy_1^2 + dy_2^2) + dz^2\right)$$

IA, Golubtsova, JHEP'15

Shock domain walls/planar shocks collision:
ENTROPY

$$\mathcal{M} = \frac{\nu}{2G_5}(8\pi G_5)^{1/(1+\nu)}s^{\frac{1}{2+\nu}}$$

To get $\mathcal{M}_{LHC} \sim s^{0.155(4)}$

Heavy Ions Collisions in Holographic Approach: shock waves collisions in 5-dimension

$$S=\int d^5x\sqrt{|g|}\left(R[g]+\Lambda-\frac{1}{2}\partial_M\phi\partial^M\phi-\frac{1}{4}e^{\lambda\phi}F^2_{(2)}\right)$$

$$ds^2=\frac{1}{z^2}\left(-dt^2+dx^2+z^{2-2/\nu}(dy_1^2+dy_2^2)+dz^2\right)$$

IA, Golubtsova, JHEP'15

Shock domain walls/planar shocks collision:

ENTROPY

$$\mathcal{M}=\frac{\nu}{2G_5}(8\pi G_5)^{1/(1+\nu)}s^{\frac{1}{2+\nu}}$$

To get $\mathcal{M}_{LHC}\sim s^{0.155(4)}$ $\qquad \nu=4.45$

Longitudinal-transversal anisotropy.

Motivation: Multiplicity

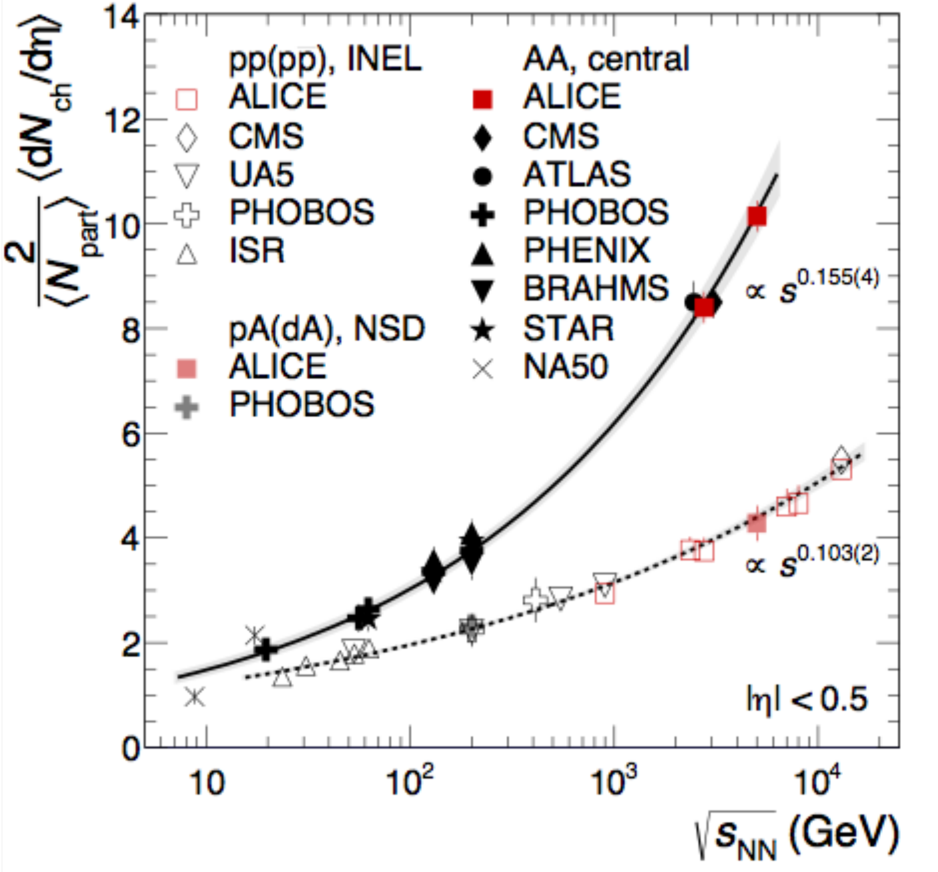

Plot from **PRL'16** (ALICE).

$$\mathcal{M}_{LHC} \sim s^{0.155}$$

Longitudinal-transversal anisotropy.

Motivation: Multiplicity

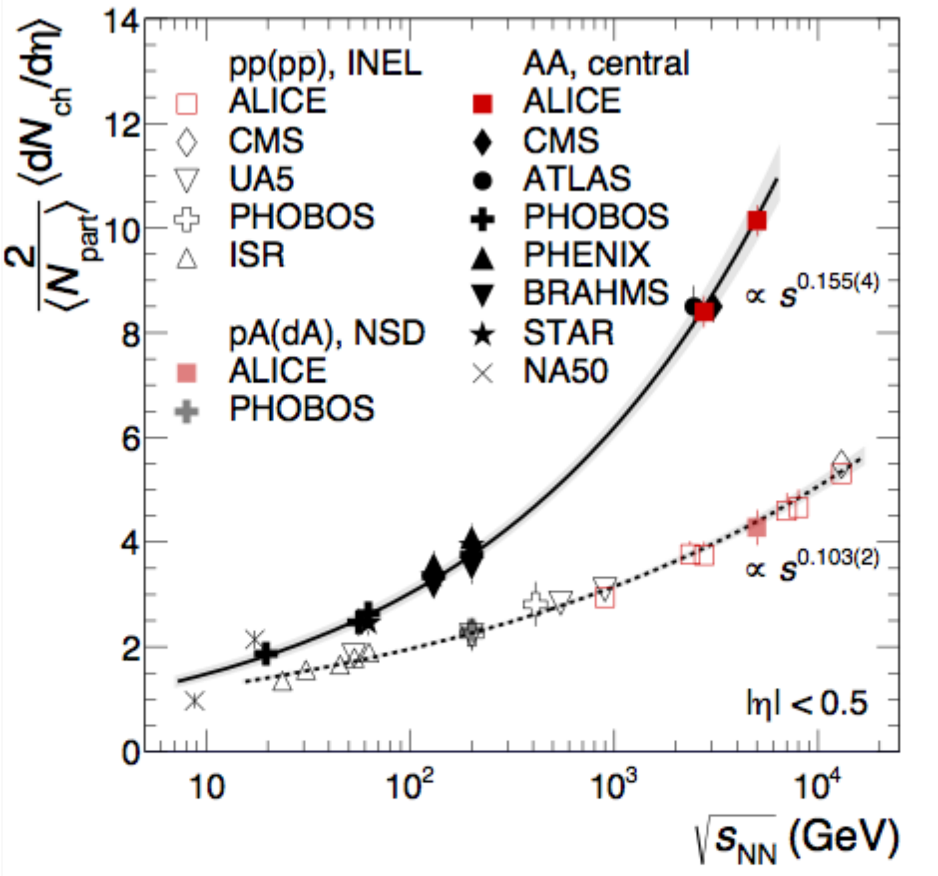

Plot from **PRL'16** (ALICE).

$$\mathcal{M}_{LP} \sim s^{0.25}$$

$$\mathcal{M}_{LHC} \sim s^{0.155}$$

Longitudinal-transversal anisotropy.

Motivation: Multiplicity

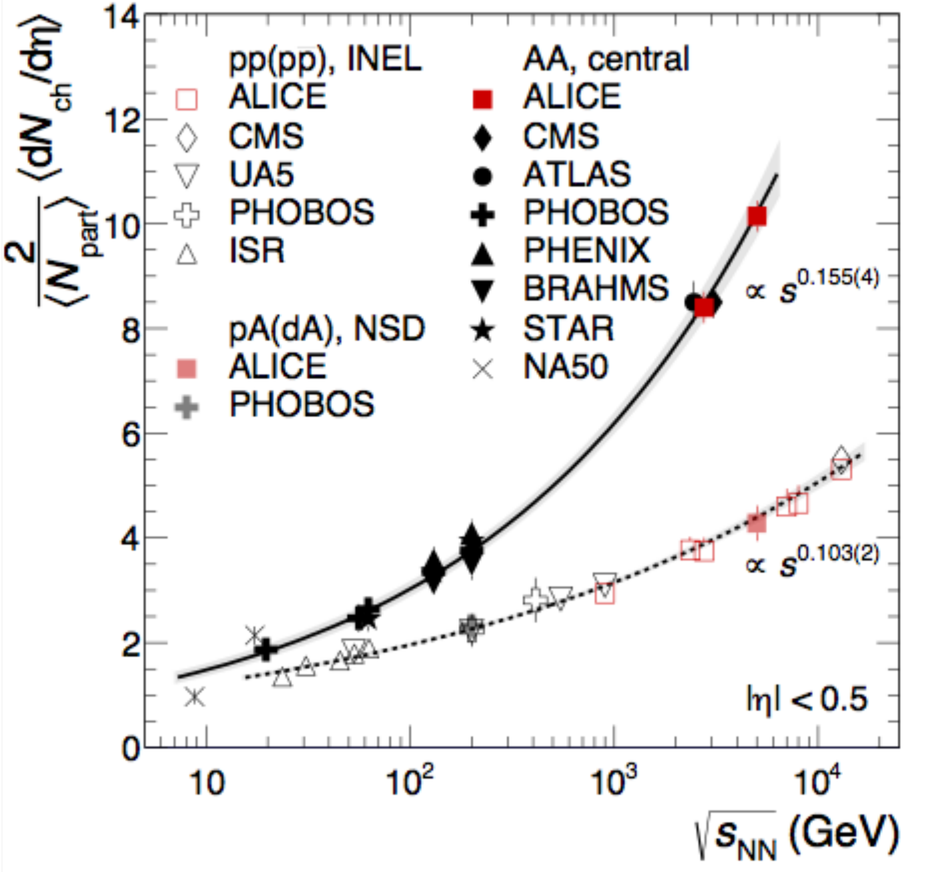

Plot from **PRL'16** (ALICE).

$$\mathcal{M}_{LP} \sim s^{0.25}$$

$$\mathcal{M}_{GPY} \sim s^{0.33}$$

$$\mathcal{M}_{LHC} \sim s^{0.155}$$

Longitudinal-transversal anisotropy.

Motivation: Multiplicity

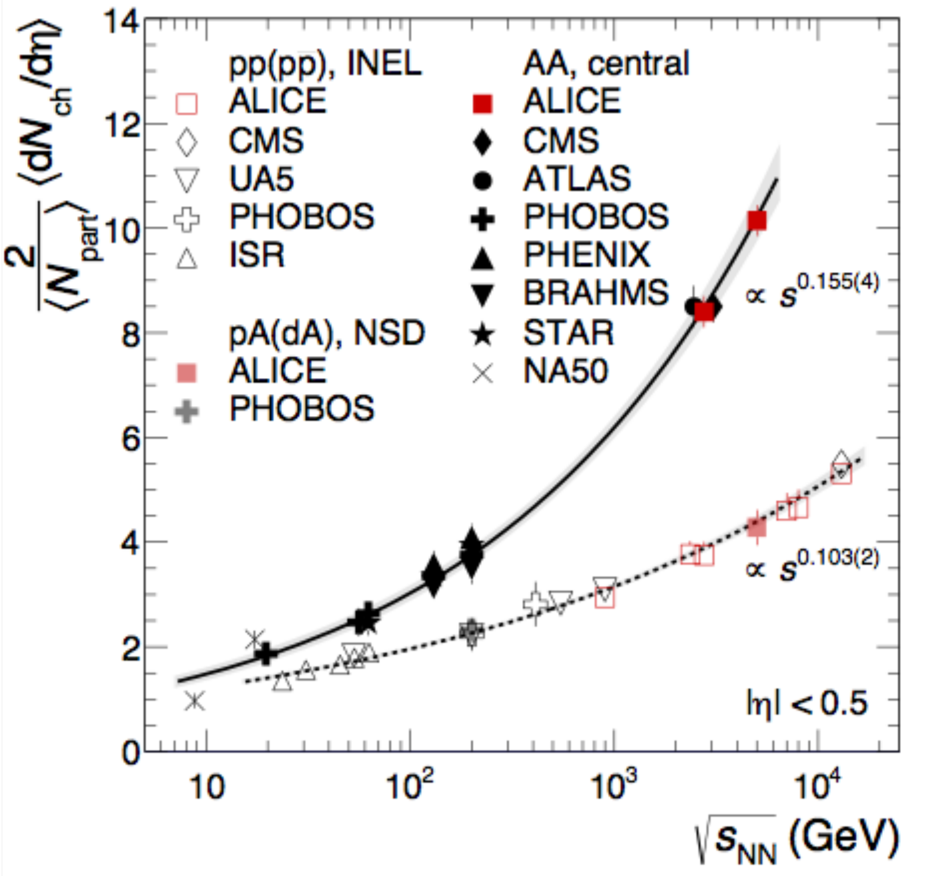

Plot from **PRL'16** (ALICE).

$$\mathcal{M}_{LP} \sim s^{0.25}$$

$$\mathcal{M}_{GPY} \sim s^{0.33}$$

$$\mathcal{M}_{AG} \sim \mathcal{M}_{LHC} \sim s^{0.155}$$

Longitudinal-transversal anisotropy.

Motivation: Multiplicity

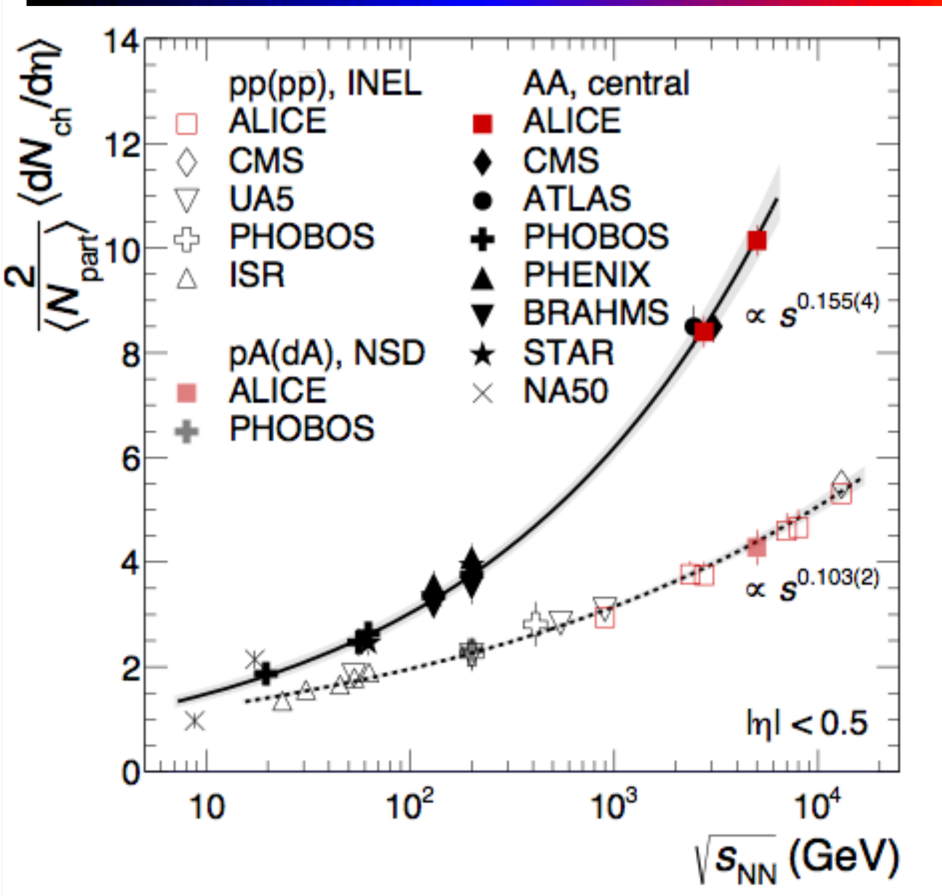

Plot from **PRL'16** (ALICE).

$$\mathcal{M}_{LP} \sim s^{0.25}$$

$$\mathcal{M}_{GPY} \sim s^{0.33}$$

IA, Golubtsova
JHEP'15

$$\mathcal{M}_{AG} \sim \mathcal{M}_{LHC} \sim s^{0.155}$$

Quark-Gluon Plasma (QGP): a new state of matter

QGP is a state of matter formed from deconfined quarks, antiquarks, and gluons at high temperature

QCD: asymptotic freedom, quark confinement

T increases, or density increases **nuclear matter** → **Deconfined phase**

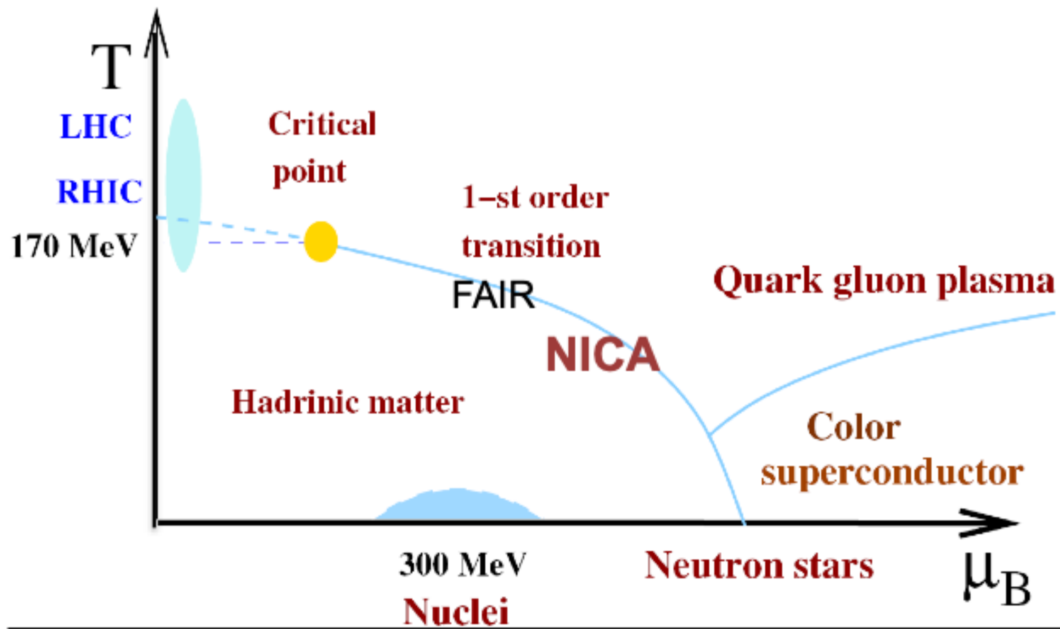

5-dim Anisotropic Background

Einstein-dilaton-two-Maxwell

$$S = \int \frac{d^5x}{16\pi G_5}\sqrt{-\det(g_{\mu\nu})}\left[R - \frac{f_1(\phi)}{4}F_{(1)}^2 - \frac{f_2(\phi)}{4}F_{(2)}^2 - \frac{1}{2}\partial_\mu\phi\partial^\mu\phi - V(\phi)\right]$$

5-dim Anisotropic Background

Einstein-dilaton-two-Maxwell

$$S=\int \frac{d^5x}{16\pi G_5}\sqrt{-\det(g_{\mu\nu})}\left[R-\frac{f_1(\phi)}{4}F_{(1)}^2-\frac{f_2(\phi)}{4}F_{(2)}^2-\frac{1}{2}\partial_\mu\phi\partial^\mu\phi-V(\phi)\right]$$

$$ds^2=\frac{Lb(z)}{z^2}\left[-g(z)dt^2+dx^2+R(z)(dy_1^2+dy_2^2)+\frac{1}{g(z)}dz^2\right]$$

$$\phi=\phi(z),\qquad A_\mu^{(1)}=A_t(z)\delta_\mu^0,\qquad F_{\mu\nu}^{(2)}=q\ dy^1\wedge dy^2$$

5-dim Anisotropic Background

Einstein-dilaton-two-Maxwell

$$S = \int \frac{d^5x}{16\pi G_5} \sqrt{-\det(g_{\mu\nu})} \left[R - \frac{f_1(\phi)}{4} F_{(1)}^2 - \frac{f_2(\phi)}{4} F_{(2)}^2 - \frac{1}{2} \partial_\mu \phi \partial^\mu \phi - V(\phi) \right]$$

$$ds^2 = \frac{Lb(z)}{z^2} \left[-g(z)dt^2 + dx^2 + R(z)(dy_1^2 + dy_2^2) + \frac{1}{g(z)} dz^2 \right]$$

$$\phi = \phi(z), \qquad A_\mu^{(1)} = A_t(z)\delta_\mu^0, \qquad F_{\mu\nu}^{(2)} = q \; dy^1 \wedge dy^2$$

We fix: $b(z), f_1(\phi), R(z)$

5-dim Anisotropic Background

Einstein-dilaton-two-Maxwell

$$S = \int \frac{d^5x}{16\pi G_5} \sqrt{-\det(g_{\mu\nu})} \left[R - \frac{f_1(\phi)}{4} F_{(1)}^2 - \frac{f_2(\phi)}{4} F_{(2)}^2 - \frac{1}{2} \partial_\mu \phi \partial^\mu \phi - V(\phi) \right]$$

$$ds^2 = \frac{Lb(z)}{z^2} \left[-g(z) dt^2 + dx^2 + R(z)(dy_1^2 + dy_2^2) + \frac{1}{g(z)} dz^2 \right]$$

$$\phi = \phi(z), \qquad A_\mu^{(1)} = A_t(z) \delta_\mu^0, \qquad F_{\mu\nu}^{(2)} = q\ dy^1 \wedge dy^2$$

We fix: $b(z), f_1(\phi), R(z)$

We find: $V(\phi), f_2(\phi), g(\phi)$

$A_t(z)$

5-dim Anisotropic Background

Einstein-dilaton-two-Maxwell

$$S = \int \frac{d^5x}{16\pi G_5}\sqrt{-\det(g_{\mu\nu})}\left[R - \frac{f_1(\phi)}{4}F_{(1)}^2 - \frac{f_2(\phi)}{4}F_{(2)}^2 - \frac{1}{2}\partial_\mu\phi\partial^\mu\phi - V(\phi)\right]$$

$$ds^2 = \frac{Lb(z)}{z^2}\left[-g(z)dt^2 + dx^2 + R(z)(dy_1^2 + dy_2^2) + \frac{1}{g(z)}dz^2\right]$$

$$\phi = \phi(z), \qquad A_\mu^{(1)} = A_t(z)\delta_\mu^0, \qquad F_{\mu\nu}^{(2)} = q\ dy^1 \wedge dy^2$$

We fix: $b(z), f_1(\phi), R(z)$

We find: $V(\phi), f_2(\phi), g(\phi)$
$A_t(z)$

"Reconstruction of potential" for zero chemical potential

White, 0701157; Pirner, Galow, 0903.2701;
He, Wu, Yang, Yuan, 1301.0385,
M.-W. Li, Y. Yang arXiv:1703.09184

Holographic RenormGroup Flow, T=0

$$\beta(\lambda) = \frac{d\lambda}{d\log E} = \lambda \frac{d\phi}{d\log \mathcal{B}}, \qquad \mathcal{B} = \frac{\sqrt{b(z)}}{z}.$$

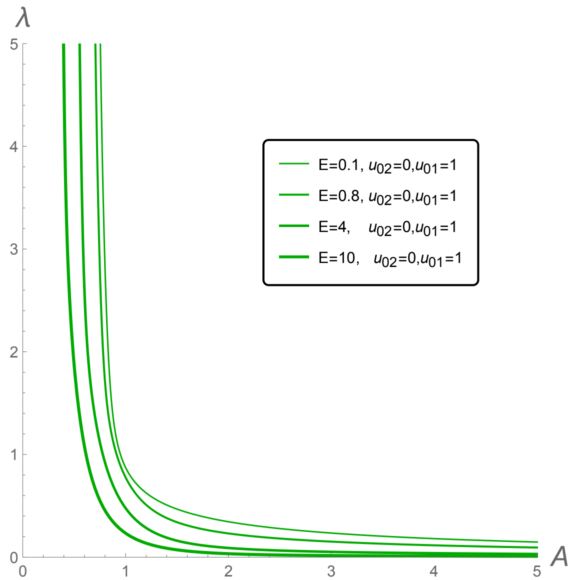

Comparing with exact integrable model

Comparing with exact integrable model

$$V_{AR}(\phi) = V_0 - C_1 e^{K_1 \phi} + C_2 e^{K_2 \phi}$$

$$V_0 = -0.6,\ K_1 = 0.8, \quad K_2(4.5) = 2.1$$
$$C_1 = 23,\ C_2 = 0.06$$

I.A., Rannu, 1802.05652

Comparing with exact integrable model

$$V_{AR}(\phi) = V_0 - C_1 e^{K_1 \phi} + C_2 e^{K_2 \phi}$$

$$V_0 = -0.6, \ K_1 = 0.8, \quad K_2(4.5) = 2.1$$
$$C_1 = 23, \ C_2 = 0.06$$

I.A., Rannu, 1802.05652

I.A.,Golubtsova, Policastro,arXiv: 1803.06764

$$V_{AGP}(\varphi) = C_1 e^{2k\varphi} + C_2 e^{\frac{32}{9k}\varphi}$$
$$\varphi = 0.47\phi \qquad k = 0.85$$

Comparing with exact integrable model

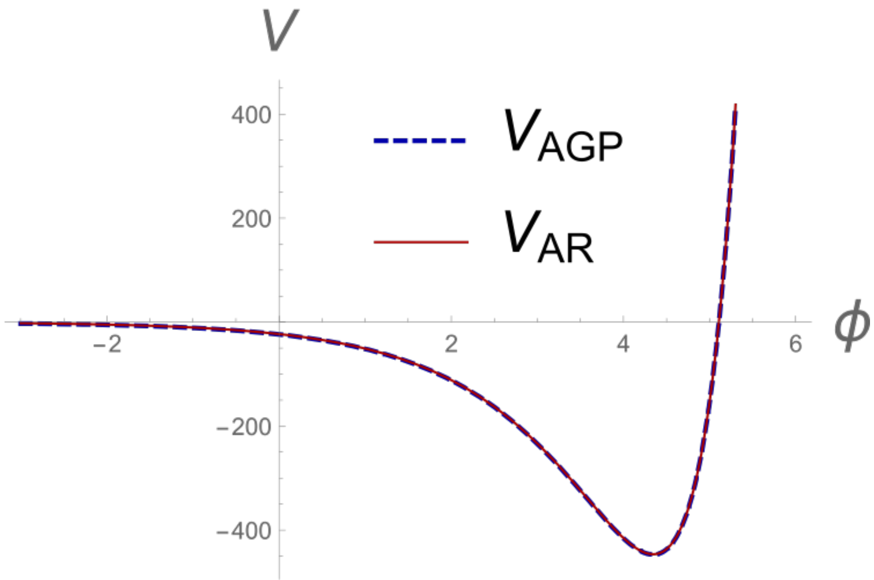

$$V_{AR}(\phi) = V_0 - C_1 e^{K_1 \phi} + C_2 e^{K_2 \phi}$$

$$V_0 = -0.6, \ K_1 = 0.8, \quad K_2(4.5) = 2.1$$
$$C_1 = 23, \ C_2 = 0.06$$

I.A., Rannu, 1802.05652

I.A.,Golubtsova, Policastro,arXiv: 1803.06764

$$V_{AGP}(\varphi) = C_1 e^{2k\varphi} + C_2 e^{\frac{32}{9k}\varphi}$$
$$\varphi = 0.47\phi \qquad k = 0.85$$

Smeared confinement/deconfinement phase transition (crossover transition) in holography for the anisotropic model

Temporal Wilson loops

Temporal Wilson loops

Energy between quarks located along x-direction

Temporal Wilson loops

Energy between quarks located along x-direction

$$W(T,X) = \langle \mathrm{Tr}_F\, e^{i \oint_{T\times X} dx_\mu A_\mu} \rangle \sim e^{-V(X)T},$$

Temporal Wilson loops

Energy between quarks located along x-direction

$$W(T,X) = \langle \mathrm{Tr}_F \, e^{i \oint_{T\times X} dx_\mu A_\mu} \rangle \sim e^{-V(X)T},$$

Holography for a probe

$$S_{xt} = \frac{1}{2\pi\alpha'} \int d\sigma^1 d\sigma^2 \sqrt{-\det(h_{\alpha\beta})}$$

The recipe by Maldacena (‘98), Rey et al (‘98), Sonnenschein et al (’98)

Temporal Wilson loops

Energy between quarks located along x-direction

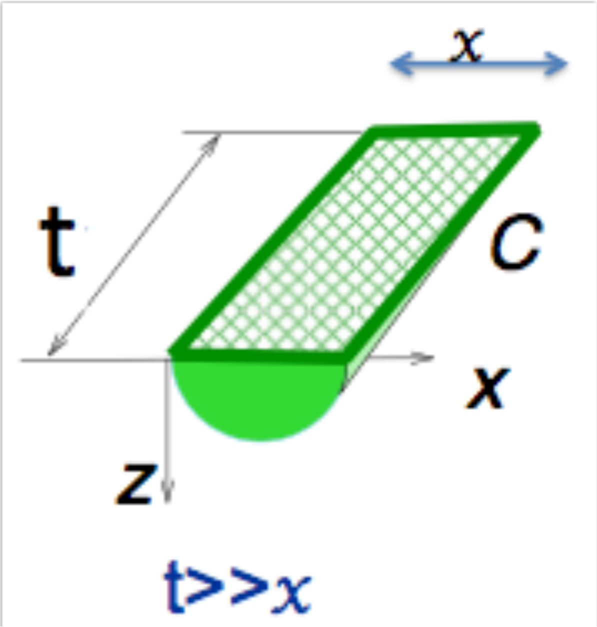

$$W(T,X) = \langle \mathrm{Tr}_F \, e^{i \oint_{T\times X} dx_\mu A_\mu} \rangle \sim e^{-V(X)T}$$

Holography for a probe

$$S_{xt} = \frac{1}{2\pi\alpha'} \int d\sigma^1 d\sigma^2 \sqrt{-\det(h_{\alpha\beta})}$$

The recipe by Maldacena ('98), Rey et al ('98), Sonnenschein et al ('98)

Temporal Wilson loops

Energy between quarks located along x-direction

$$W(T,X) = \langle \mathrm{Tr}_F\, e^{i \oint_{T\times X} dx_\mu A_\mu} \rangle \sim e^{-V(X)T}$$

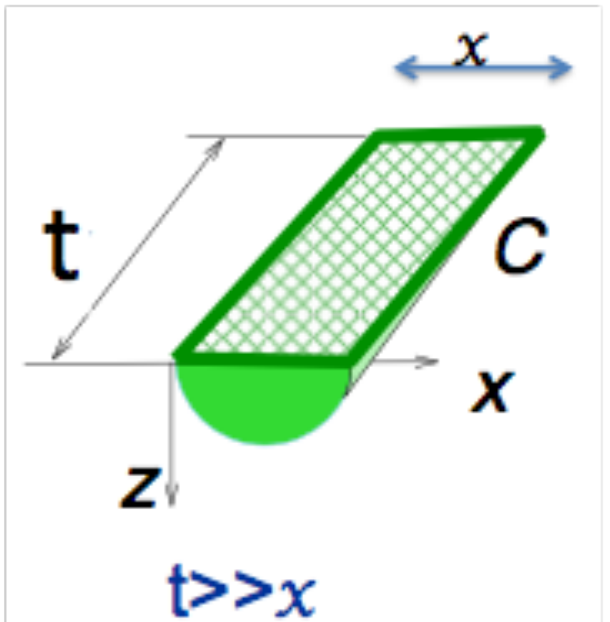

Holography for a probe

$$S_{xt} = \frac{1}{2\pi\alpha'} \int d\sigma^1 d\sigma^2 \sqrt{-\det(h_{\alpha\beta})}$$

The recipe by Maldacena (‘98), Rey et al (‘98), Sonnenschein et al (’98)

Contour approach in YM in 80’

Temporal Wilson loops

Energy between quarks located along x-direction

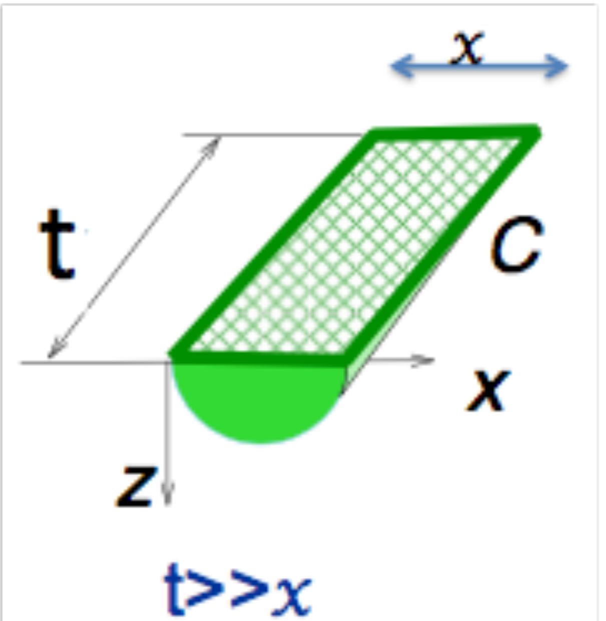

$$W(T,X) = \langle \mathrm{Tr}_F \, e^{i \oint_{T\times X} dx_\mu A_\mu} \rangle \sim e^{-V(X)T}$$

Holography for a probe

$$S_{xt} = \frac{1}{2\pi\alpha'} \int d\sigma^1 d\sigma^2 \sqrt{-\det(h_{\alpha\beta})}$$

The recipe by Maldacena ('98), Rey et al ('98), Sonnenschein et al ('98)

2-dim Born-Infeld dynamical system

Contour approach in YM in 80'

Temporal Wilson loops

Energy between quarks located along x-direction

$$W(T,X) = \langle \mathrm{Tr}_F \, e^{i \oint_{T\times X} dx_\mu A_\mu} \rangle \sim e^{-V(X)T}$$

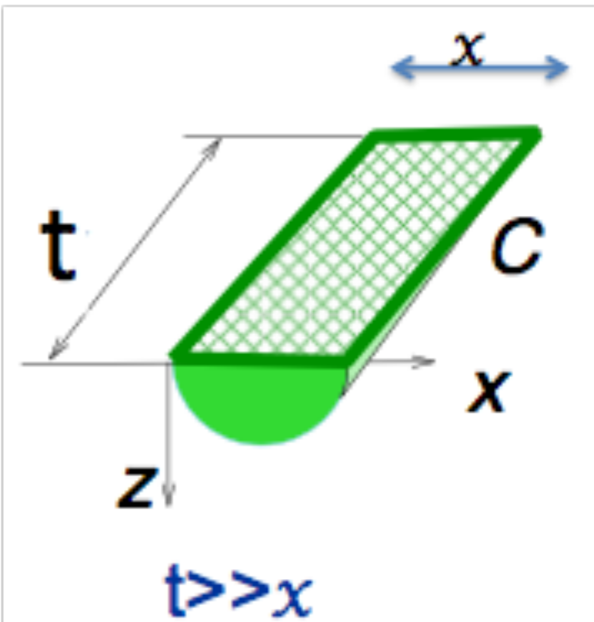

Contour approach in YM in 80'

Holography for a probe

$$S_{xt} = \frac{1}{2\pi\alpha'} \int d\sigma^1 d\sigma^2 \sqrt{-\det(h_{\alpha\beta})}$$

The recipe by Maldacena ('98), Rey et al ('98), Sonnenschein et al ('98)

2-dim Born-Infeld dynamical system

$$S_{xt} = \frac{\mathcal{T}}{2\pi\alpha'} \int \frac{b(z)}{z^2} \sqrt{g(z) + z'^2} \, dx.$$

Temporal Wilson loops

Energy between quarks located along x-direction

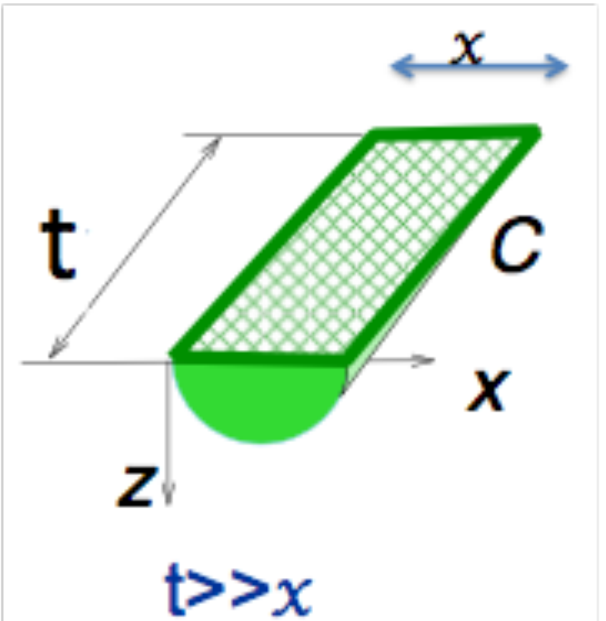

Contour approach in YM in 80'

$$W(T,X) = \langle \mathrm{Tr}_F\, e^{i\oint_{T\times X} dx_\mu A_\mu} \rangle \sim e^{-V(X)T},$$

Holography for a probe

$$S_{xt} = \frac{1}{2\pi\alpha'}\int d\sigma^1 d\sigma^2 \sqrt{-\det(h_{\alpha\beta})}$$

The recipe by Maldacena ('98), Rey et al ('98), Sonnenschein et al ('98)

2-dim Born-Infeld dynamical system

$$S_{xt} = \frac{\mathcal{T}}{2\pi\alpha'}\int \frac{b(z)}{z^2}\sqrt{g(z)+z'^2}\,dx.$$

$$S_{yt} = \frac{\mathcal{T}}{2\pi\alpha'}\int \frac{b(z)}{z^2}\sqrt{z^{2-2/\nu}g(z)+z'^2}\,dx.$$

Temporal Wilson loops

Energy between quarks located along x-direction

$$W(T,X) = \langle \mathrm{Tr}_F\, e^{i\oint_{T\times X} dx_\mu A_\mu} \rangle \sim e^{-V(X)T},$$

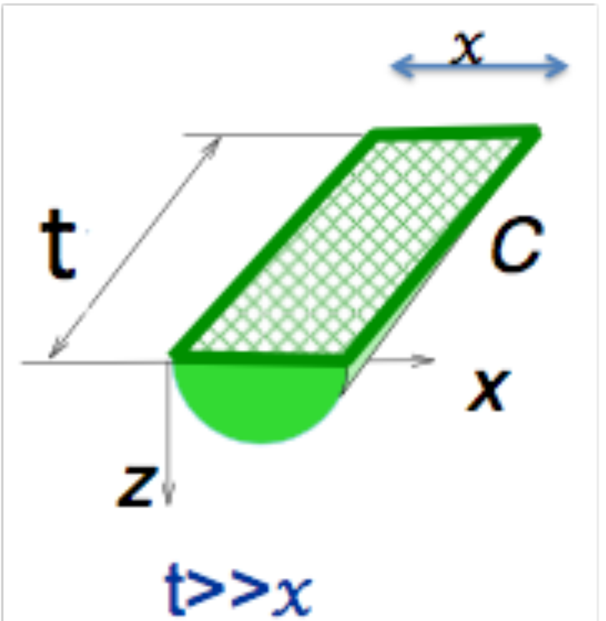

Holography for a probe

$$S_{xt} = \frac{1}{2\pi\alpha'} \int d\sigma^1 d\sigma^2 \sqrt{-\det(h_{\alpha\beta})}$$

The recipe by Maldacena ('98), Rey et al ('98), Sonnenschein et al ('98)

Contour approach in YM in 80'

2-dim Born-Infeld dynamical system

$$S_{xt} = \frac{\mathcal{T}}{2\pi\alpha'} \int \frac{b(z)}{z^2} \sqrt{g(z) + z'^2}\, dx.$$

$$S_{yt} = \frac{\mathcal{T}}{2\pi\alpha'} \int \frac{b(z)}{z^2} \sqrt{z^{2-2/\nu} g(z) + z'^2}\, dx.$$

Effective actions depend on orientation

Temporal Wilson loops

Energy between quarks located along x-direction

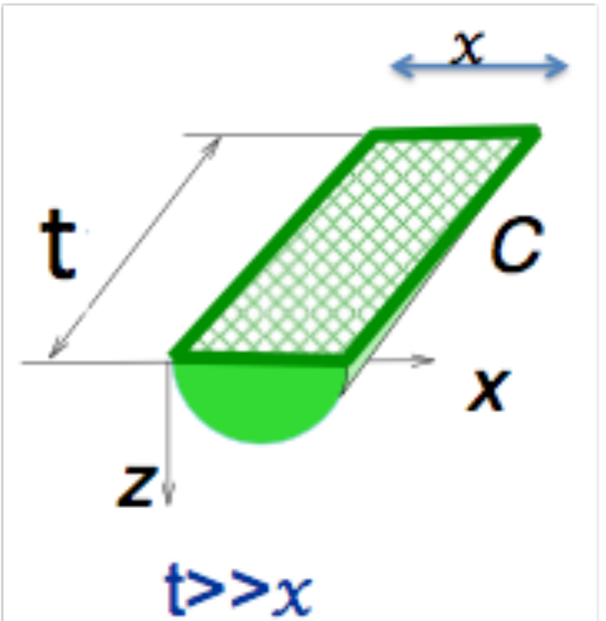

Contour approach in YM in 80'

$$W(T,X) = \langle \mathrm{Tr}_F\, e^{i\oint_{T\times X} dx_\mu A_\mu} \rangle \sim e^{-V(X)T},$$

Holography for a probe

$$S_{xt} = \frac{1}{2\pi\alpha'}\int d\sigma^1 d\sigma^2 \sqrt{-\det(h_{\alpha\beta})}$$

The recipe by Maldacena ('98), Rey et al ('98), Sonnenschein et al ('98)

2-dim Born-Infeld dynamical system

$$S_{xt} = \frac{\mathcal{T}}{2\pi\alpha'}\int \frac{b(z)}{z^2}\sqrt{g(z)+z'^2}\,dx.$$

$$S_{yt} = \frac{\mathcal{T}}{2\pi\alpha'}\int \frac{b(z)}{z^2}\sqrt{z^{2-2/\nu}g(z)+z'^2}\,dx.$$

Effective actions depend on orientation

$$\mathcal{V}_x = \frac{e^{P(z)+\sqrt{\frac{2}{3}}\phi(z)}}{z^2}\sqrt{g(z)},$$

$$\mathcal{V}_y = \frac{e^{P(z)+\sqrt{\frac{2}{3}}\phi(z)}}{z^{1/\nu+1}}\sqrt{g(z)}.$$

Dynamical domain wall

Dynamical domain wall

$$\mathcal{V}_x'(z_{\,DW\,x}) = 0$$

$$\mathcal{V}_y'(z_{\,DW\,y}) = 0$$

Dynamical domain wall

$$\mathcal{V}_x'(z_{DWx}) = 0$$

$$\mathcal{V}_y'(z_{DWy}) = 0$$

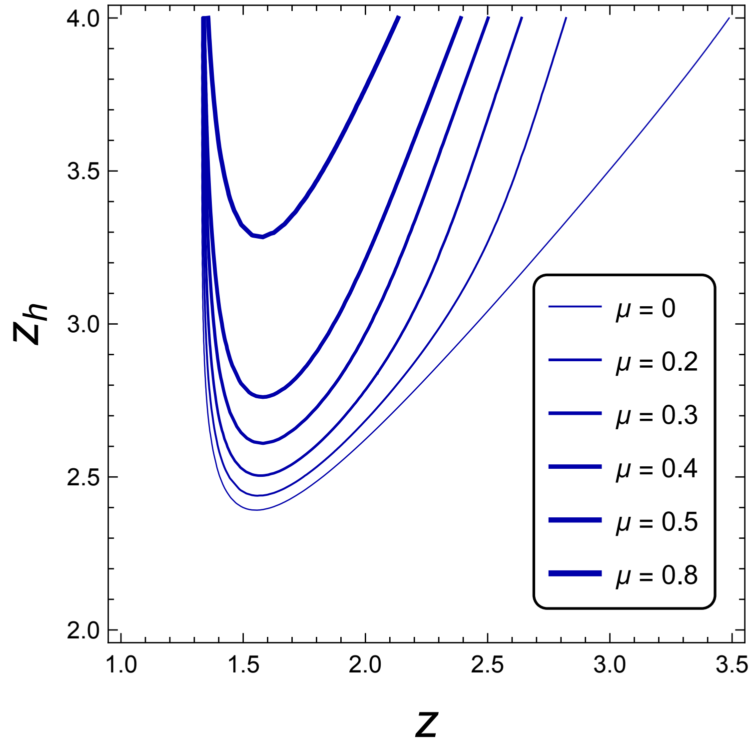

Dynamical domain wall

$$\mathcal{V}'_x(z_{DWx}) = 0$$
$$\mathcal{V}'_y(z_{DWy}) = 0$$

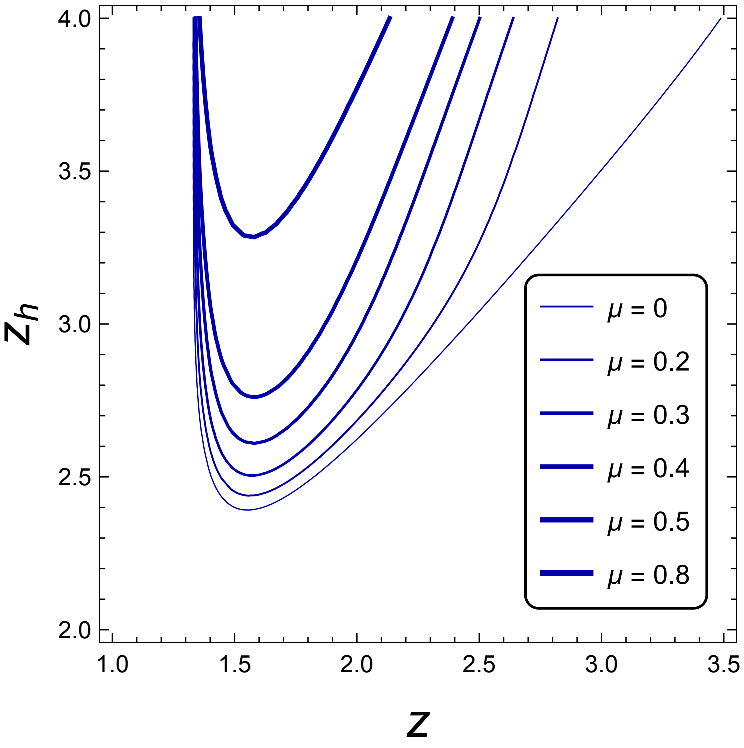

$$V_{Cornell}(x) \equiv V_{Q\bar{Q}}(x) = -\frac{\kappa}{x} + \sigma_{str}x + V_0$$

Holographic anisotropic QCD phase diagram

Holographic anisotropic QCD phase diagram

W_{xT}

Holographic anisotropic QCD phase diagram

W_{xT} W_{yT}

Holographic anisotropic QCD phase diagram

W_{xT} W_{yT}

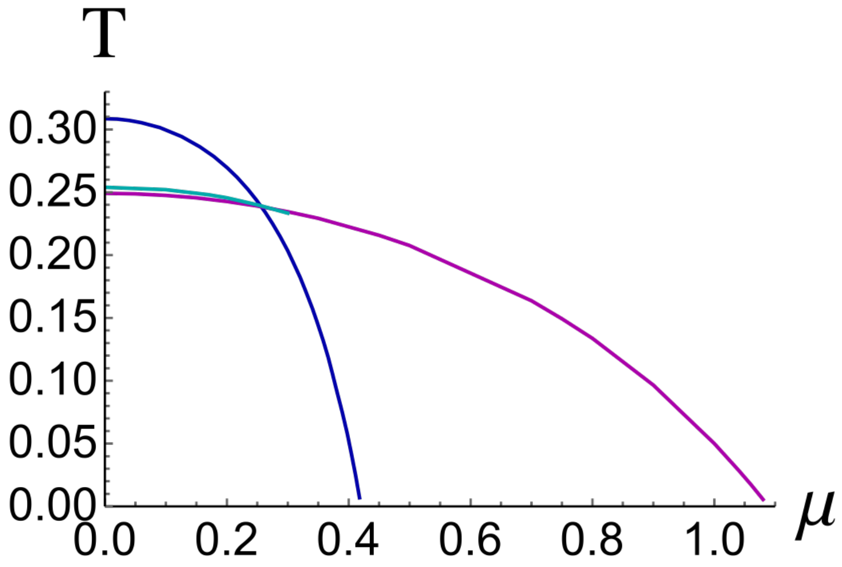

Holographic anisotropic QCD phase diagram

W_{xT} W_{yT}

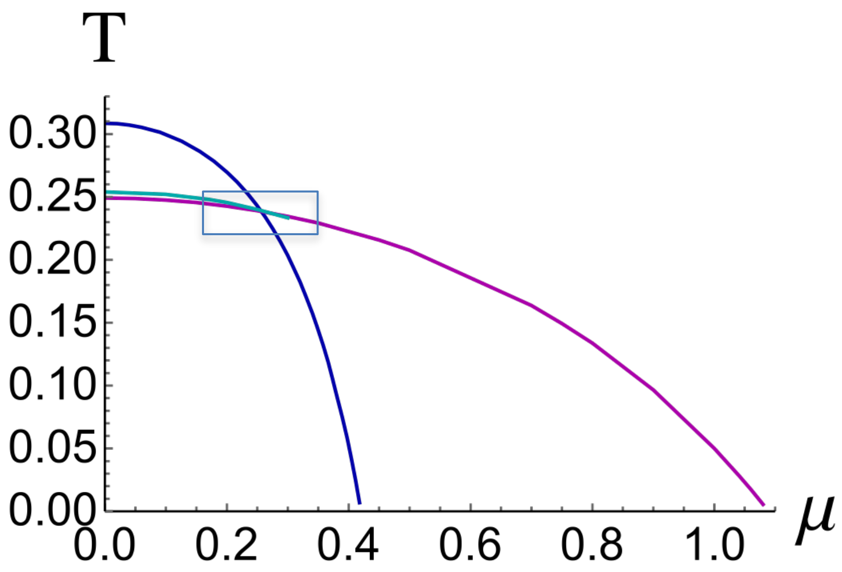

Holographic anisotropic QCD phase diagram

W_{xT} W_{yT}

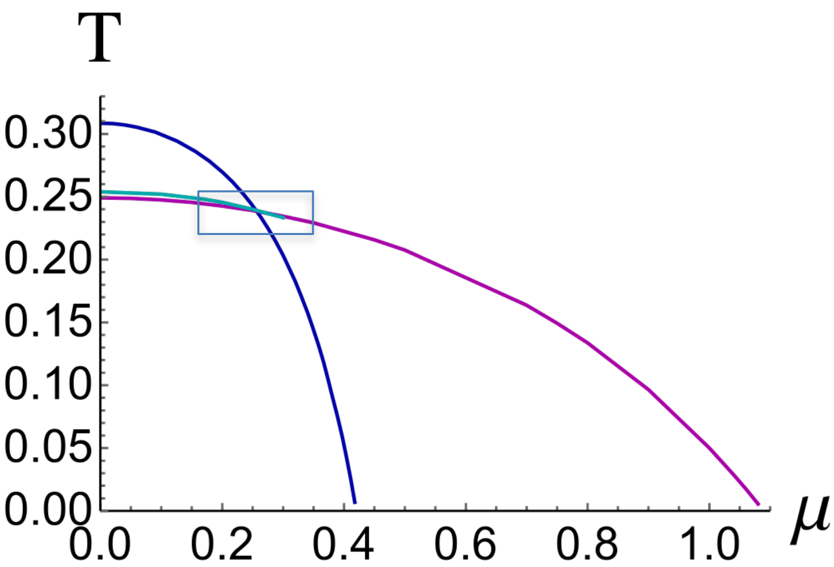

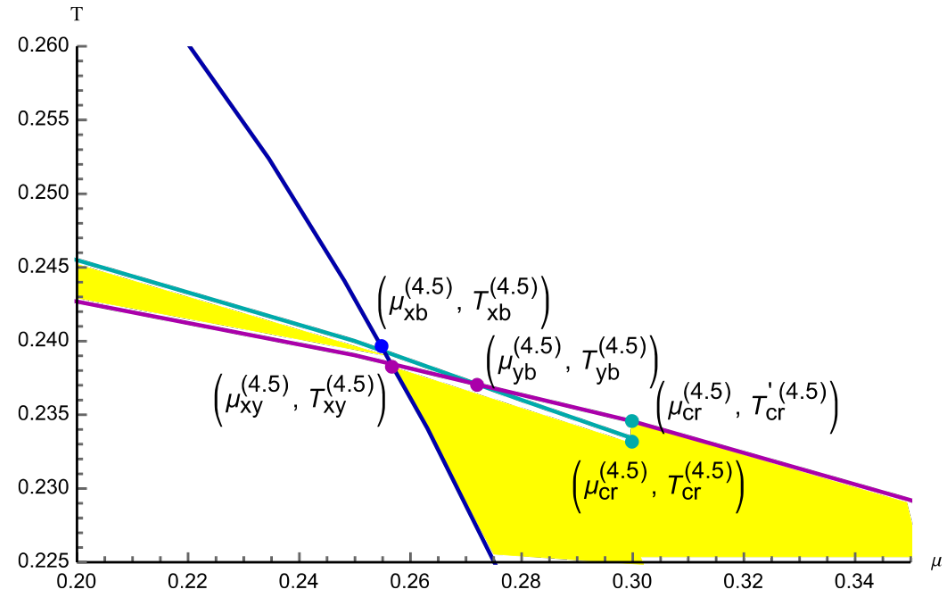

Holographic anisotropic QCD phase diagram

W_{xT} W_{yT}

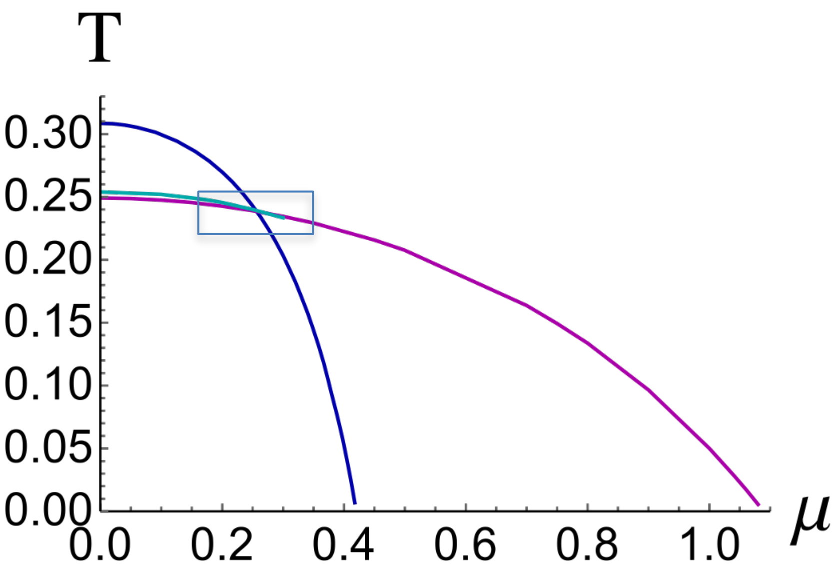

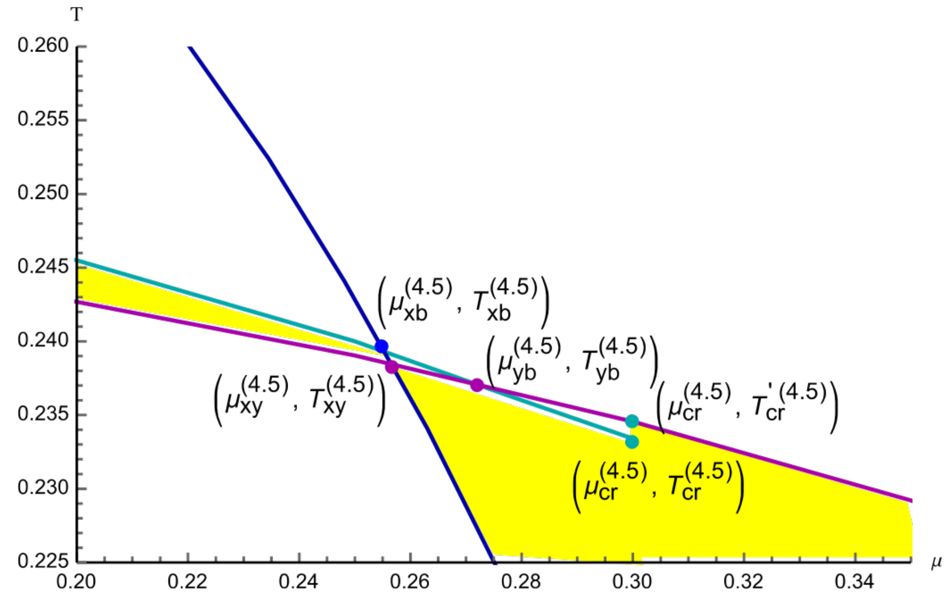

Smeared confinement/deconfinement phase transition

Holographic anisotropic QCD phase diagram

W_{xT} W_{yT}

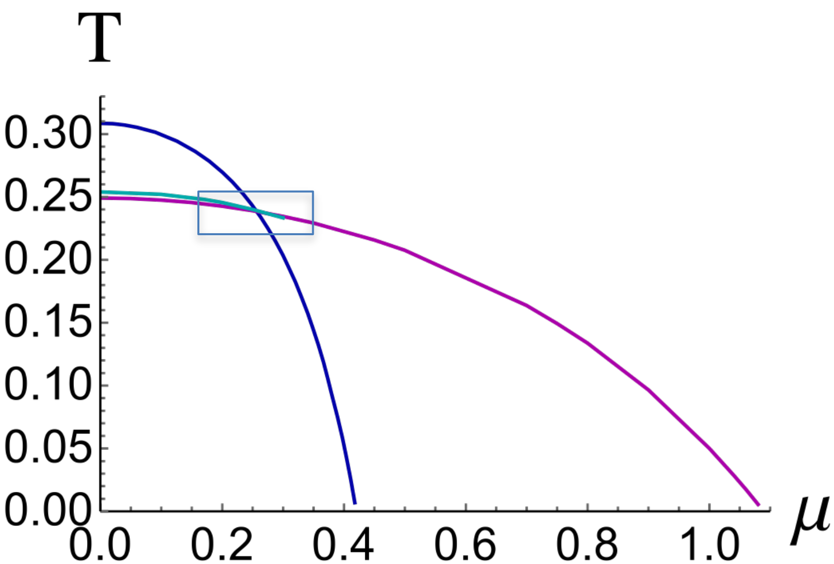

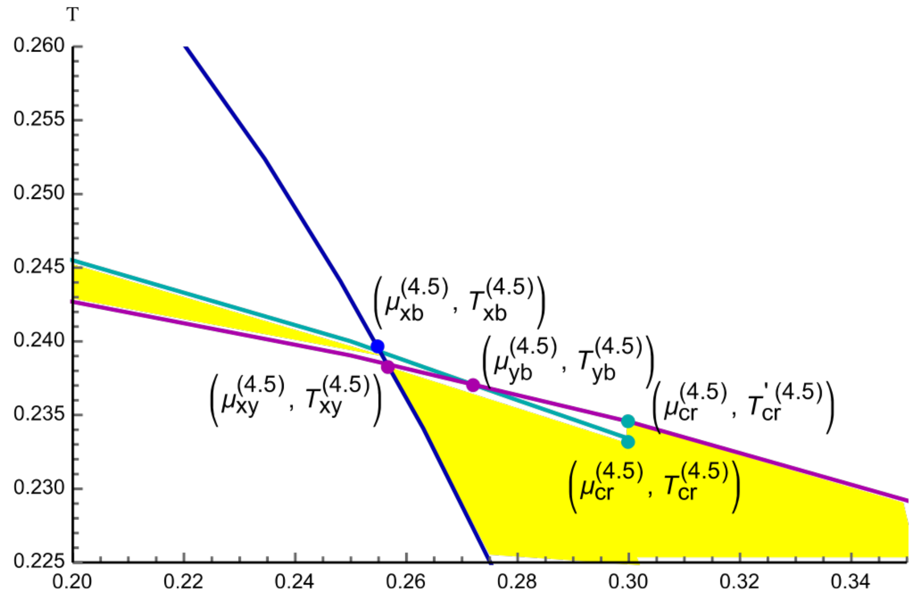

Smeared confinement/deconfinement phase transition

Arbitrary angle: IA, K.Rannu, P.Slepov,PLB'19

Holographic anisotropic QCD phase diagram

W_{xT} W_{yT}

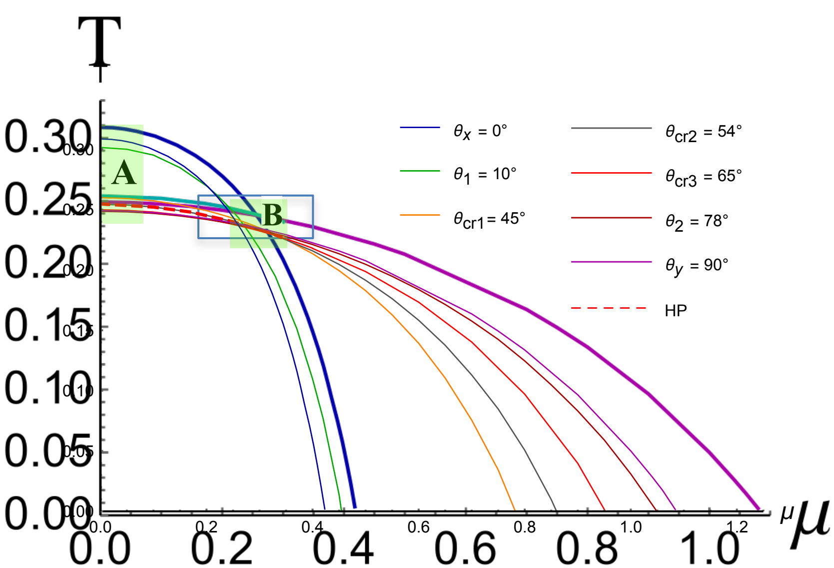

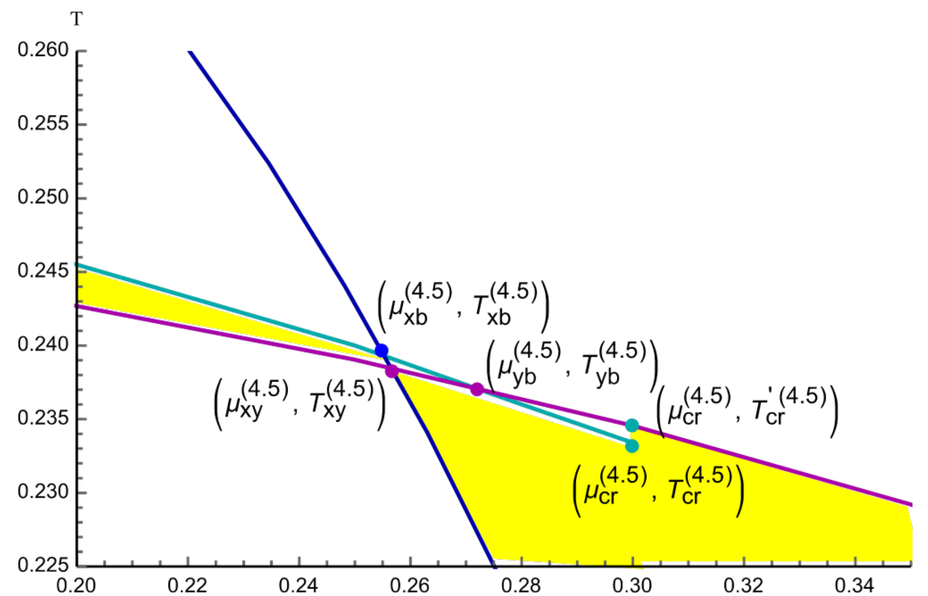

Smeared confinement/deconfinement phase transition

Arbitrary angle: IA, K.Rannu, P.Slepov,PLB'19

Thermodynamics of the background

Temperature as function of horizon

Temperature as function of horizon

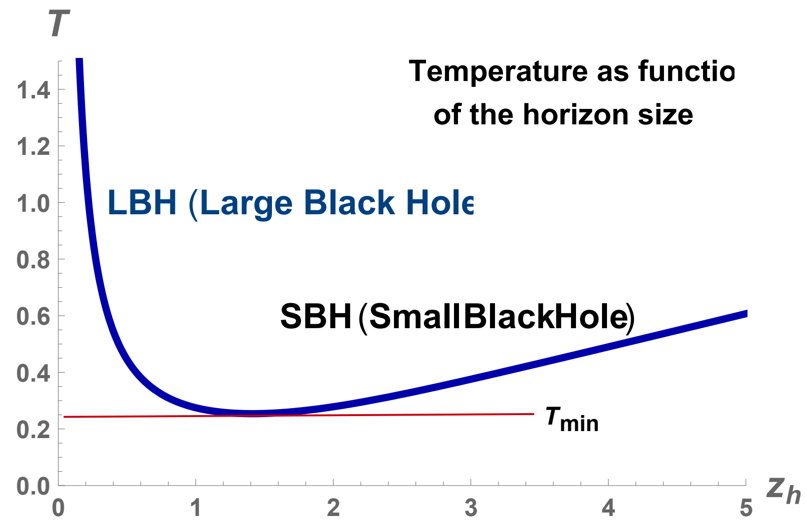

Temperature as function of horizon

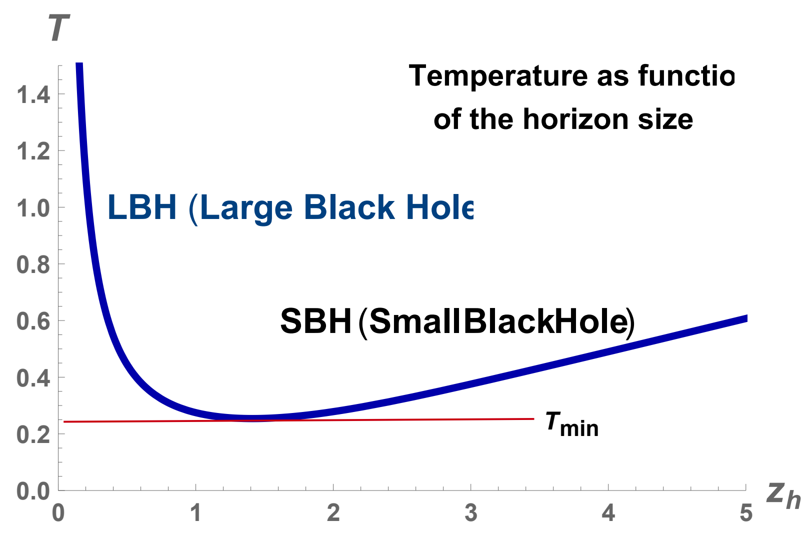

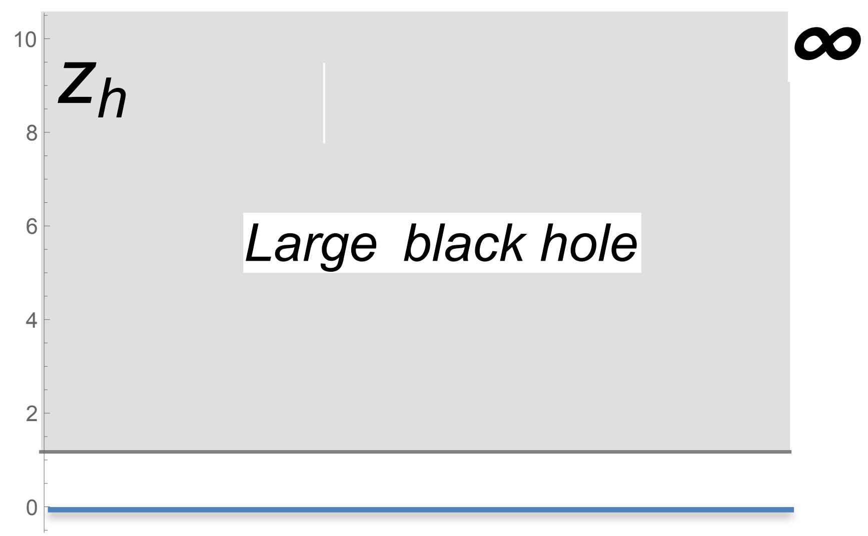

Temperature as function of horizon

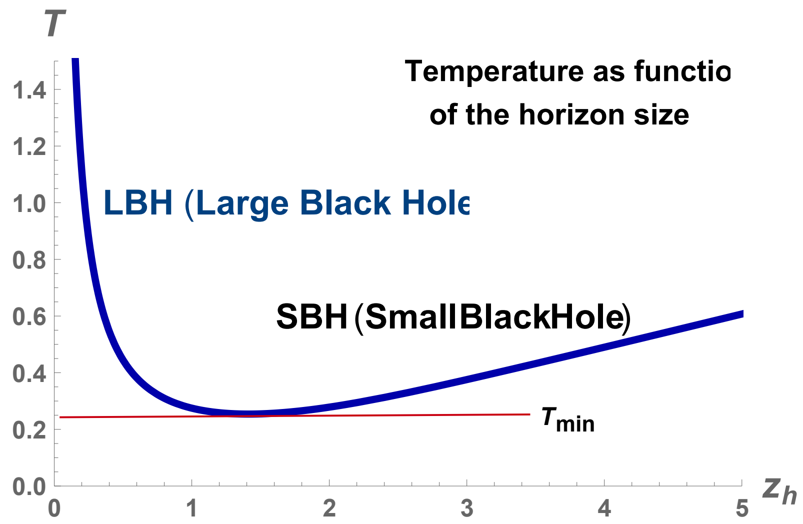

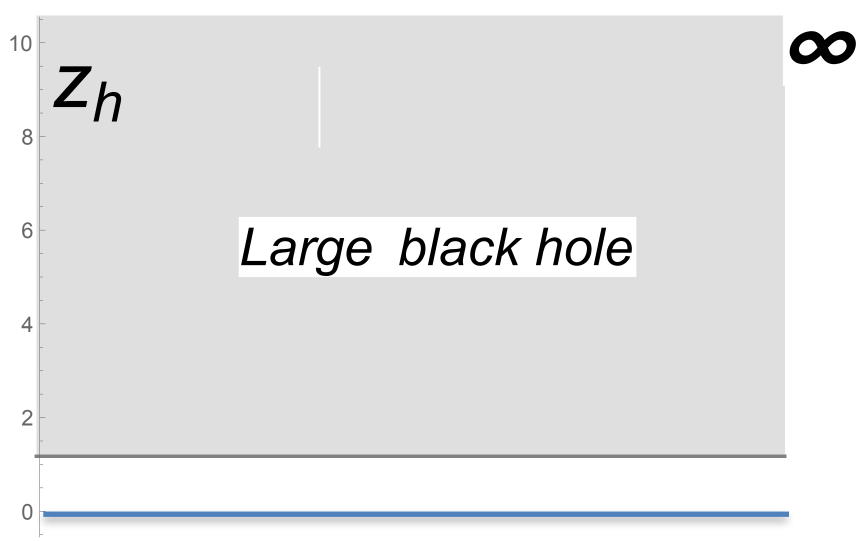

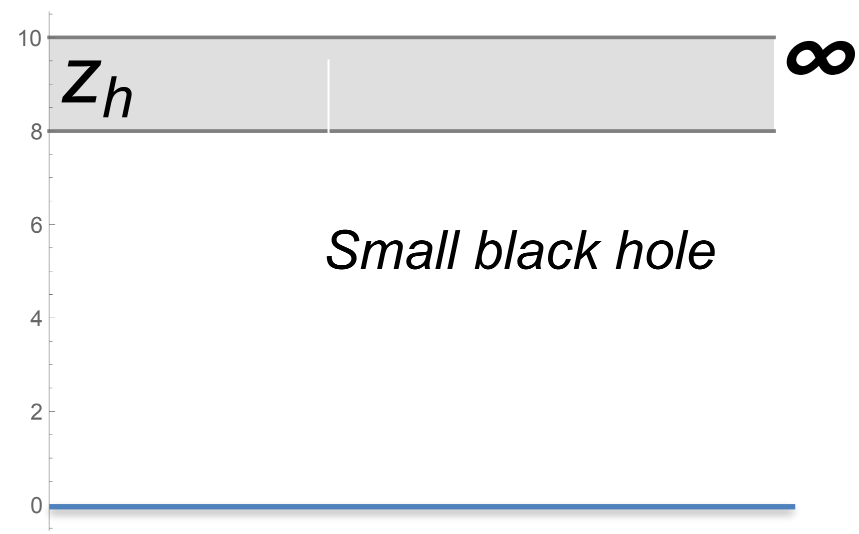

Disappearance of local max and min

Disappearance of local max and min

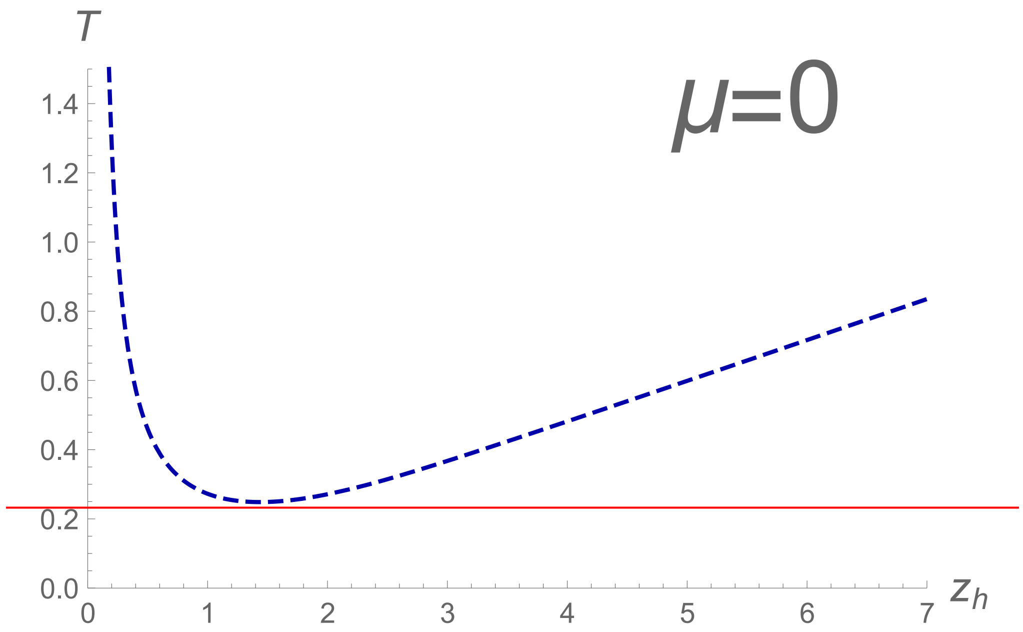

Disappearance of local max and min

Disappearance of local max and min

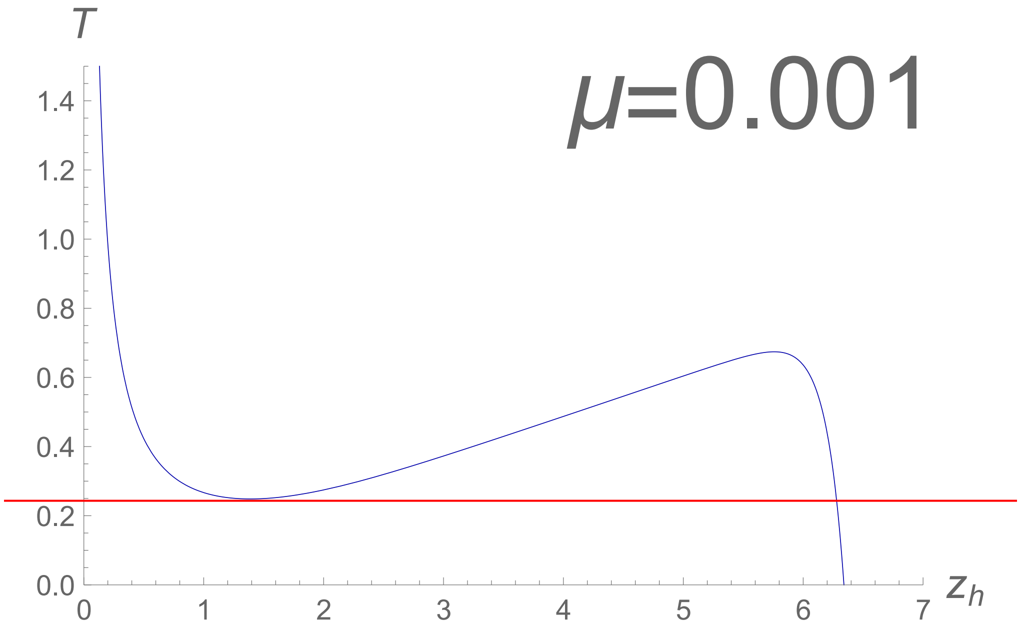

Disappearance of local max and min

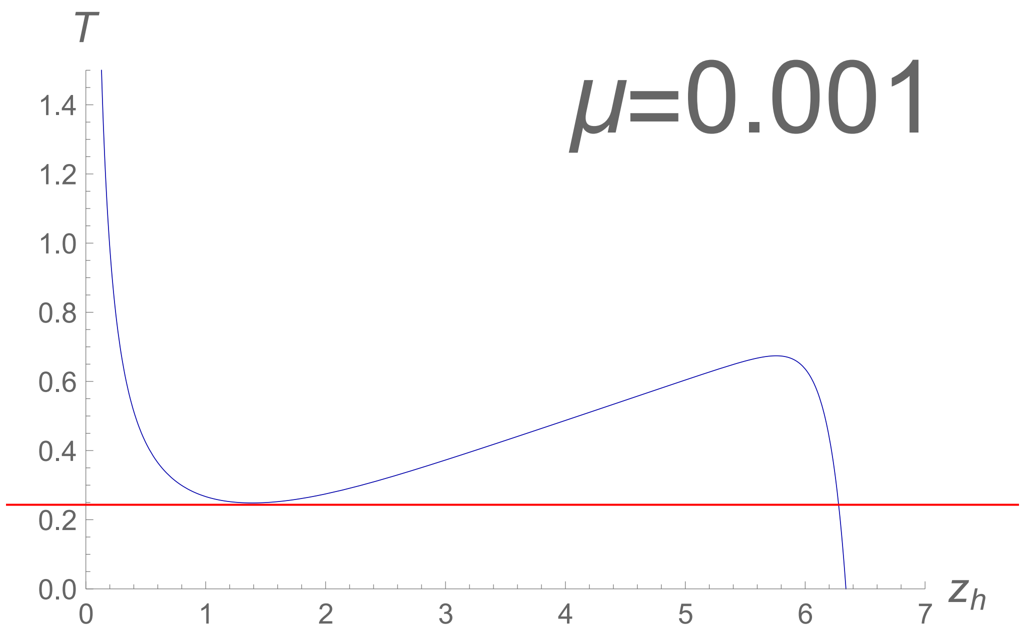

The appearance of second horizon

Disappearance of local max and min

The appearance of second horizon

Disappearance of local max and min

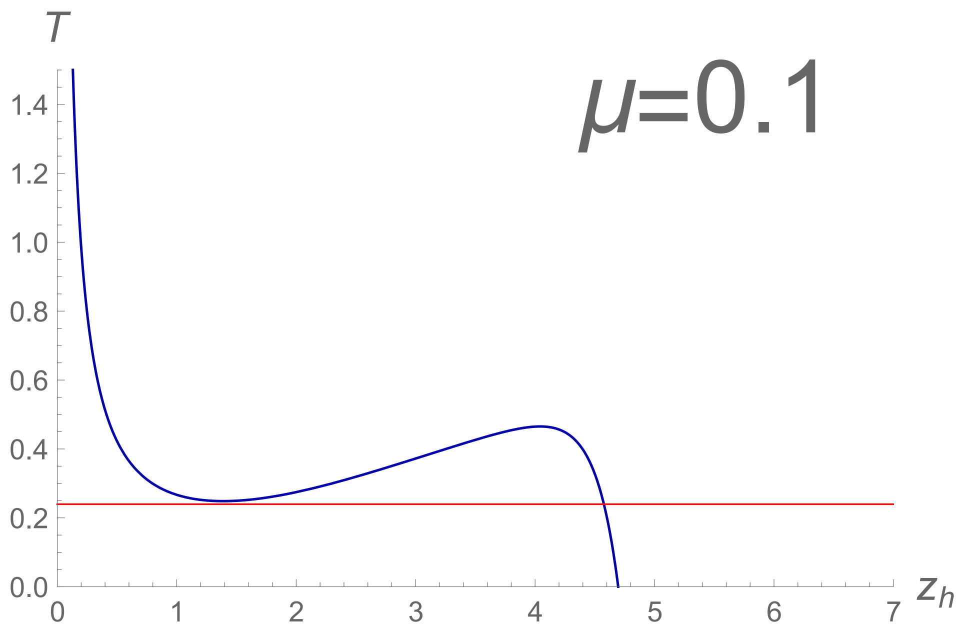

The appearance of second horizon

Disappearance of local max and min

The appearance of second horizon

Disappearance of local max and min

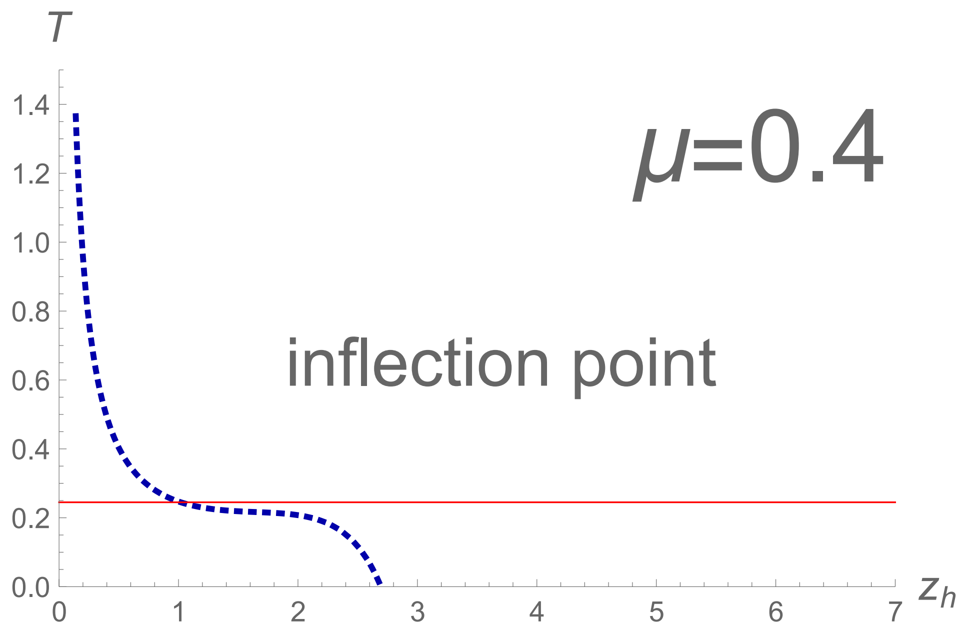

The appearance of second horizon

Disappearance of local max and min

The appearance of second horizon

Disappearance of local max and min

The appearance of second horizon

The disappearance of local max and min

Disappearance of local max and min

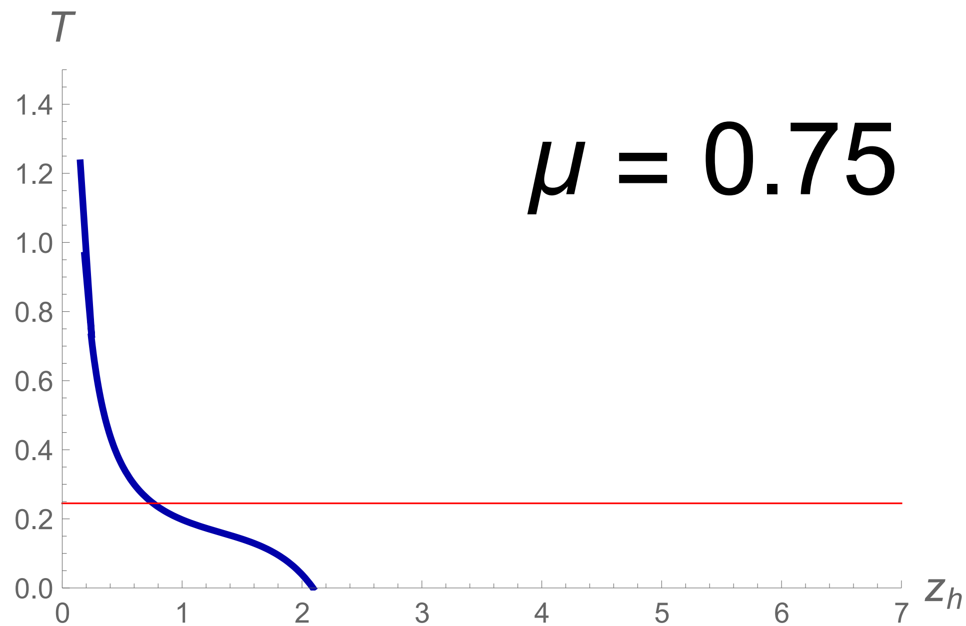

The appearance of second horizon

The disappearance of local max and min

Disappearance of local max and min

The appearance of second horizon

The disappearance of local max and min

Disappearance of local max and min

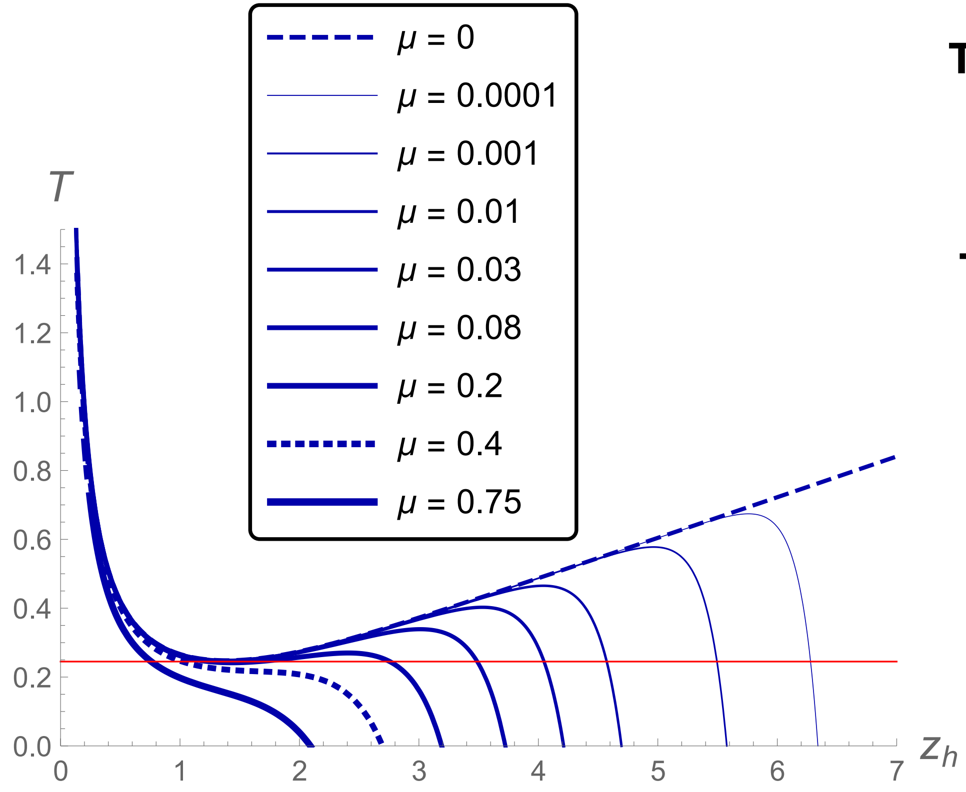

The appearance of second horizon

The disappearance of local max and min

Disappearance of local max and min

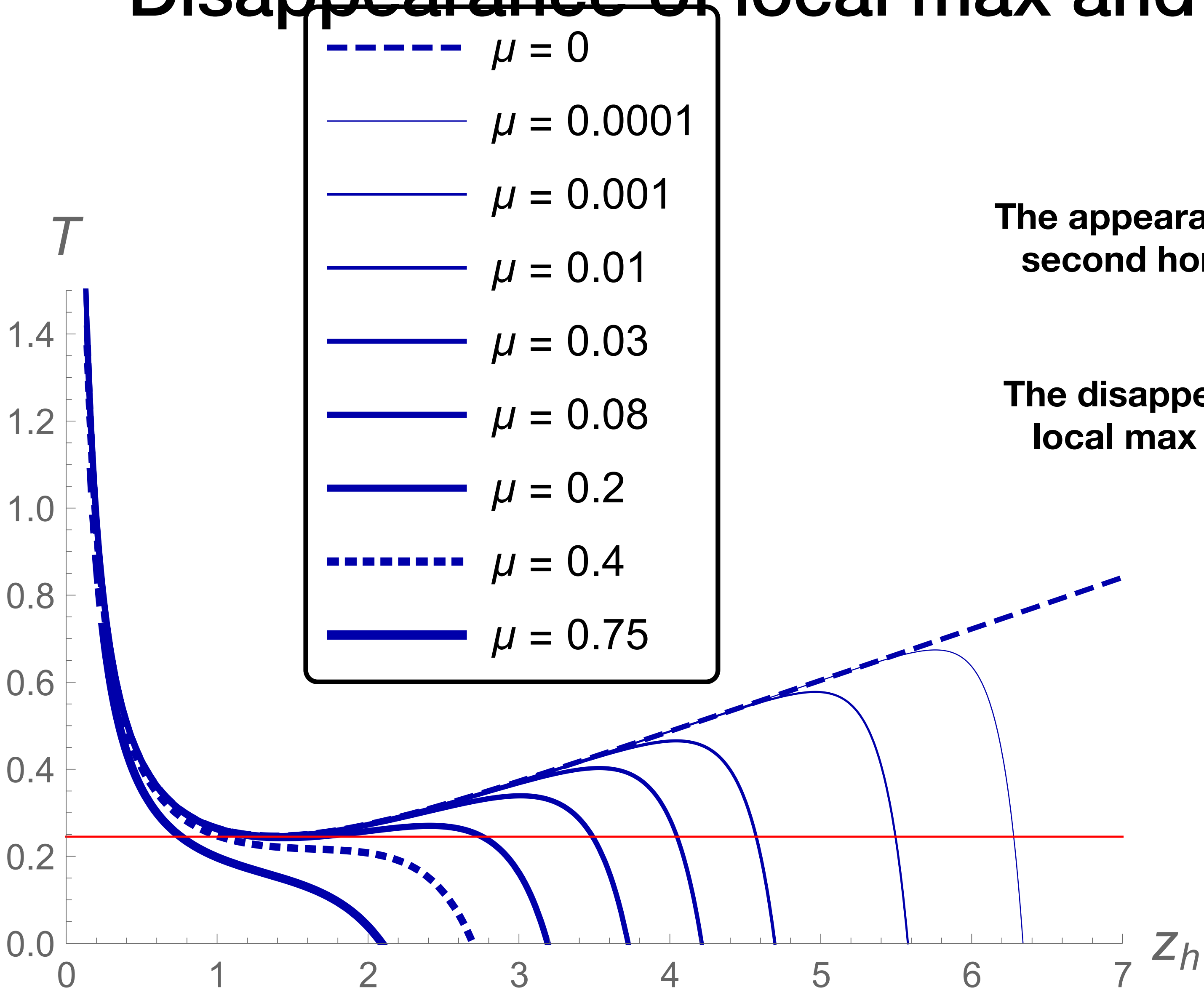

The appearance of second horizon

The disappearance of local max and min

Disappearance of local max and min

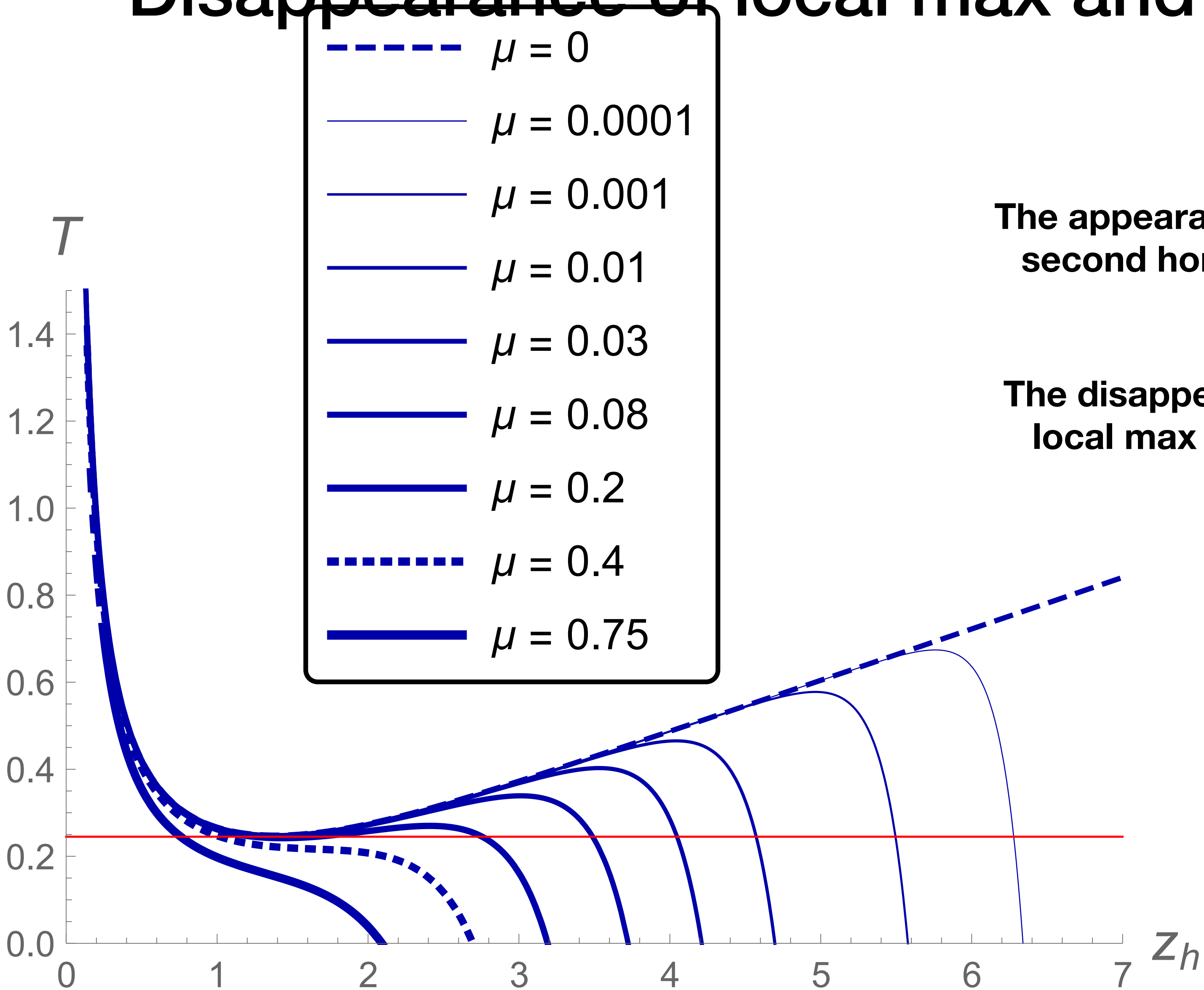

The appearance of second horizon

The disappearance of local max and min

Disappearance of local max and min

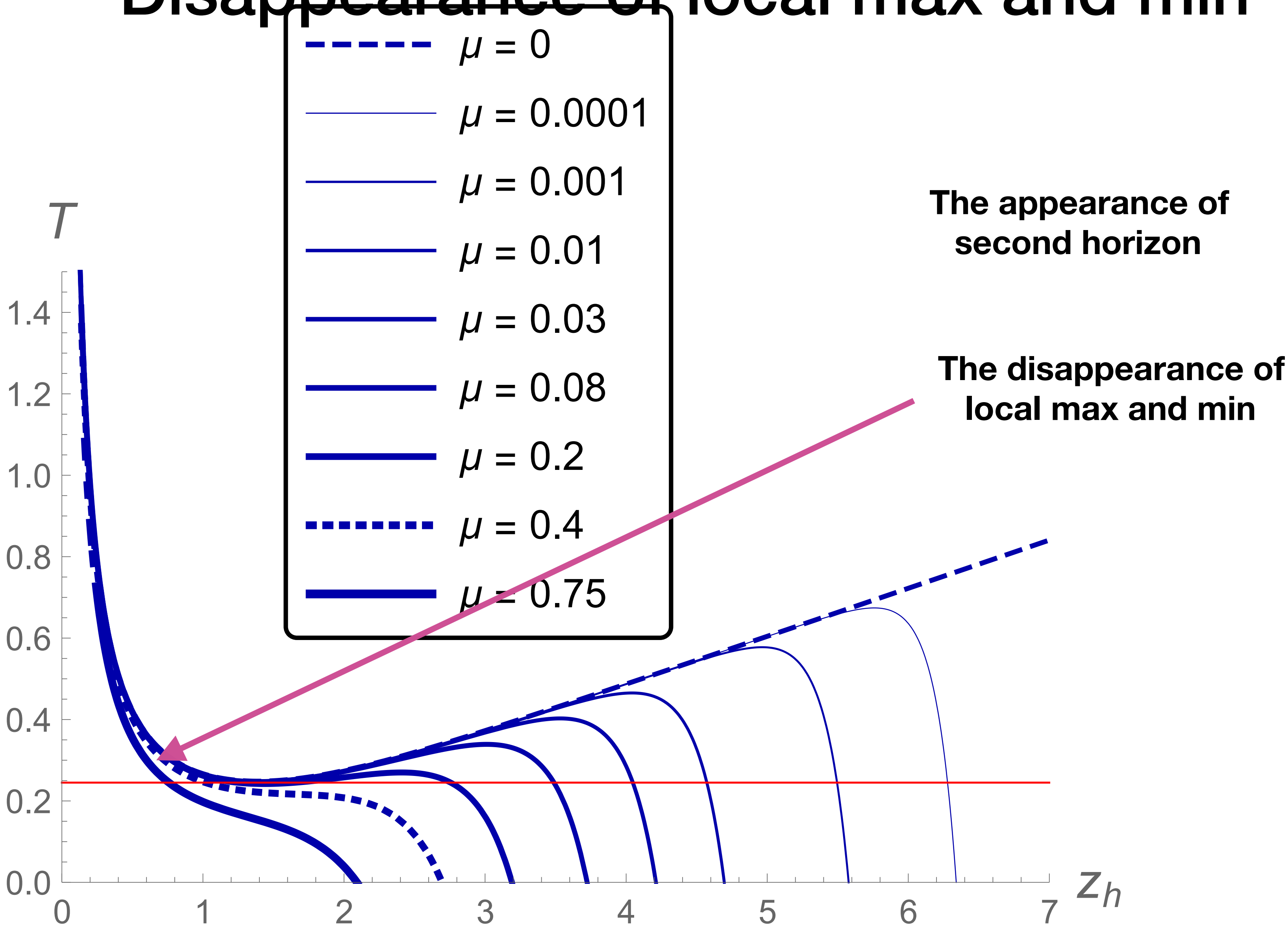

Entropy as function of the temperature

$$s(z_h, c, \nu) = \frac{e^{\frac{3}{4}cz_h^2}}{4}\, z_h^{-\frac{(\nu+2)}{\nu}}$$

Entropy as function of the temperature

$$s(z_h, c, \nu) = \frac{e^{\frac{3}{4}cz_h^2}}{4}\, z_h^{-\frac{(\nu+2)}{\nu}}$$

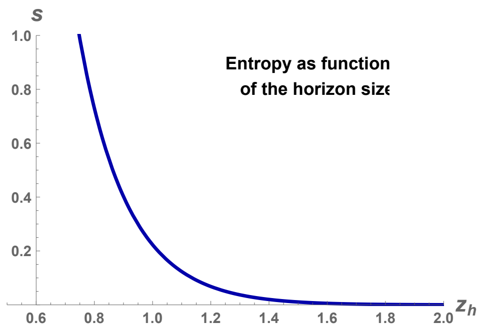

Entropy as function of the temperature

$$s(z_h, c, \nu) = \frac{e^{\frac{3}{4} c z_h^2}}{4}\, z_h^{-\frac{(\nu+2)}{\nu}}$$

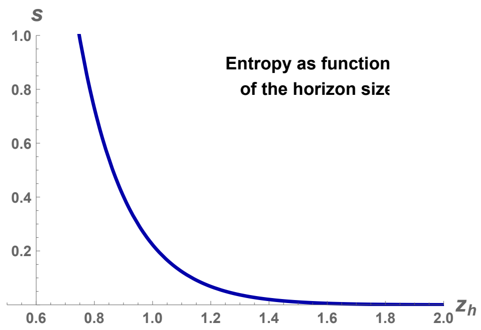

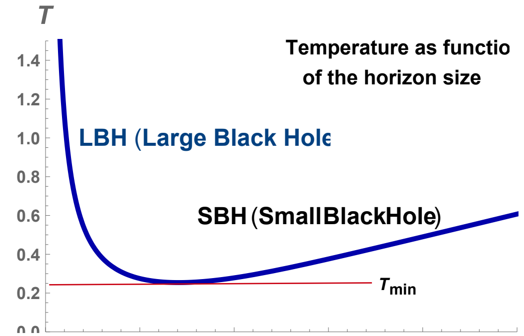

Entropy as function of the temperature

$$s(z_h, c, \nu) = \frac{e^{\frac{3}{4}cz_h^2}}{4}\, z_h^{-\frac{(\nu+2)}{\nu}}$$

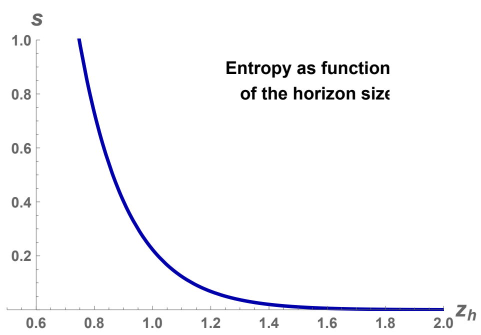

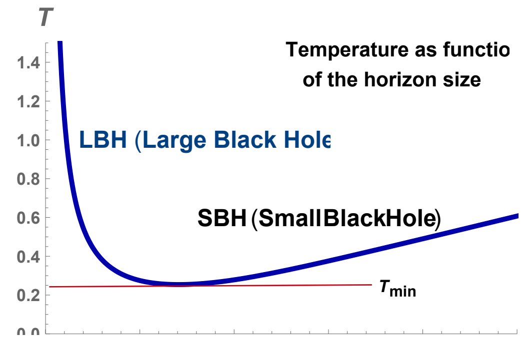

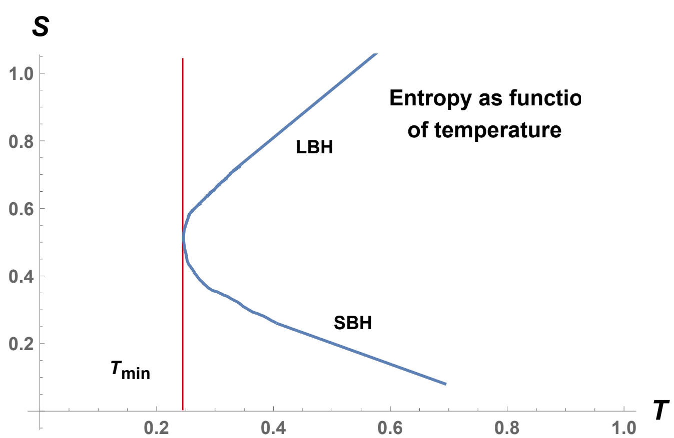

Entropy as function of the temperature

$$s(z_h, c, \nu) = \frac{e^{\frac{3}{4}cz_h^2}}{4}\, z_h^{-\frac{(\nu+2)}{\nu}}$$

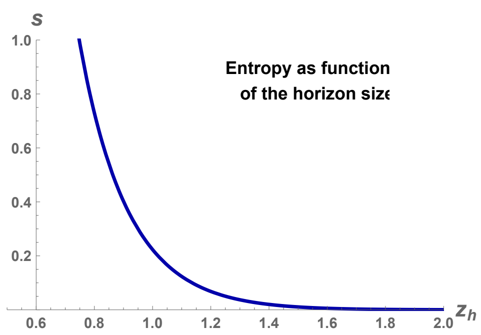

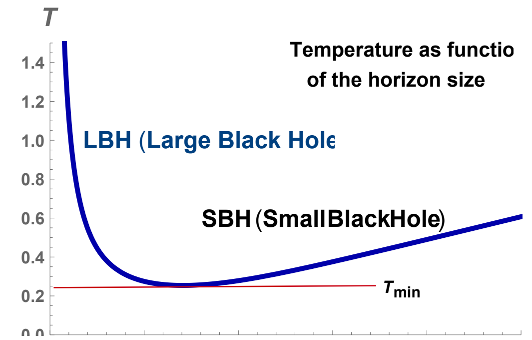

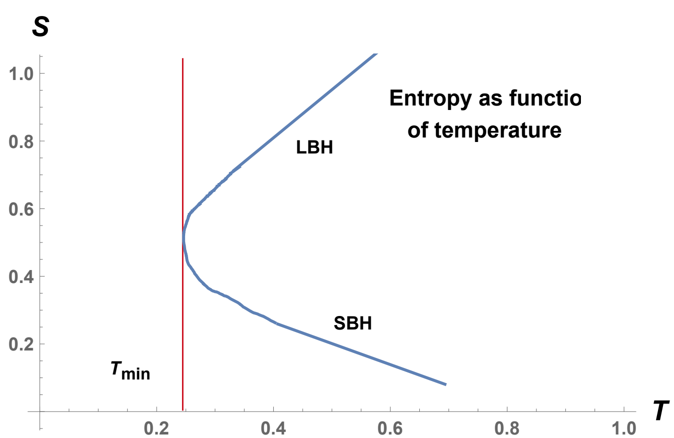

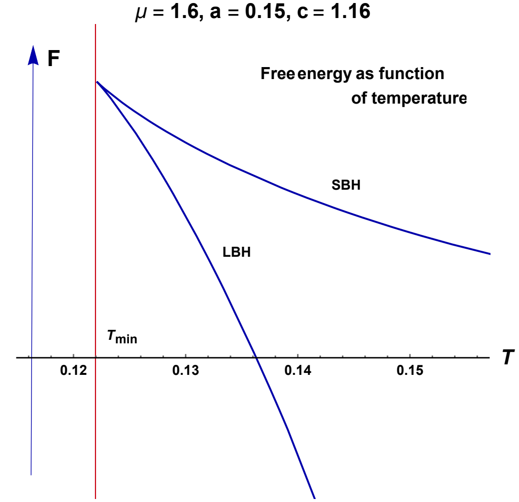

Free energy as function of temperature

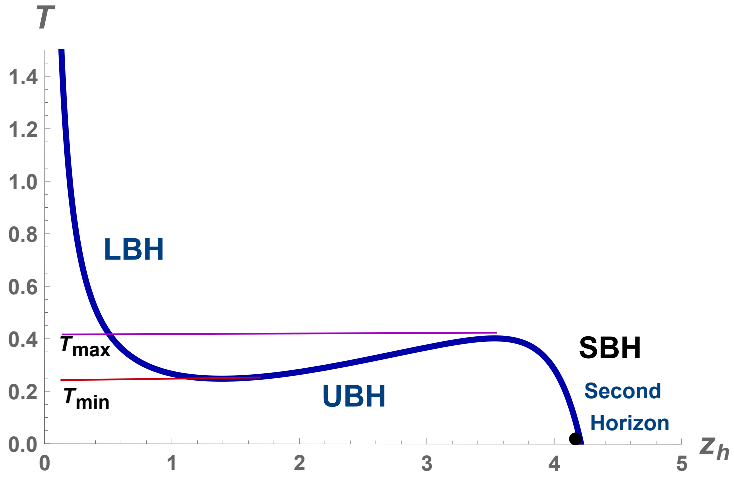

Free energy as function of temperature

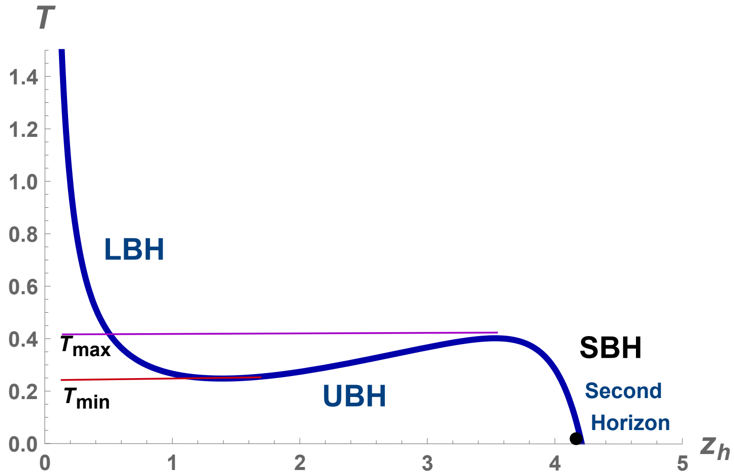

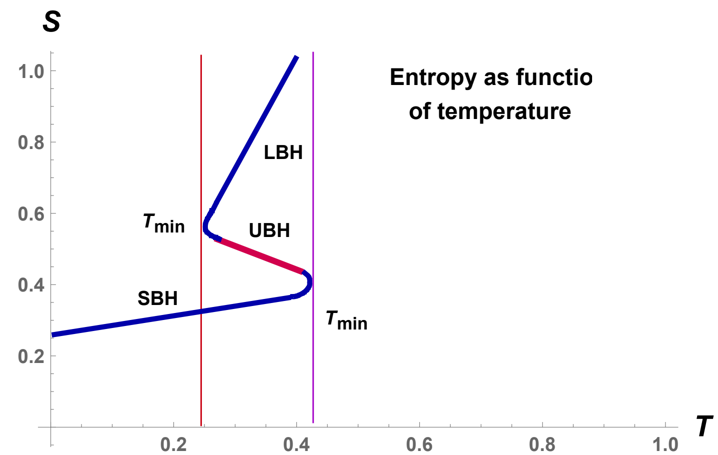

Free energy as function of temperature

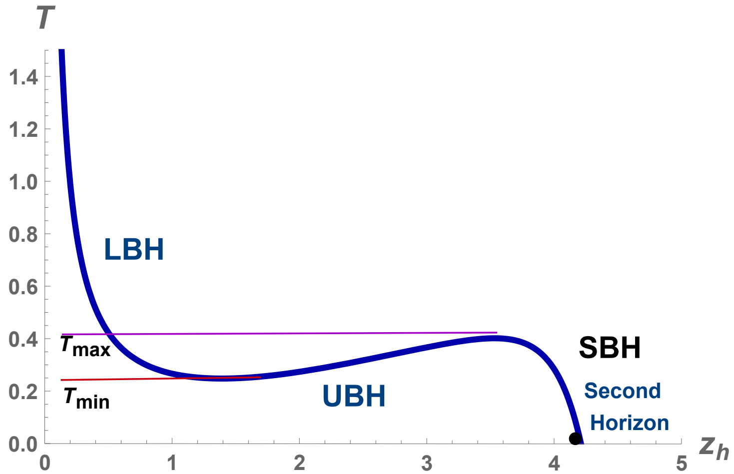

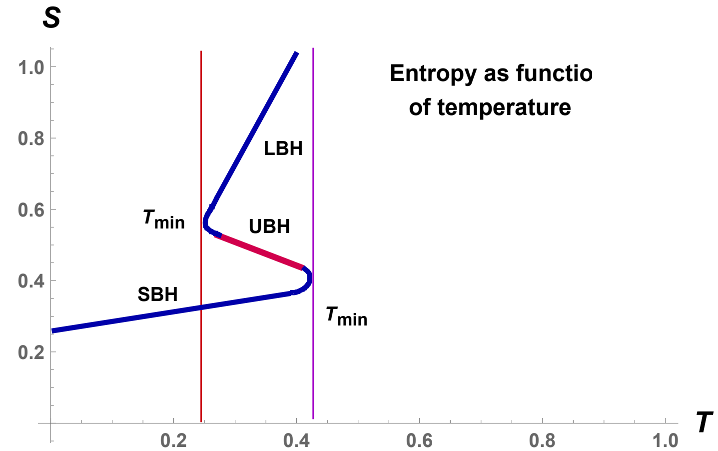

$$F(z_h, c, \nu) = \int_{z_h}^{\infty} s(z_h, c, \nu)\, T'(z_h, c, \nu)\, dz_h$$

Free energy as function of temperature

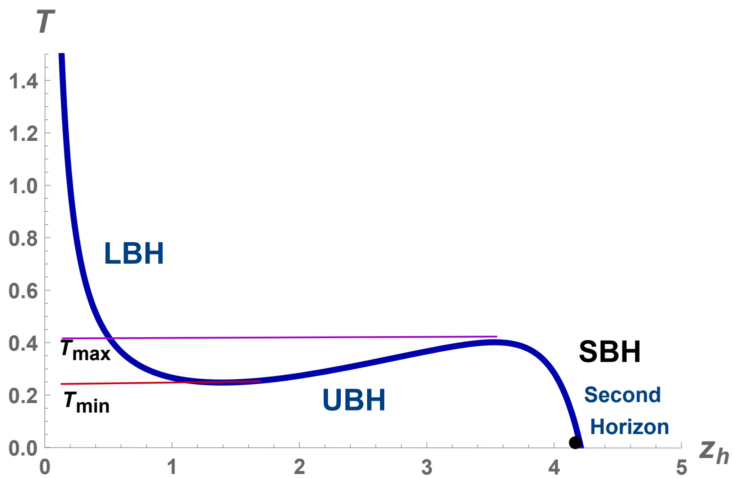

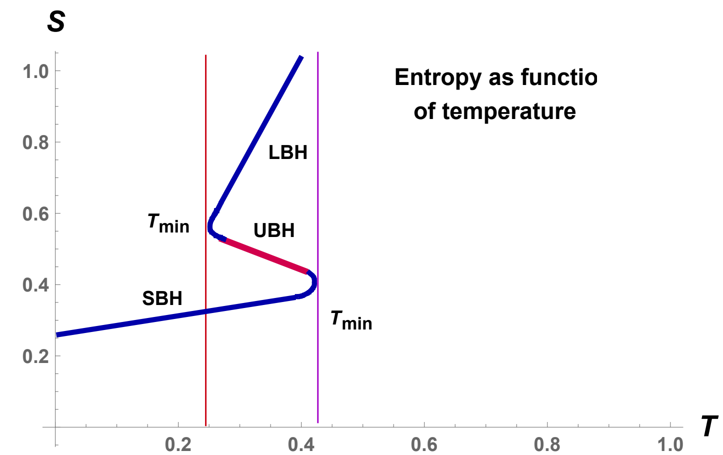

$$F(z_h, c, \nu) = \int_{z_h}^{\infty} s(z_h, c, \nu)\, T'(z_h, c, \nu)\, dz_h$$

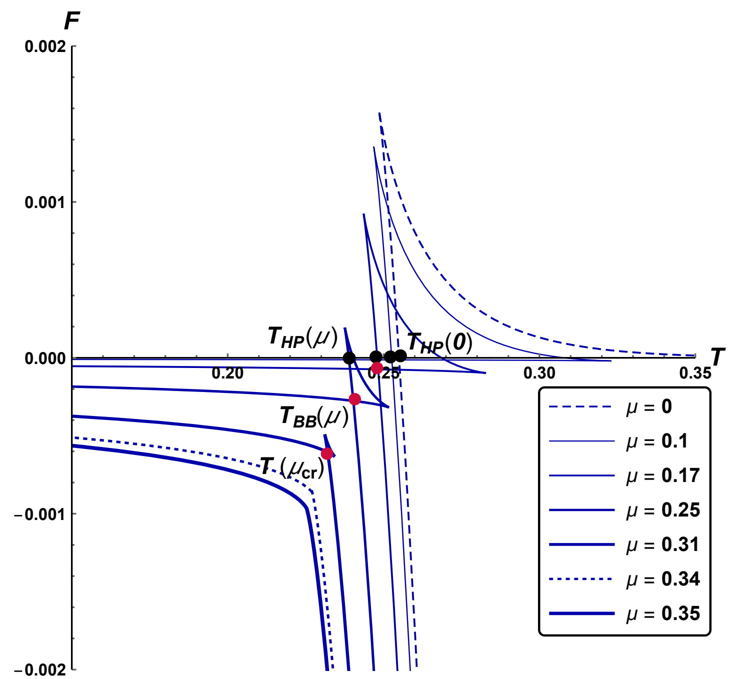

Free energy as function of temperature

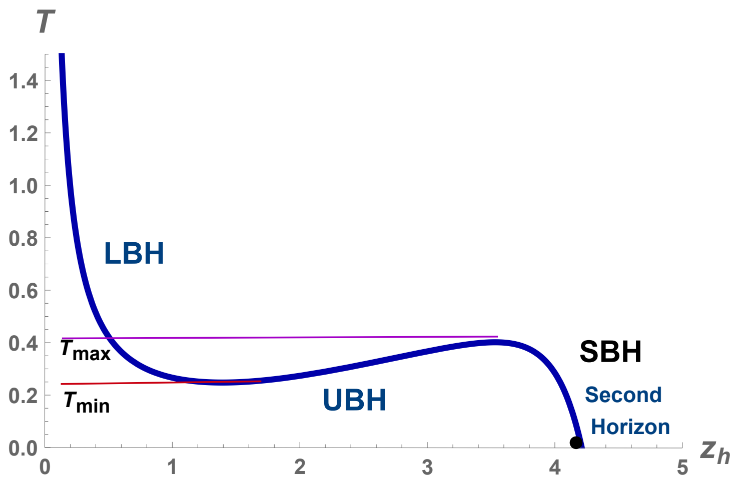

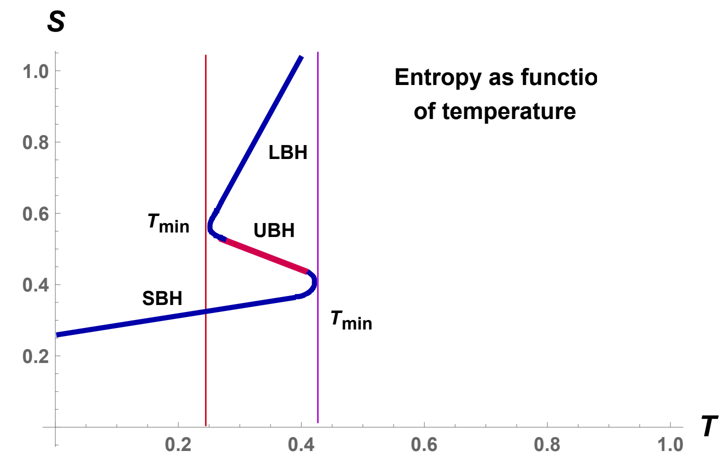

$$F(z_h, c, \nu) = \int_{z_h}^{\infty} s(z_h, c, \nu)\, T'(z_h, c, \nu)\, dz_h$$

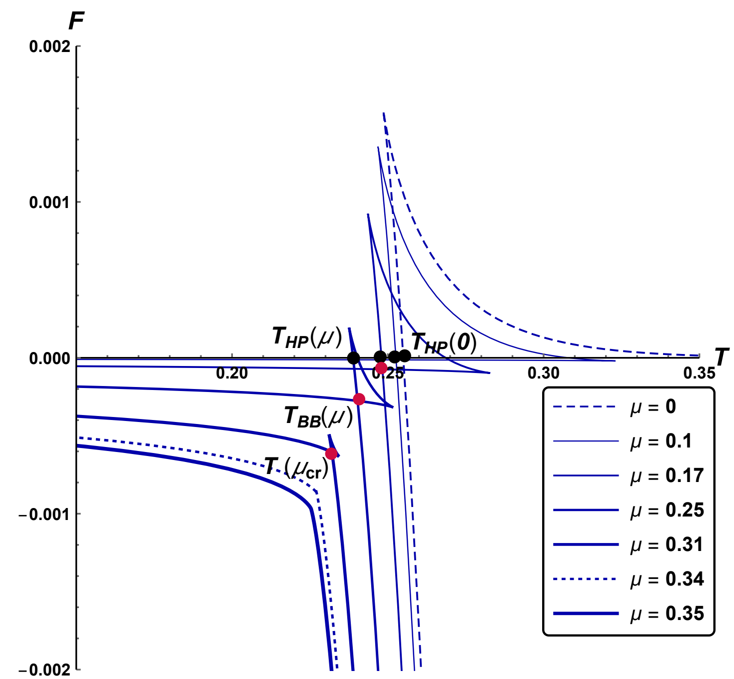

The swallow-tailed shape

Free energy as function of temperature for Isotropic and Anisotropic

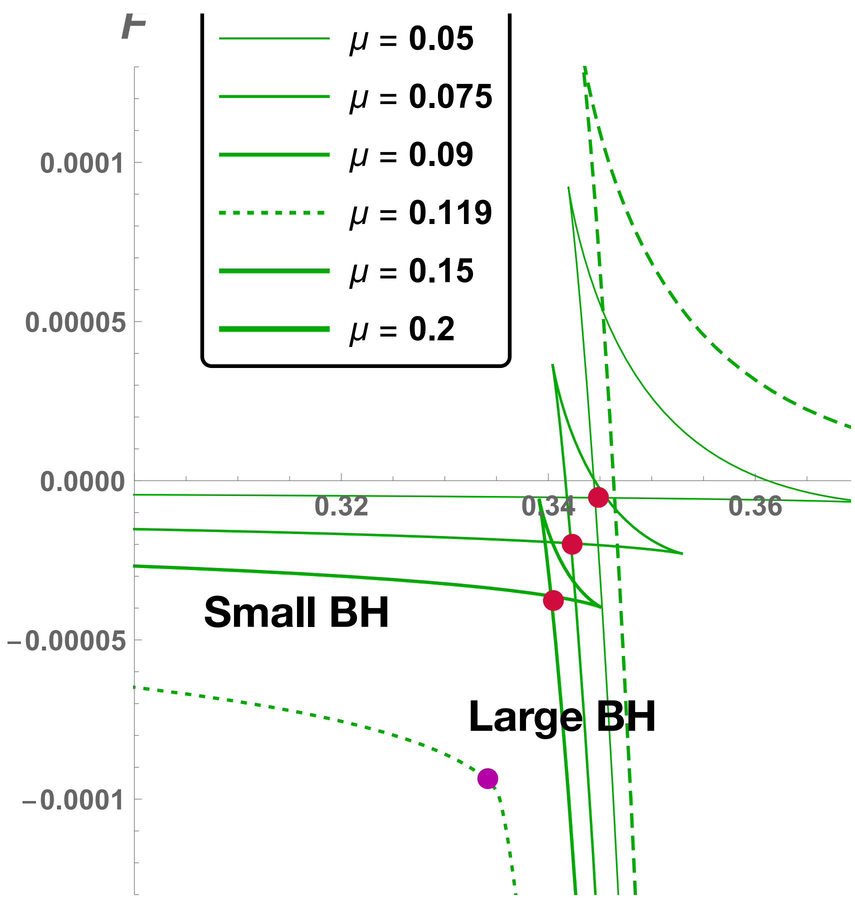

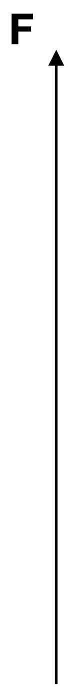

Free energy as function of temperature for Isotropic and Anisotropic

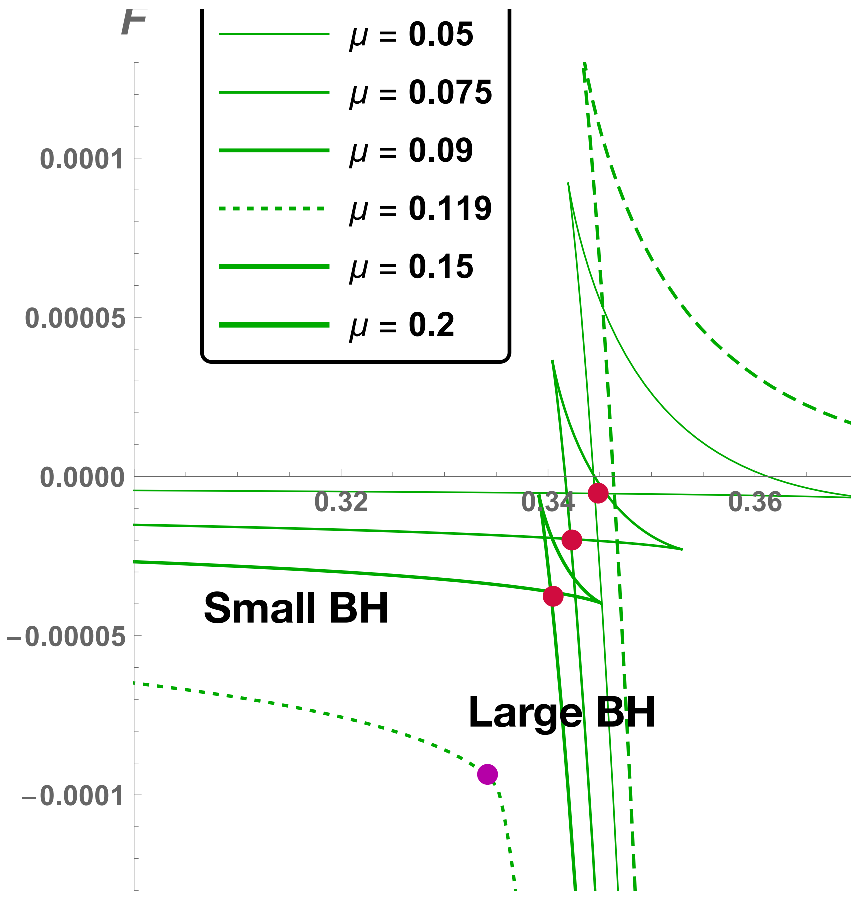

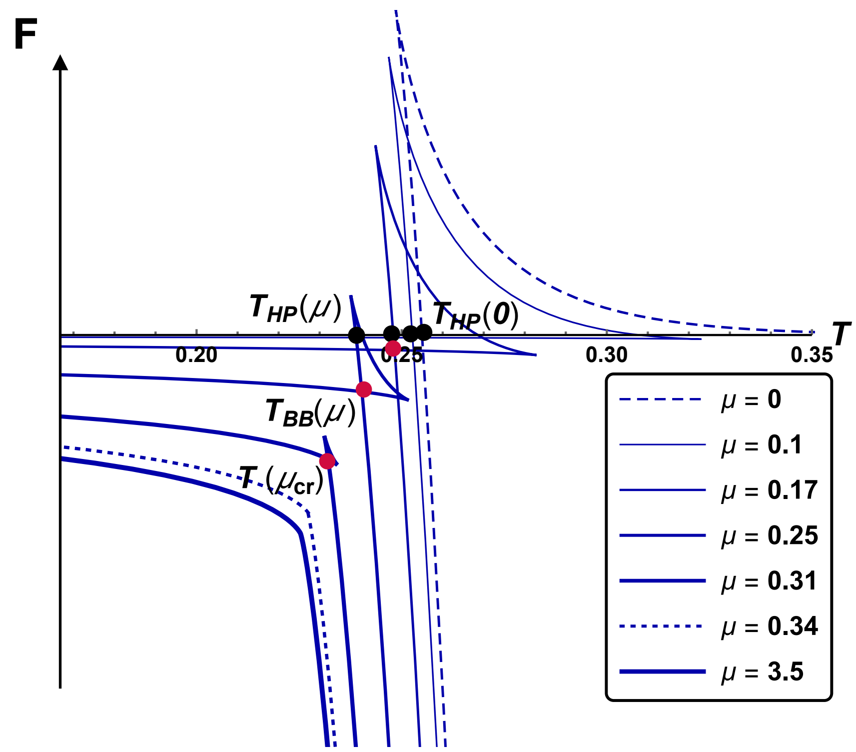

Thermodynamics of the Anisotropic background as compare with Isotropic one

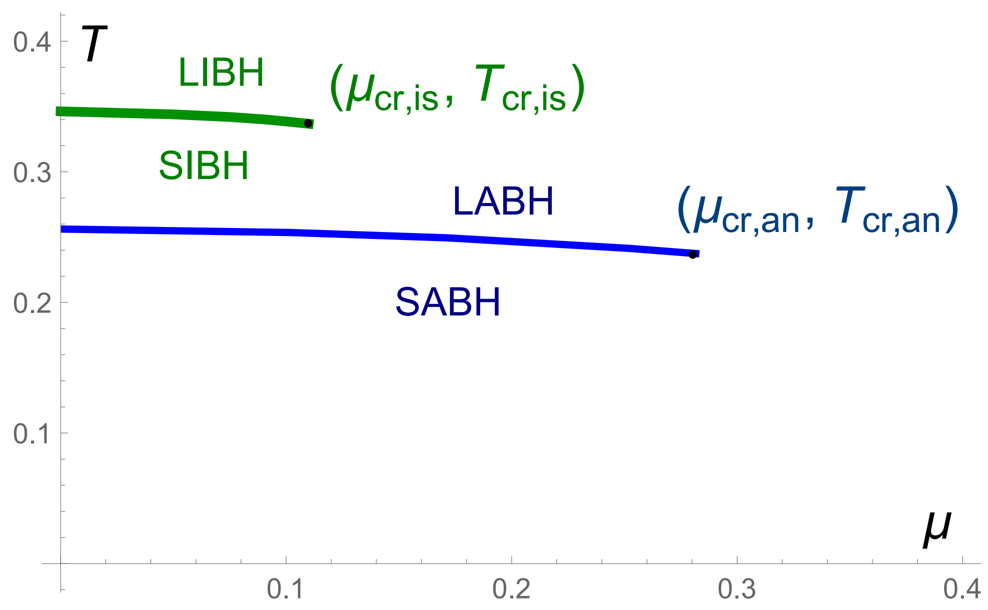

Background instability leads to 1-order confinement/deconfinement phase transition

Dynamical domain wall position

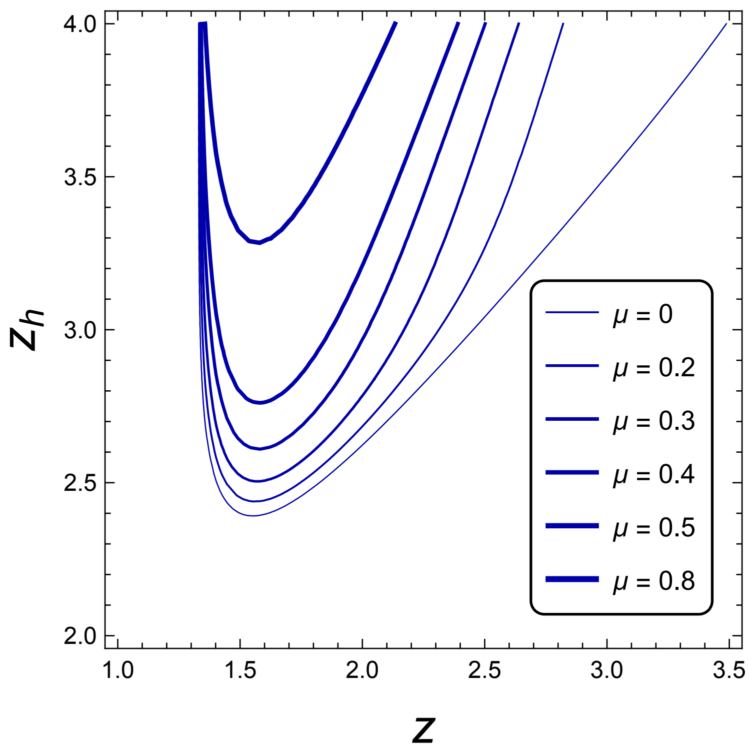

Background instability leads to 1-order confinement/deconfinement phase transition

Dynamical domain wall position

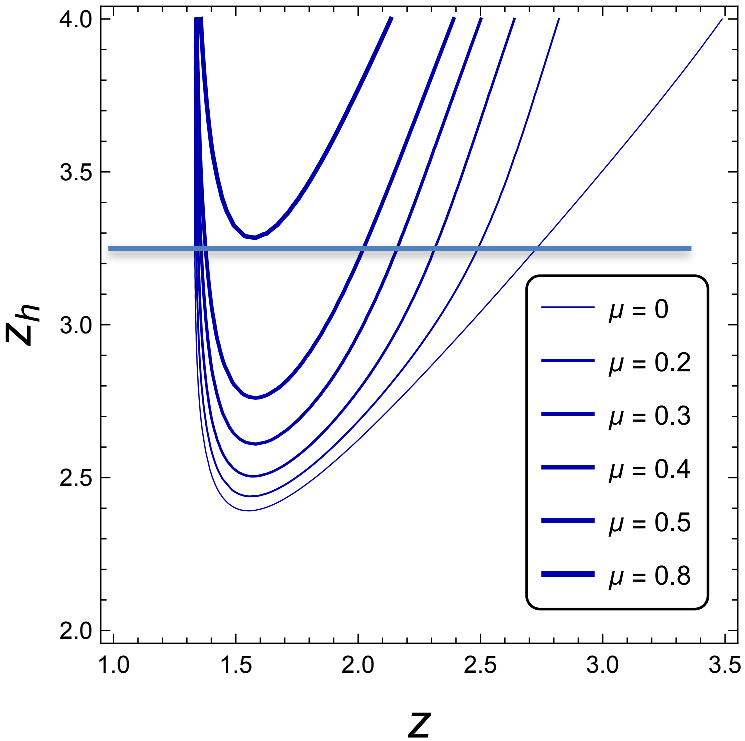

Background instability leads to 1-order confinement/deconfinement phase transition

Dynamical domain wall position

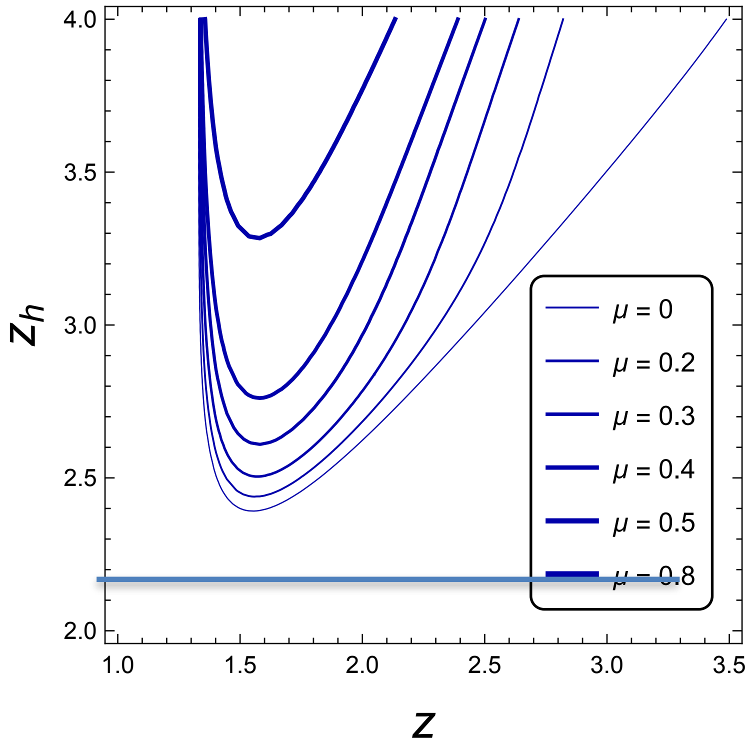

Background instability leads to 1-order confinement/deconfinement phase transition

Dynamical domain wall position

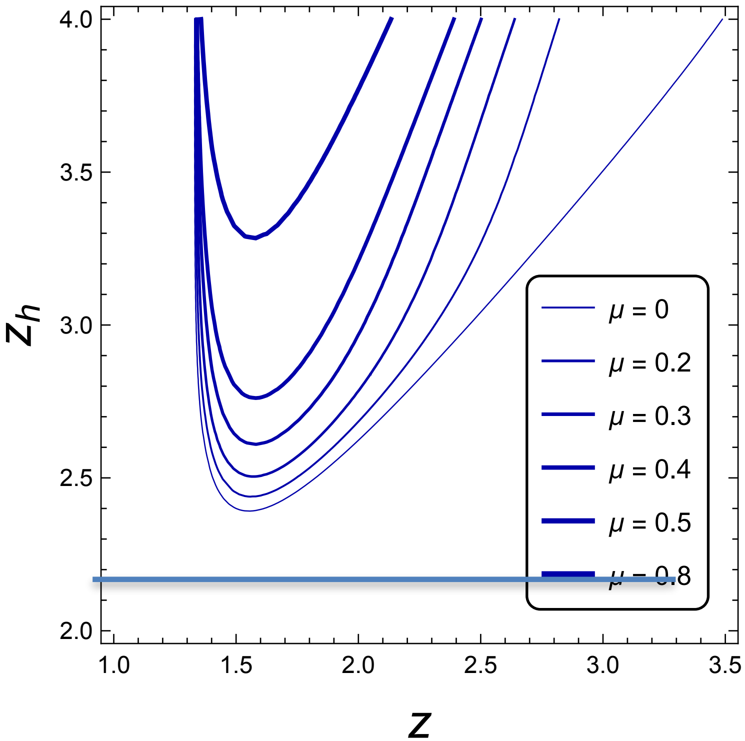

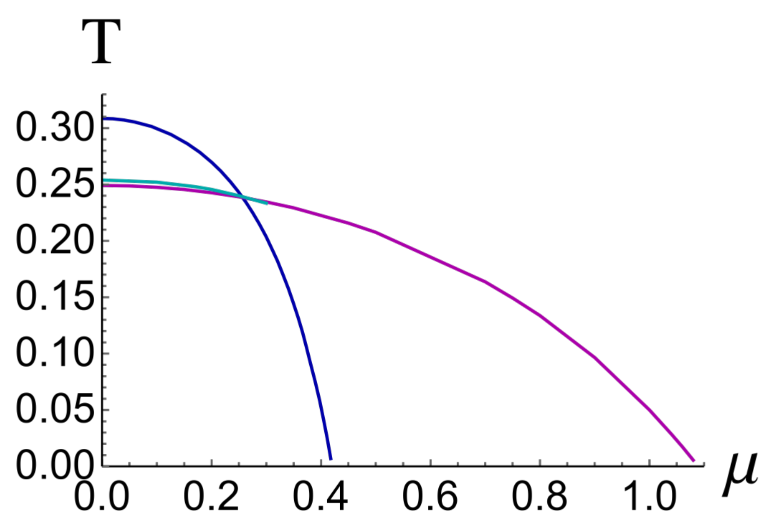

HQCD phase diagram in magnetic field

HQCD phase diagram in magnetic field

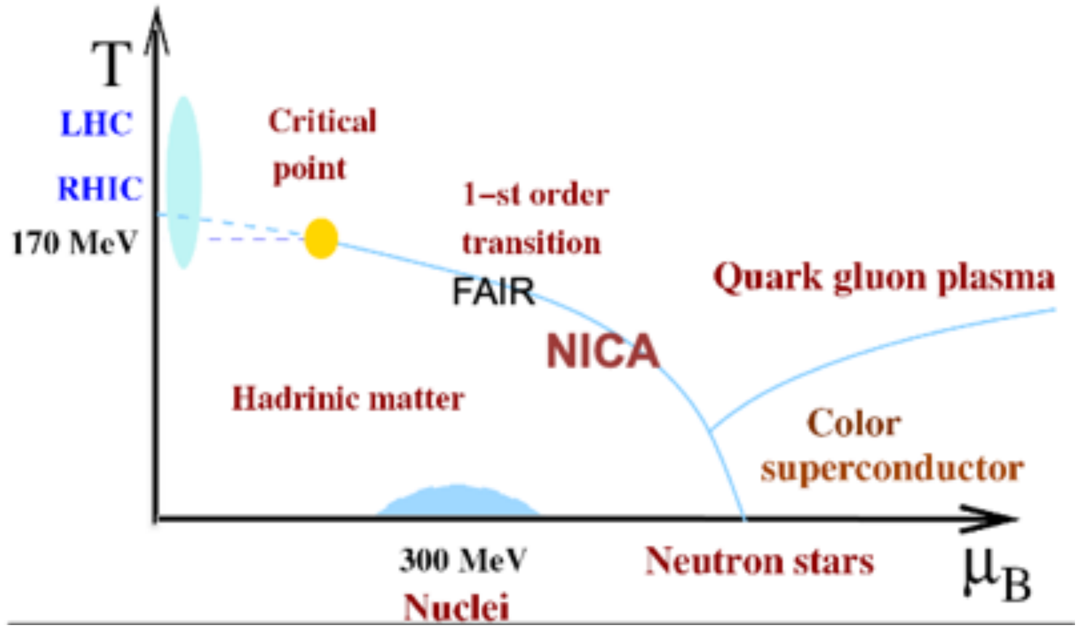

HQCD phase diagram in magnetic field

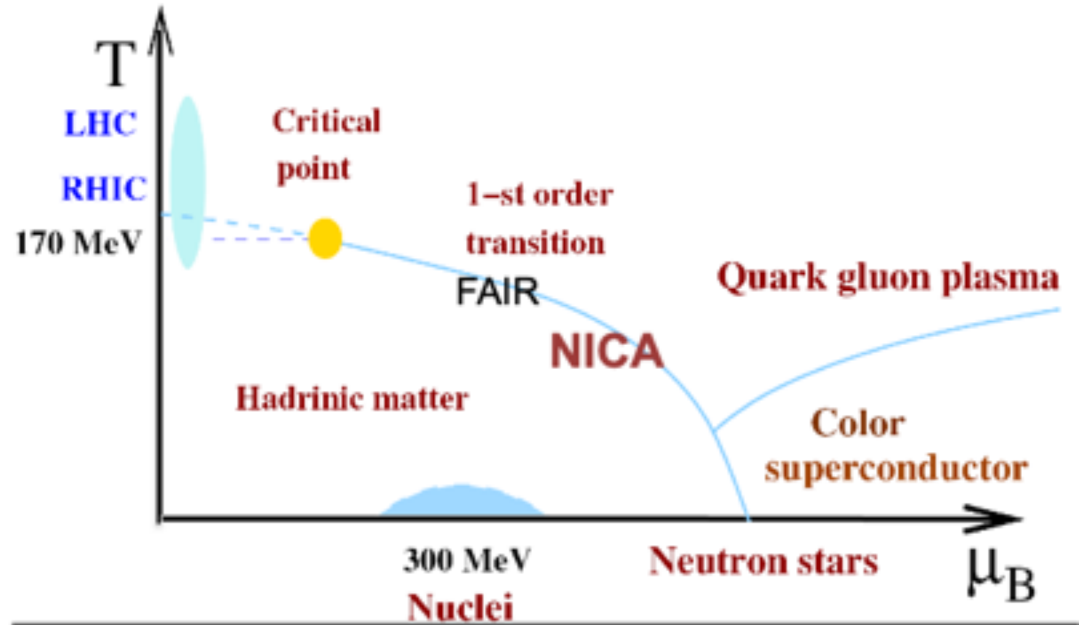

Magnetic field

HQCD phase diagram in magnetic field

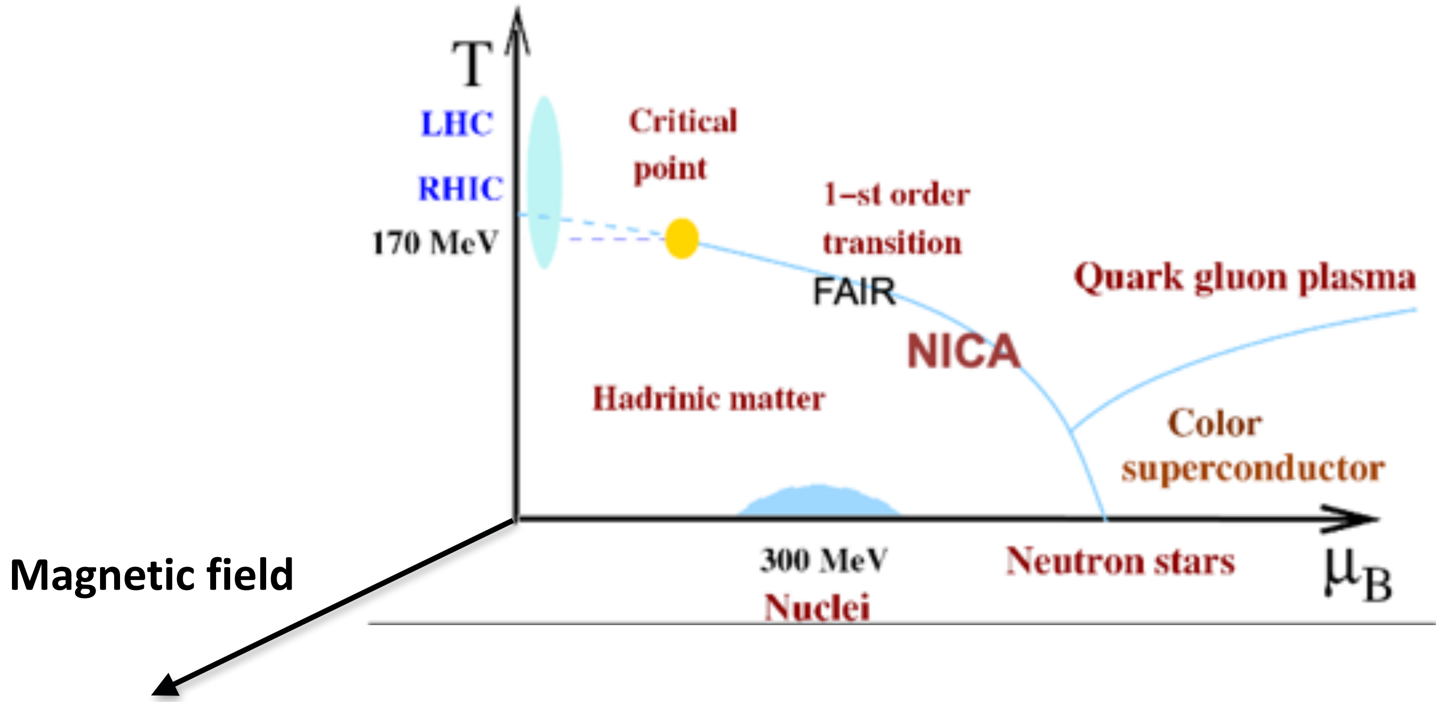

HQCD phase diagram in magnetic field

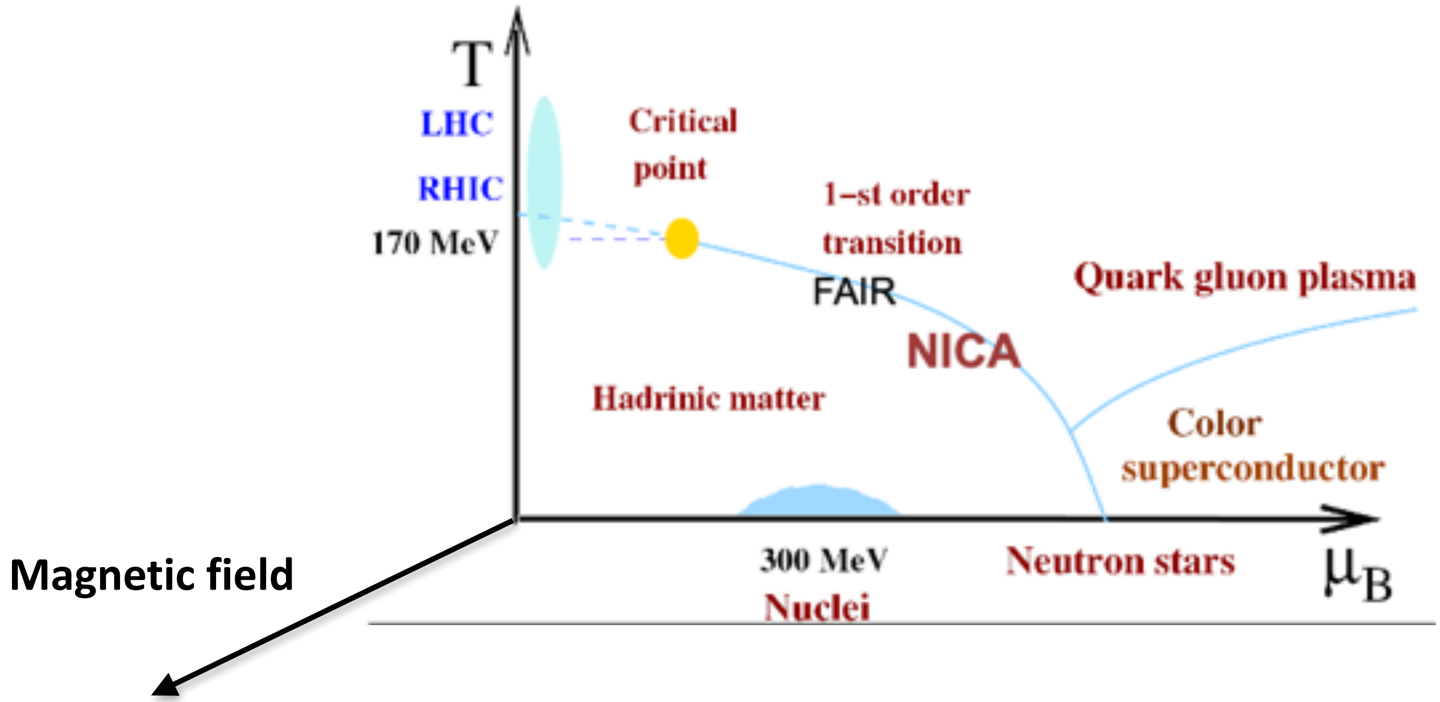

In HIC magnetic field: a largest known magnitude ~ $10^{18}\ Gauss$

HQCD phase diagram in magnetic field

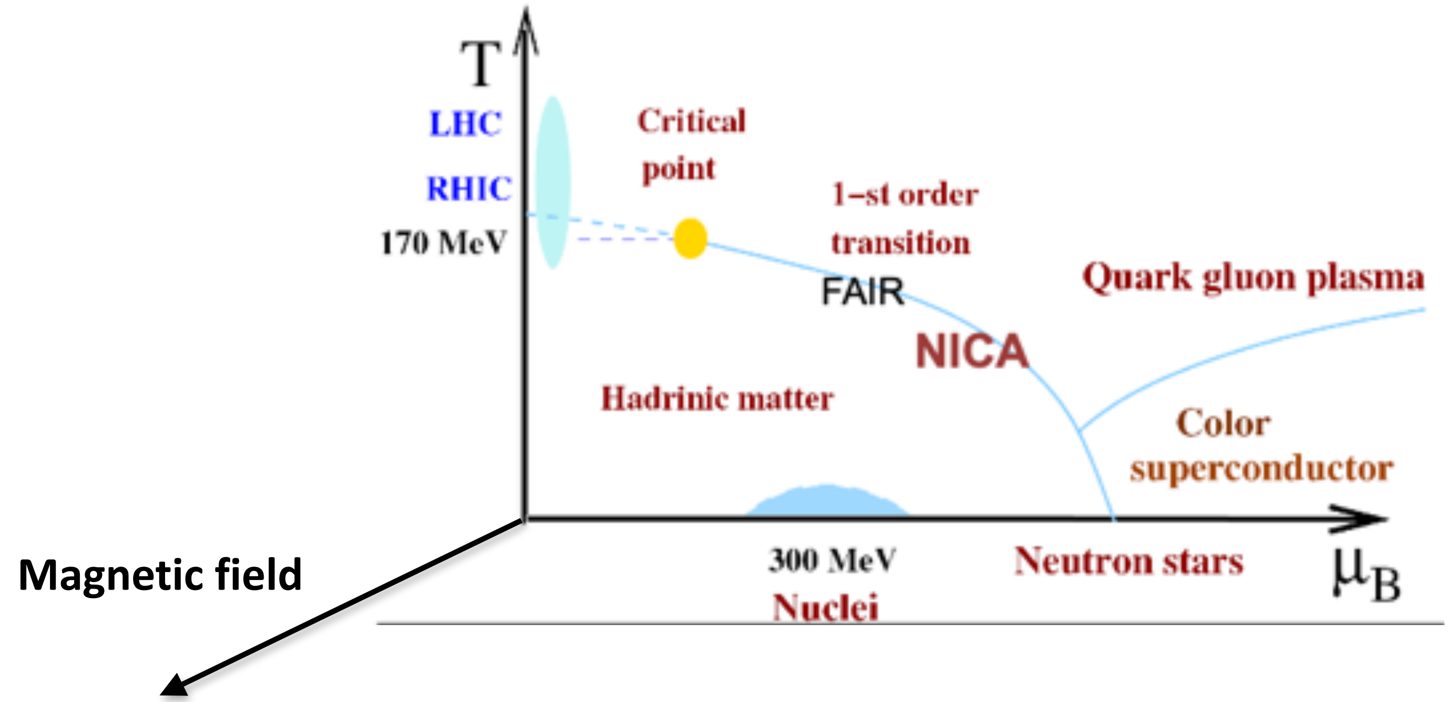

Lattice data (mu=0) IMC (inverse magnetic catalysis)

In HIC magnetic field: a largest known magnitude ~ $10^{18}\, Gauss$

Heavy ion collisions: largest known magnitude ~ 10^{18} Gauss

Heavy ion collisions: largest known magnitude ~ 10^{18} Gauss

Peripheral HIC

Heavy ion collisions: largest known magnitude ~ 10^{18} Gauss

Peripheral HIC

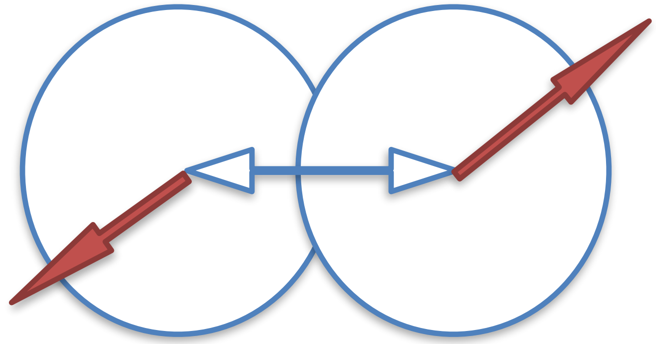

Heavy ion collisions: largest known magnitude ~ 10^{18} Gauss

Peripheral HIC

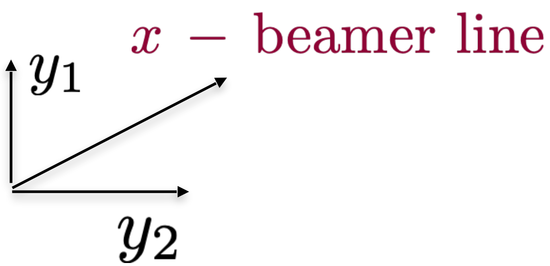

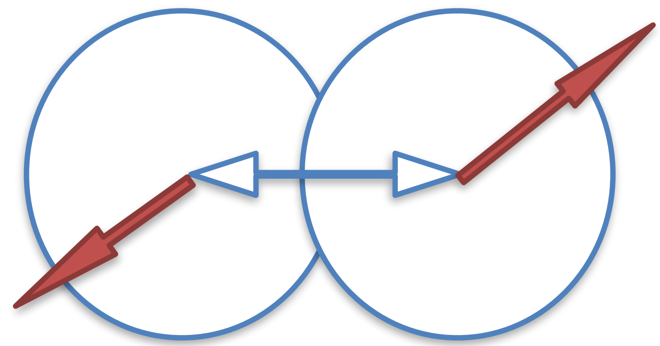

Heavy ion collisions: largest known magnitude ~ 10^{18} Gauss

Peripheral HIC

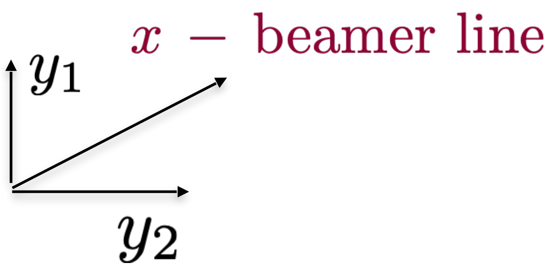

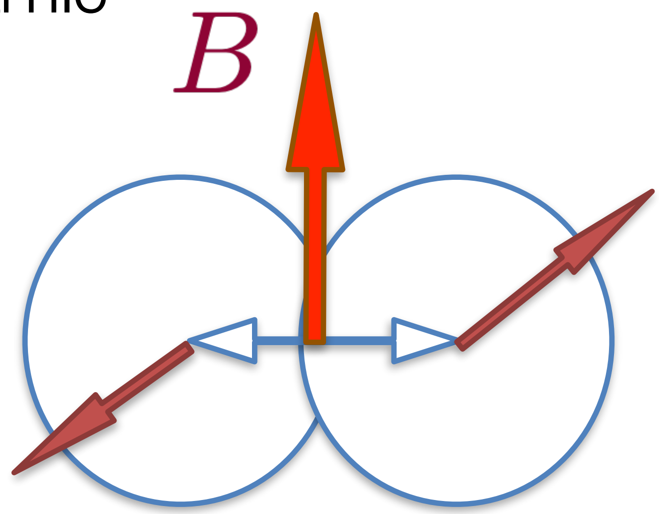

Heavy ion collisions: largest known magnitude ~ 10^{18} Gauss

Peripheral HIC

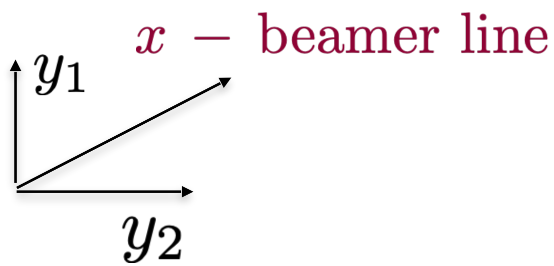

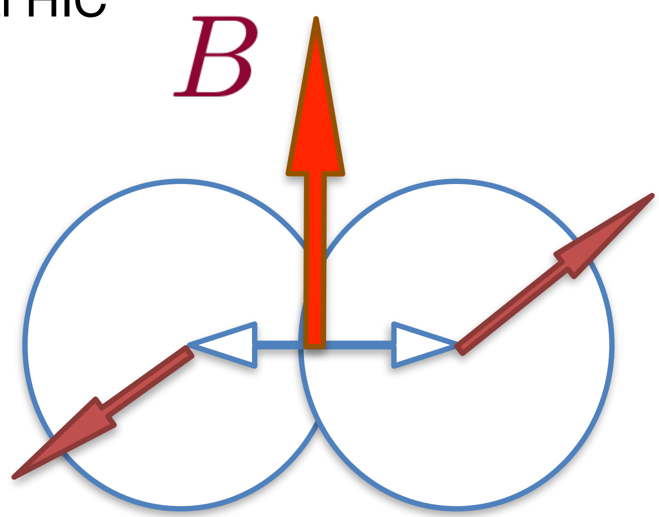

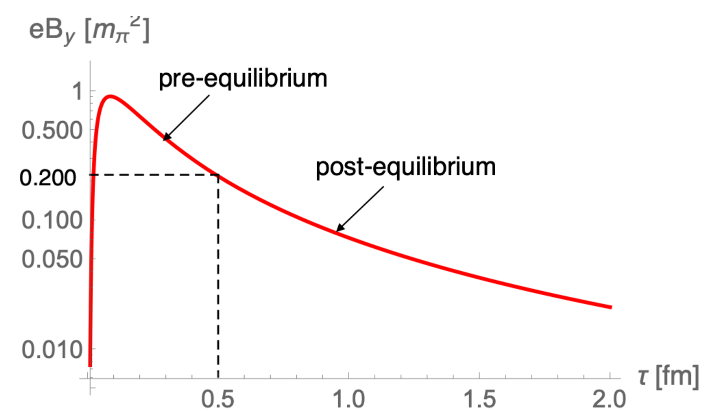

Heavy ion collisions: largest known magnitude ~ 10^{18} Gauss

Peripheral HIC

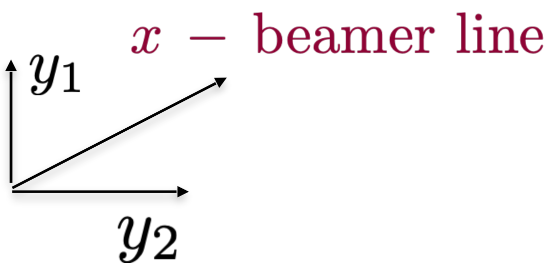

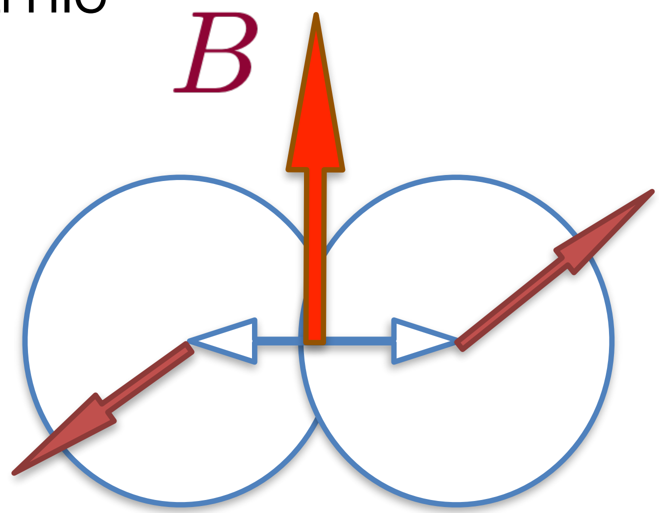

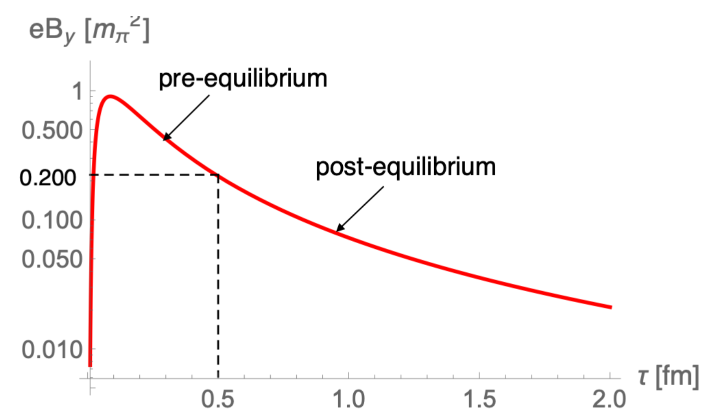

V.Skokov, et al., 0907.1396
V.Tonev, O.Rogachevsky, et al., 1604.0623

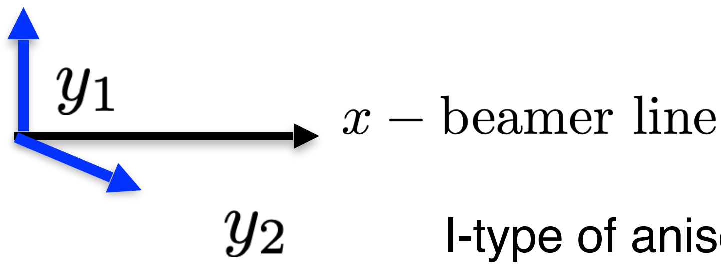

I-type of anisotropy (transverse to beam vs. along beam)

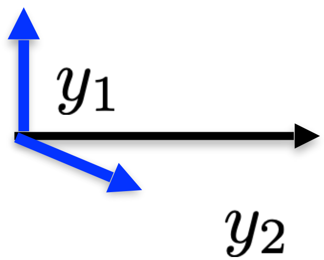

I-type of anisotropy (transverse to beam vs. along beam)

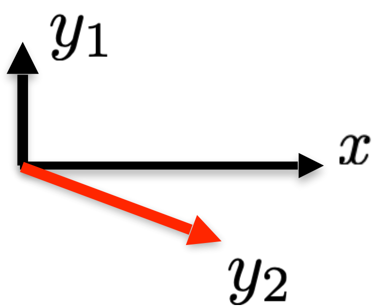

II-type of anisotropy (within y-plane
due to magnetic field)

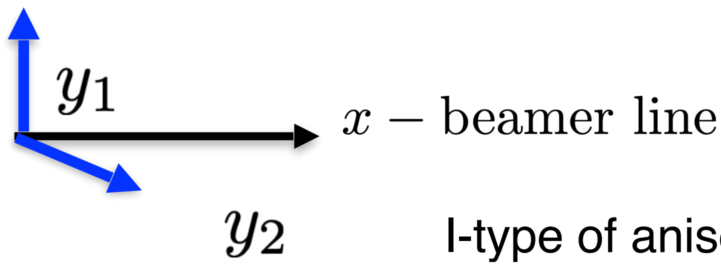

I-type of anisotropy (transverse to beam vs. along beam)

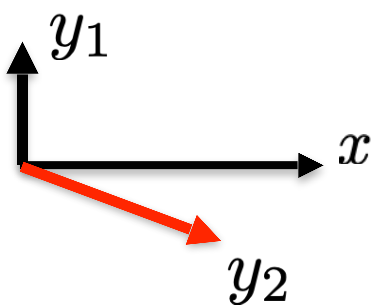

II-type of anisotropy (within y-plane
due to magnetic field)

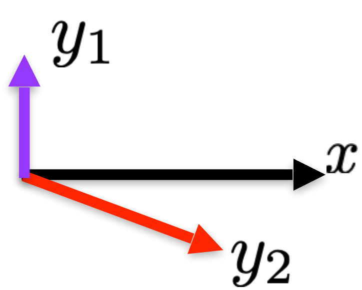

III-type of anisotropy (general anisotropy)

5-dim Anisotropic Background at Large Magnetic Field

5-dim Anisotropic Background at Large Magnetic Field

Compare with anisotropic model Einstein-Axion-Dilaton action:

$$ds^2 = \frac{L\,b(z)}{z^2}\left[-g_A(z)dt^2 + dx^2 + dy_1^2 + R_A(z)(dy_2^2) + \frac{dz^2}{g_A(z)}\right]$$

Physical motivations: peripheral HIC

Gursoy, et al 1708.05691, 1811.1172

5-dim Anisotropic Background at Large Magnetic Field

Compare with anisotropic model Einstein-Axion-Dilaton action:

$$ds^2 = \frac{L\, b(z)}{z^2}\left[-g_A(z)dt^2 + dx^2 + dy_1^2 + R_A(z)(dy_2^2) + \frac{dz^2}{g_A(z)}\right]$$

Physical motivations: peripheral HIC

Gursoy, et al 1708.05691, 1811.1172

Einstein-dilaton-two-Maxwell

5-dim Anisotropic Background at Large Magnetic Field

Compare with anisotropic model Einstein-Axion-Dilaton action:

$$ds^2 = \frac{L\,b(z)}{z^2}\left[-g_A(z)dt^2 + dx^2 + dy_1^2 + R_A(z)(dy_2^2) + \frac{dz^2}{g_A(z)}\right]$$

Physical motivations: peripheral HIC

Gursoy, et al 1708.05691, 1811.1172

Einstein-dilaton-two-Maxwell

$$ds^2 = \frac{Lb(z)}{z^2}\left[-g(z)dt^2 + dx^2 + R(z)(dy_1^2 + dy_2^2) + \frac{1}{g(z)}dz^2\right]$$

IA, K.Rannu, 1802.05652
D.Dudal et al, 1907.01852

Temperature vs horizon

Temperature vs horizon

$$ds^2 = \frac{Lb(z)}{z^2}\left[-g(z)dt^2 + dx^2 + R(z)(dy_1^2 + dy_2^2) + \frac{1}{g(z)}dz^2\right]$$

Temperature vs horizon

$$ds^2 = \frac{Lb(z)}{z^2}\left[-g(z)dt^2 + dx^2 + R(z)(dy_1^2 + dy_2^2) + \frac{1}{g(z)}dz^2\right]$$

$$R(z) = e^{B^2 z^2}$$

Temperature vs horizon

$$ds^2 = \frac{Lb(z)}{z^2}\left[-g(z)dt^2 + dx^2 + R(z)(dy_1^2 + dy_2^2) + \frac{1}{g(z)}dz^2\right]$$

$$R(z) = e^{B^2 z^2}$$

D.Dudal et al, 1907.01852

Temperature vs horizon

$$ds^2 = \frac{Lb(z)}{z^2}\left[-g(z)dt^2 + dx^2 + R(z)(dy_1^2 + dy_2^2) + \frac{1}{g(z)}dz^2\right]$$

$$R(z) = e^{B^2 z^2}$$

D.Dudal et al, 1907.01852

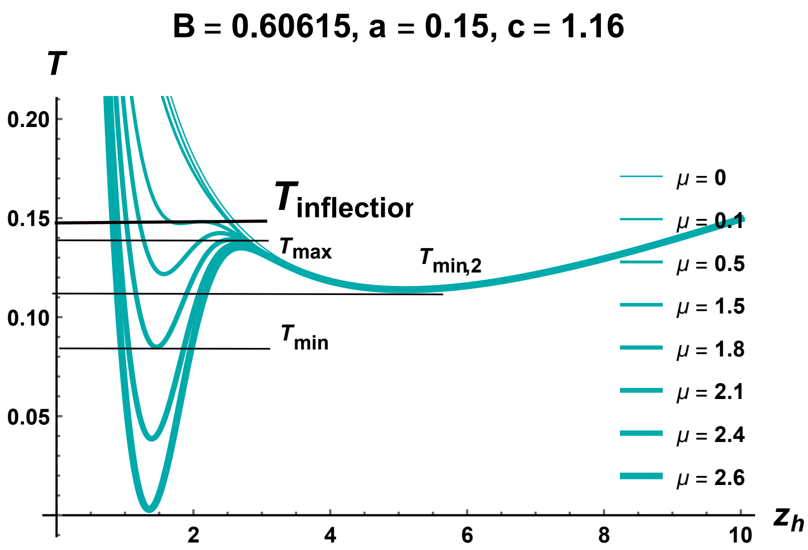

Temperature vs horizon

$$ds^2 = \frac{Lb(z)}{z^2}\left[-g(z)dt^2 + dx^2 + R(z)(dy_1^2 + dy_2^2) + \frac{1}{g(z)}dz^2\right]$$

$$R(z) = e^{B^2 z^2}$$

D.Dudal et al, 1907.01852

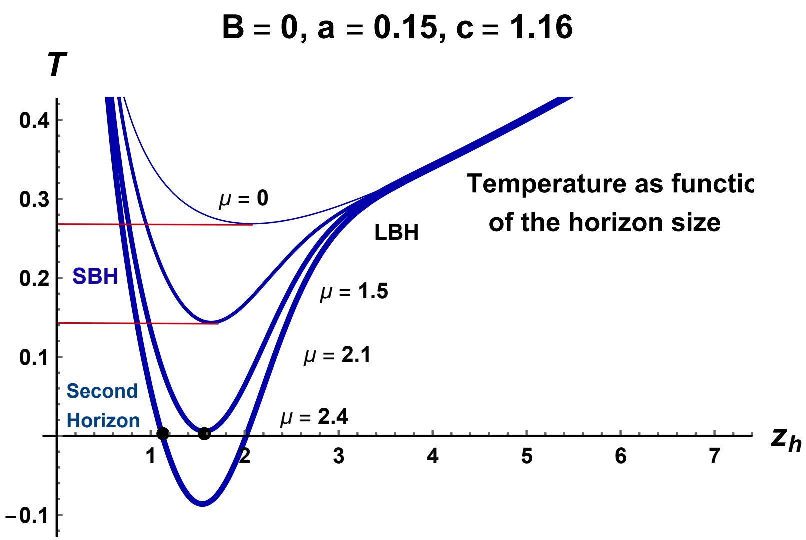

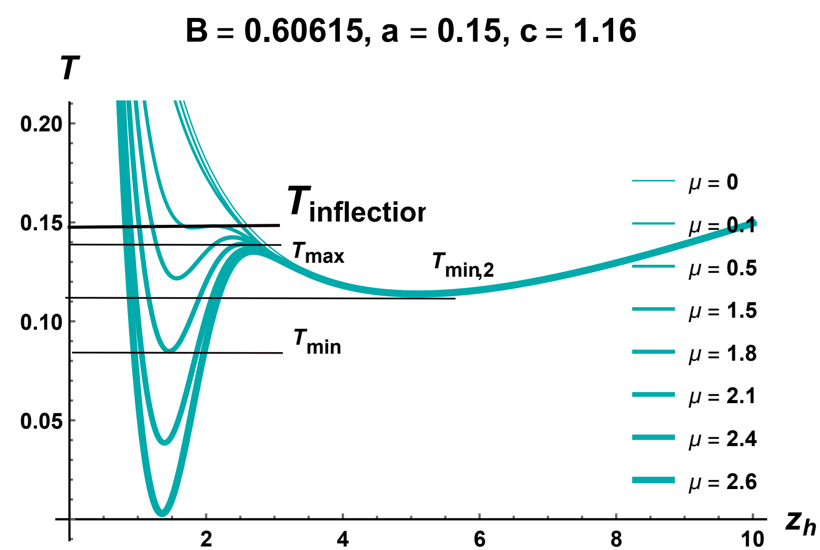

Confinement/deconfinement phase diagram in the magnetic field

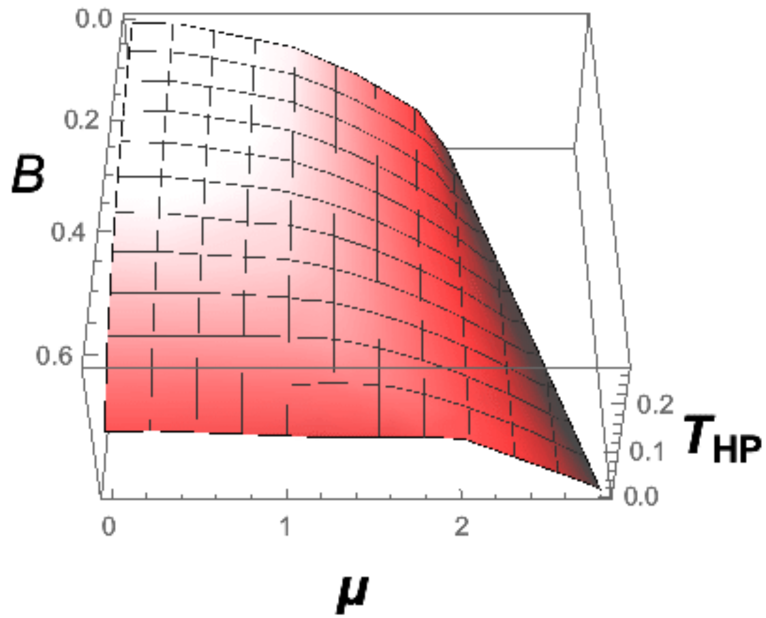

D.Dudal et al, 1907.01852

Work in progress:

IA, K.Rannu, P.SlepoV

Confinement/deconfinement phase diagram in the magnetic field

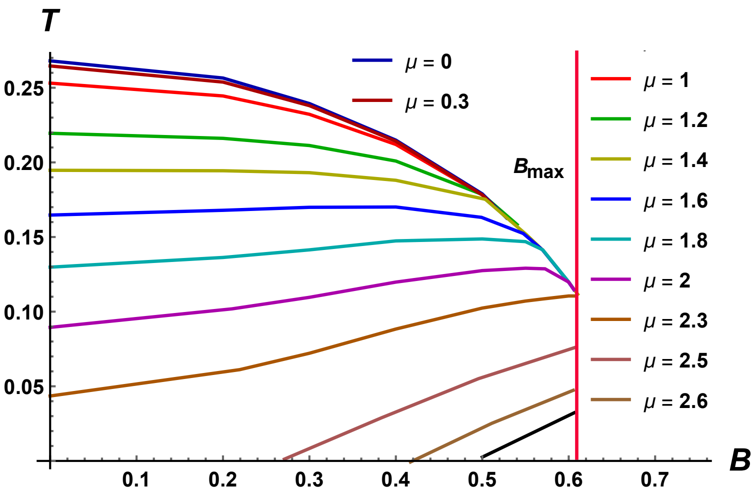

D.Dudal et al, 1907.01852

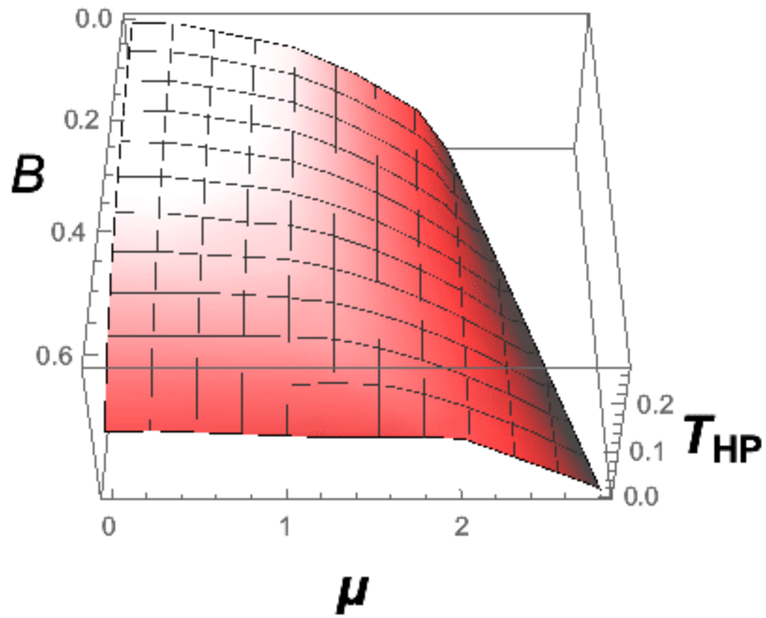

Work in progress:

IA, K.Rannu, P.SlepoV

Confinement/deconfinement phase diagram in the magnetic field

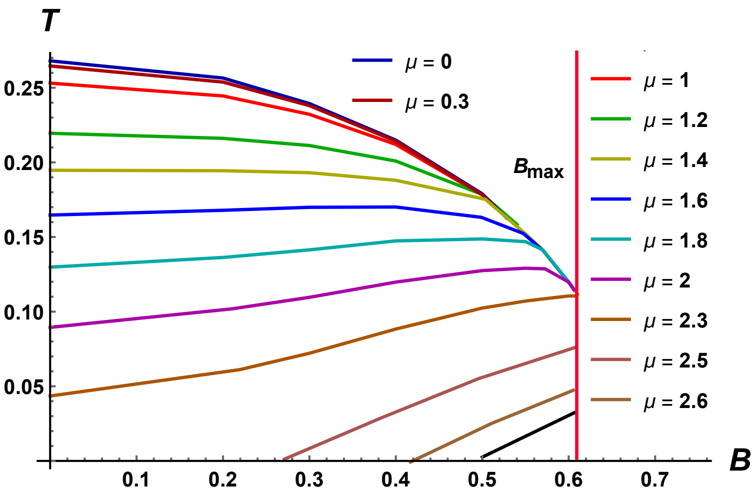

D.Dudal et al, 1907.01852

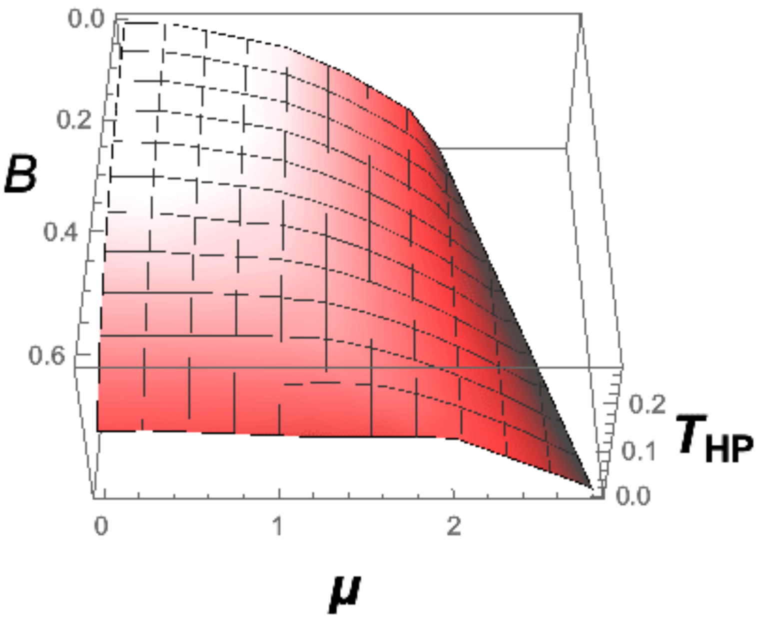

Work in progress:

IA, K.Rannu, P.SlepoV

Confinement/deconfinement phase diagram in the magnetic field

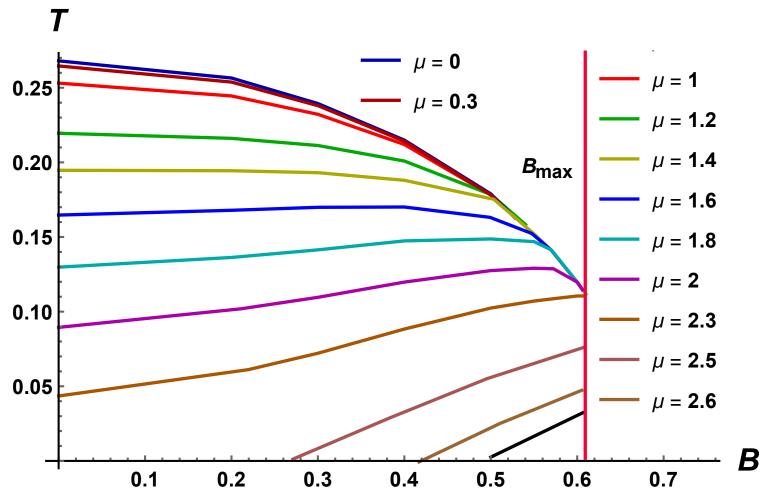

D.Dudal et al, 1907.01852

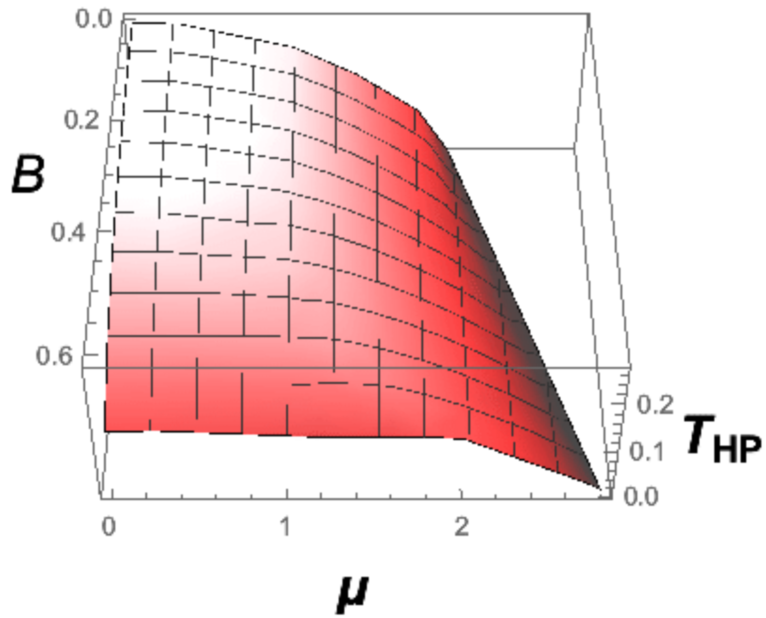

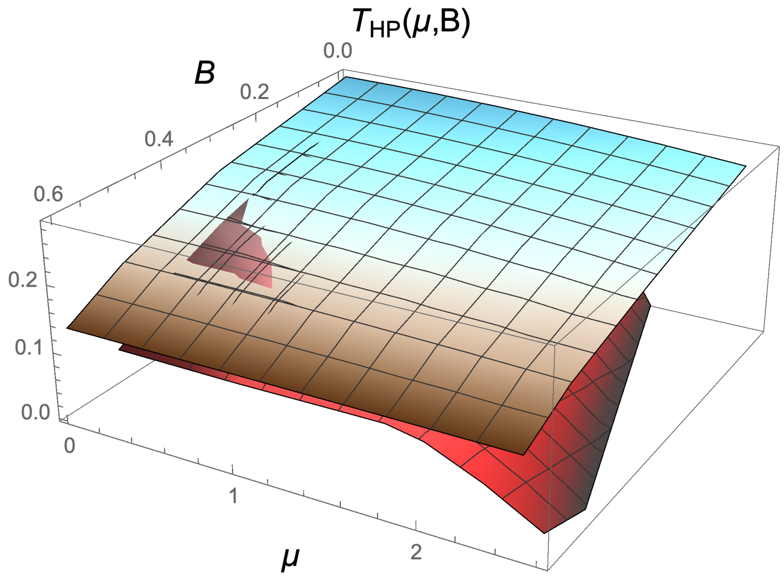

Work in progress:

IA, K.Rannu, P.SlepoV

Confinement/deconfinement phase diagram in the magnetic field

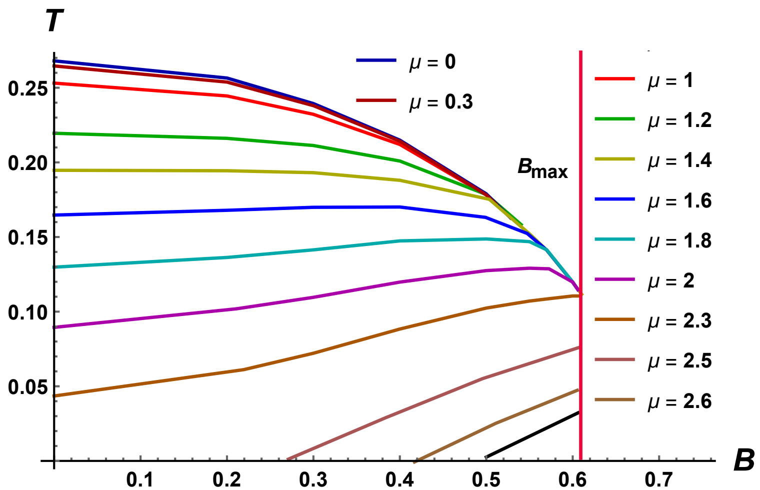

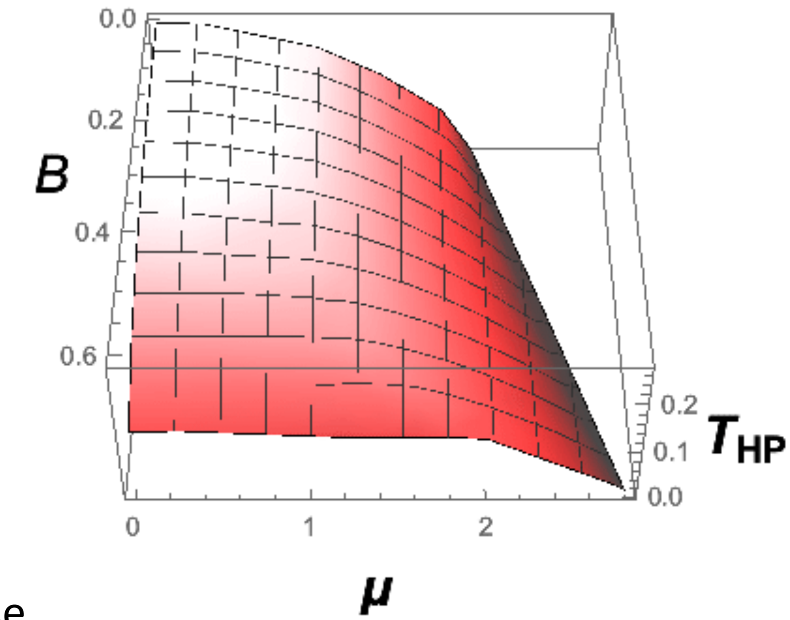

D.Dudal et al, 1907.01852

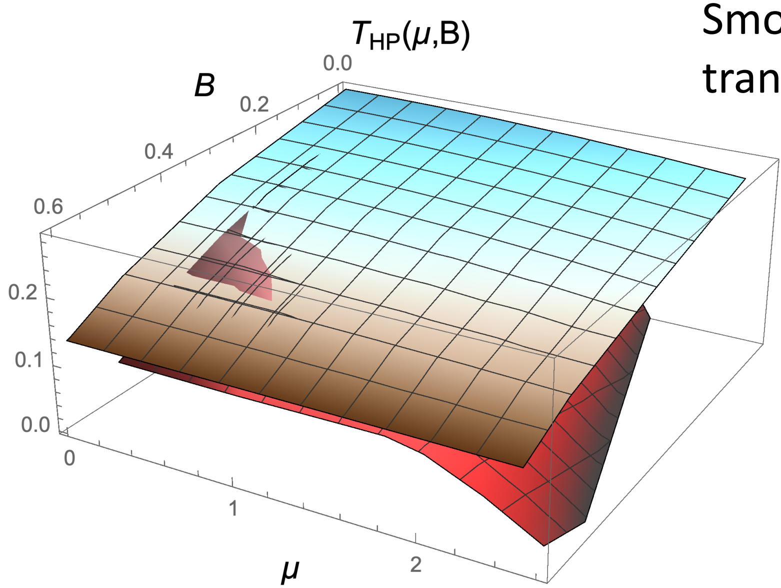

Smooth phase transition

Work in progress:

IA, K.Rannu, P.SlepoV

Confinement/deconfinement phase diagram in the magnetic field

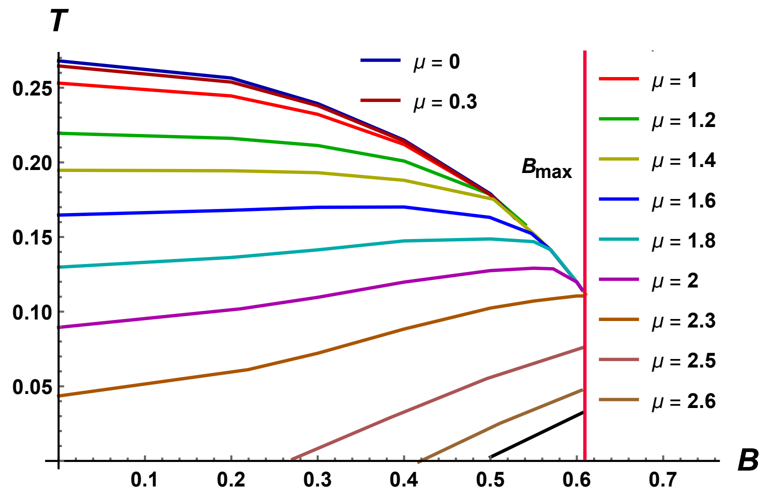

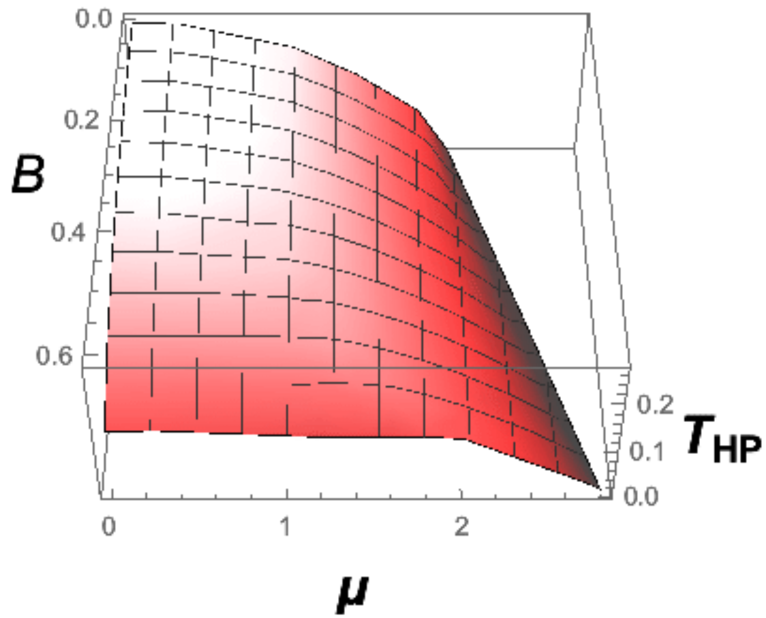

D.Dudal et al, 1907.01852

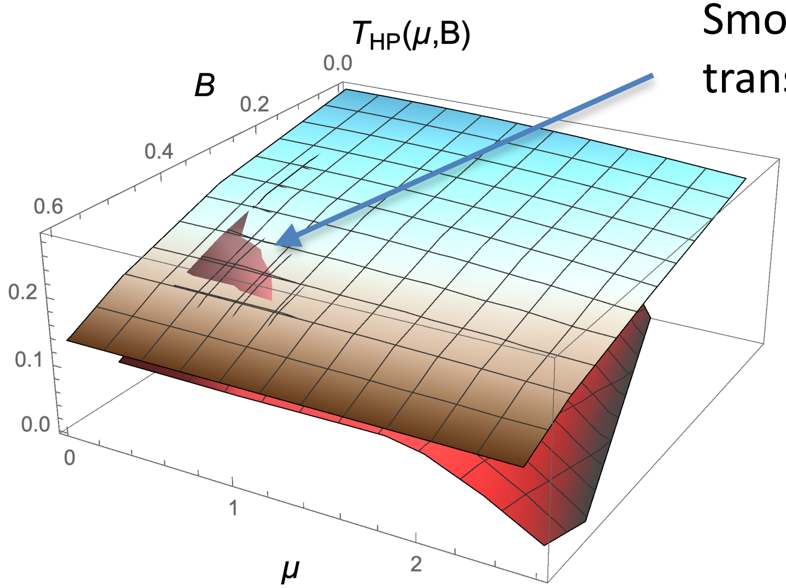

Smooth phase transition

Work in progress:

IA, K.Rannu, P.SlepoV

Confinement/deconfinement phase diagram in the magnetic field

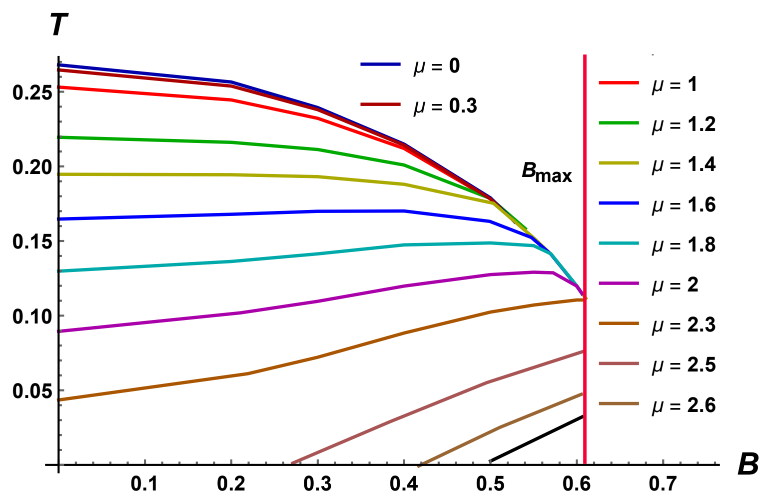

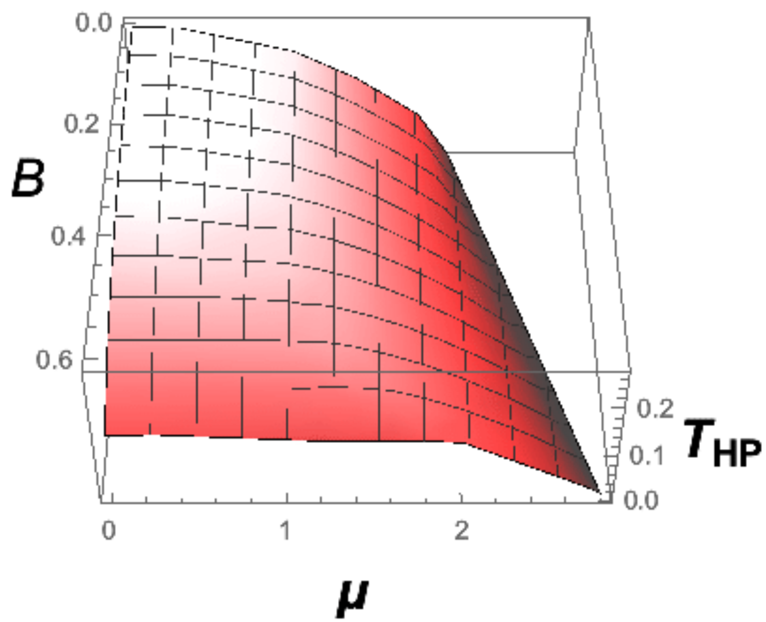

D.Dudal et al, 1907.01852

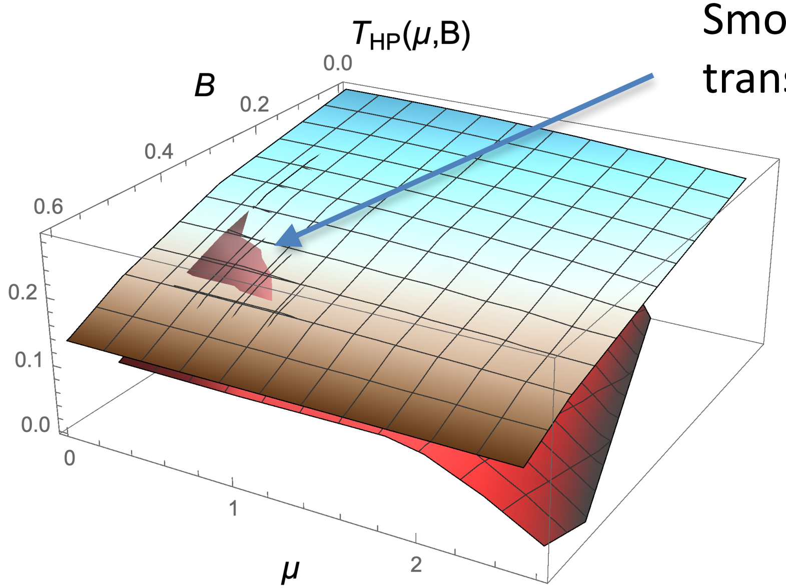

Smooth phase transition

Conf/deconf -> first order

Work in progress:

IA, K.Rannu, P.SlepoV

Confinement/deconfinement phase diagram in the magnetic field

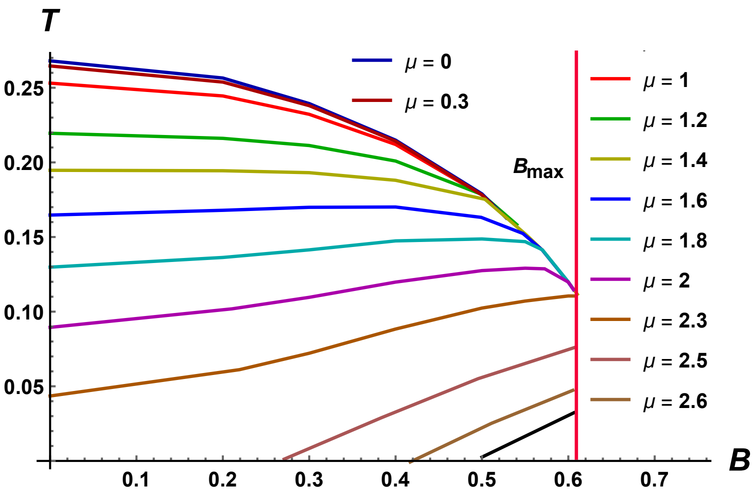

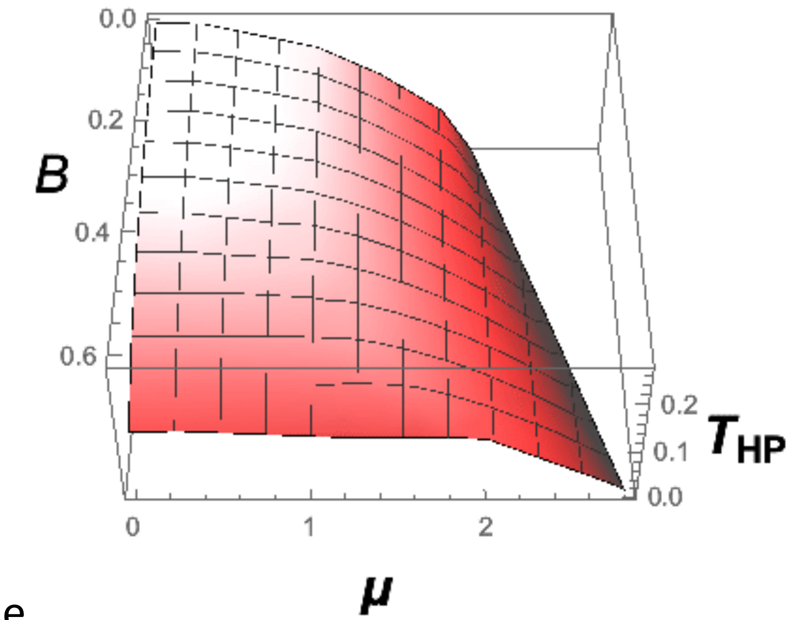

D.Dudal et al, 1907.01852

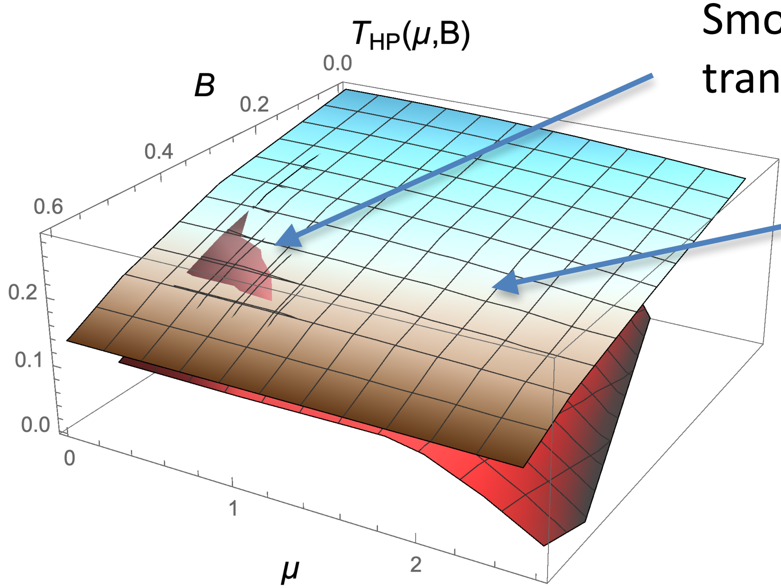

Smooth phase transition

Conf/deconf -> first order

Work in progress:

IA, K.Rannu, P.SlepoV

Confinement/deconfinement phase diagram in the magnetic field

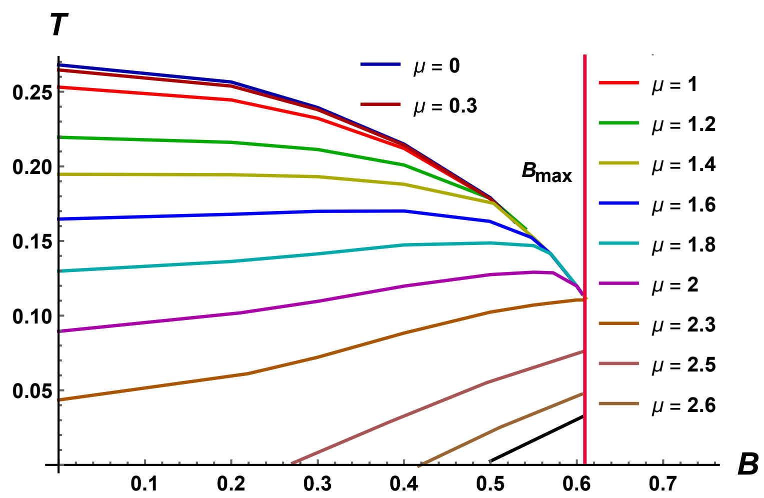

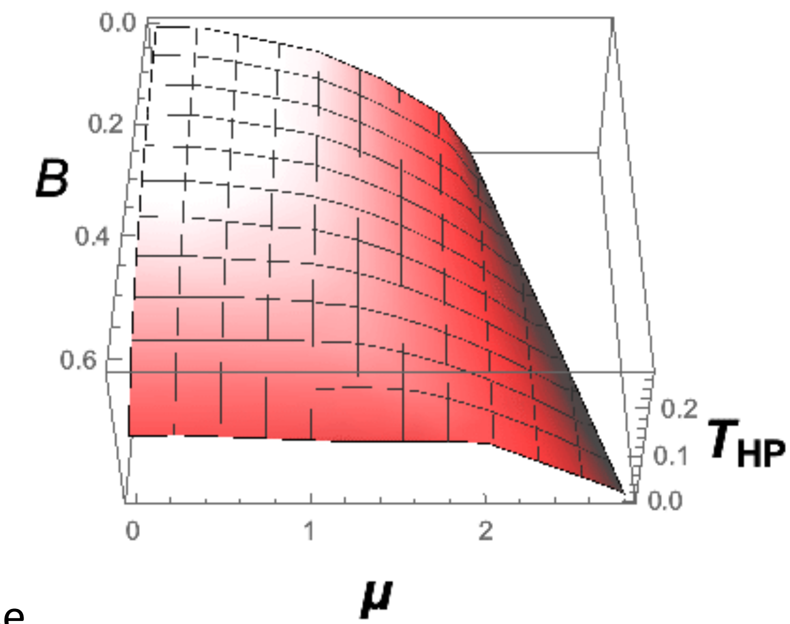

D.Dudal et al, 1907.01852

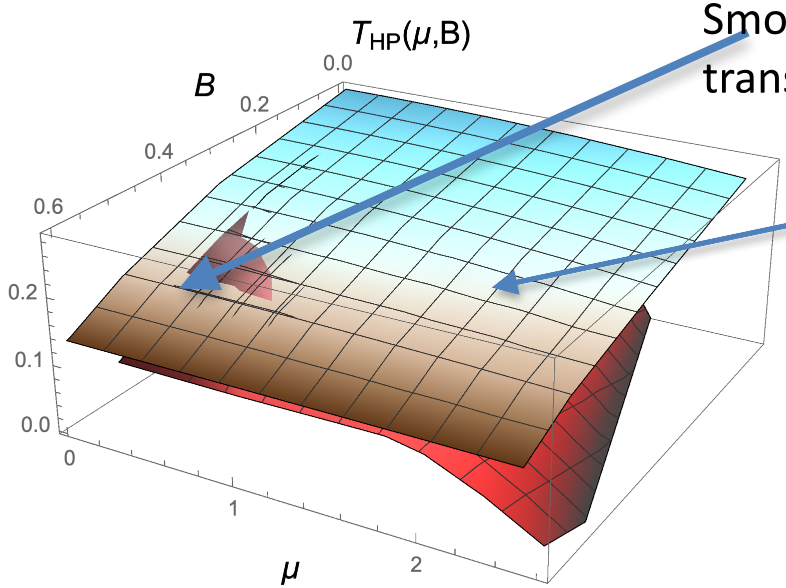

Smooth phase transition

Conf/deconf -> first order

Work in progress:

IA, K.Rannu, P.SlepoV

Spatial Wilson loops /Drag Forces/Diffusion coefficients

Gubser, 0605182

$$V_{xY}(z) = \frac{b(z)}{z^2}\sqrt{f(z)}$$

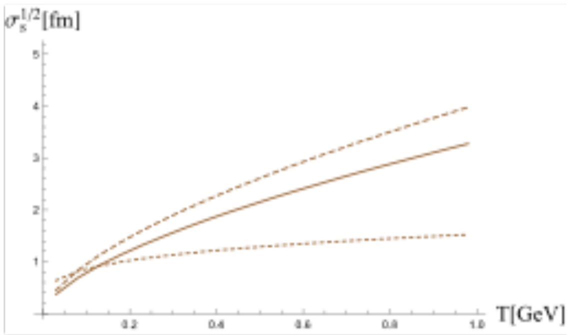

solid - Xy plane
dashed – xY plane,
dotted $y_1 Y_2$ plane.

Ageev, IA, Golubtsova, Gourgoulhon, NPB'18

Spatial Wilson loops /Drag Forces/Diffusion coefficients

Gubser, 0605182

$$V_{xY}(z) = \frac{b(z)}{z^2}\sqrt{f(z)}$$

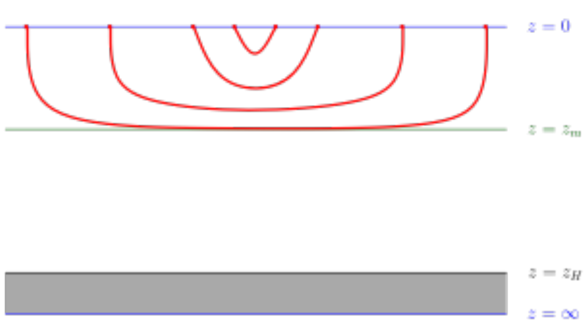

Small black hole

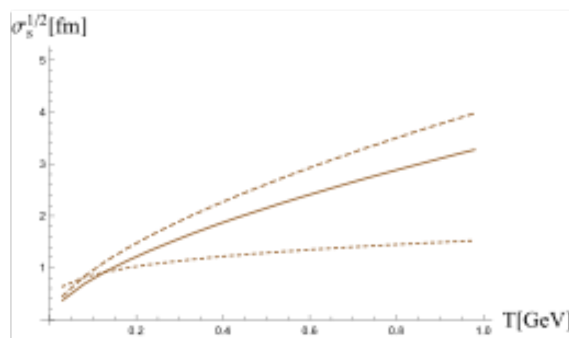

solid - Xy plane
dashed – xY plane,
dotted y_1Y_2 plane.

Ageev, IA, Golubtsova, Gourgoulhon, NPB'18

Spatial Wilson loops /Drag Forces/Diffusion coefficients

Gubser, 0605182

$$V_{xY}(z) = \frac{b(z)}{z^2}\sqrt{f(z)}$$

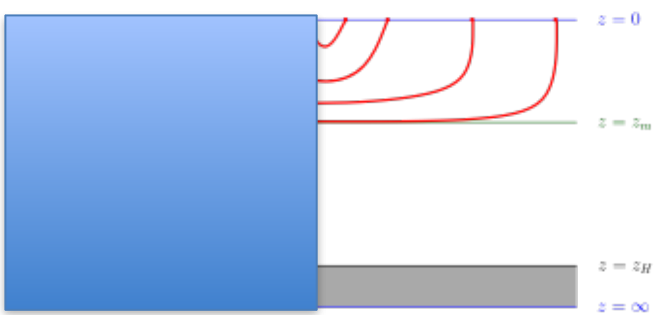

Small black hole

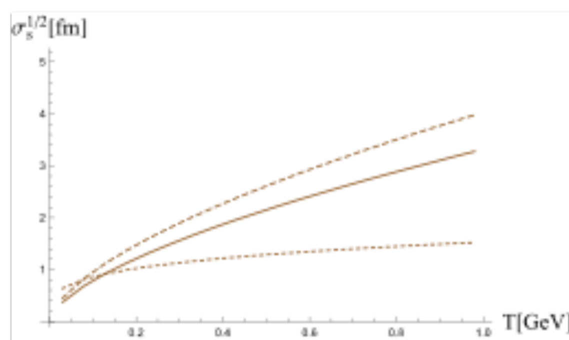

solid - Xy plane
dashed – xY plane,
dotted y_1Y_2 plane.

Ageev, IA, Golubtsova, Gourgoulhon, NPB'18

Spatial Wilson loops /Drag Forces/Diffusion coefficients

Gubser, 0605182

$$V_{xY}(z) = \frac{b(z)}{z^2}\sqrt{f(z)}$$

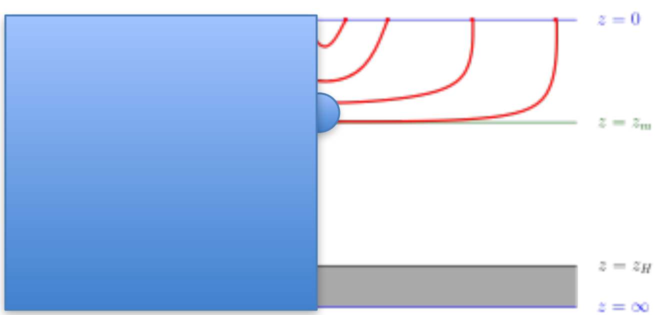

Small black hole

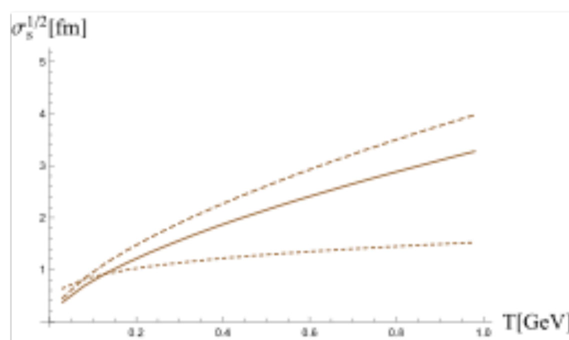

solid - Xy plane
dashed – xY plane,
dotted y_1Y_2 plane.

Ageev, IA, Golubtsova, Gourgoulhon, NPB'18

Spatial Wilson loops /Drag Forces/Diffusion coefficients

Gubser, 0605182

$$V_{xY}(z) = \frac{b(z)}{z^2}\sqrt{f(z)}$$

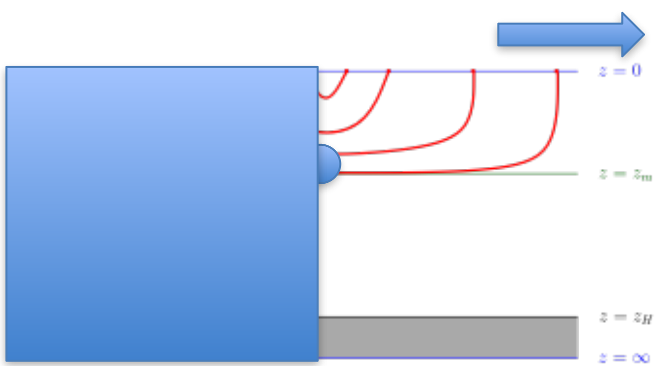

Small black hole

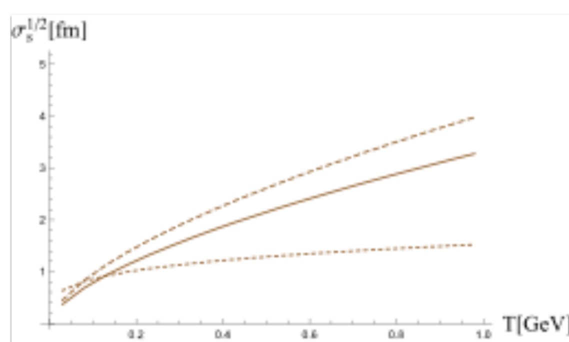

solid - Xy plane
dashed – xY plane,
dotted y_1Y_2 plane.

Ageev, IA, Golubtsova, Gourgoulhon, NPB'18

Spatial Wilson loops /Drag Forces/Diffusion coefficients

$$S_{xY}(\ell)$$

Gubser, 0605182

$$V_{xY}(z) = \frac{b(z)}{z^2}\sqrt{f(z)}$$

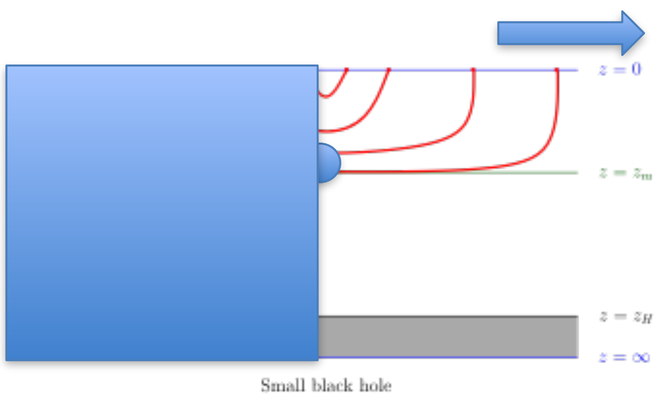

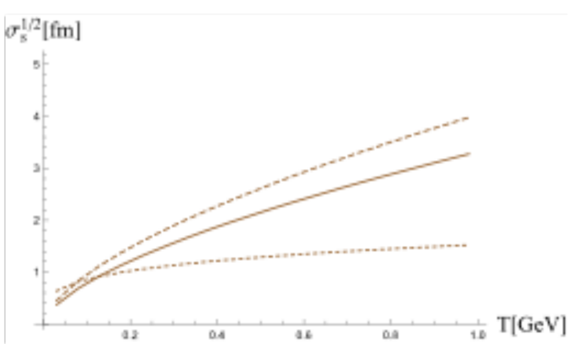

solid - Xy plane
dashed – xY plane,
dotted y_1Y_2 plane.

Ageev, IA, Golubtsova, Gourgoulhon, NPB'18

Spatial Wilson loops /Drag Forces/Diffusion coefficients

$$S_{xY}(\ell)$$

Drag forces

Gubser, 0605182

$$V_{xY}(z) = \frac{b(z)}{z^2}\sqrt{f(z)}$$

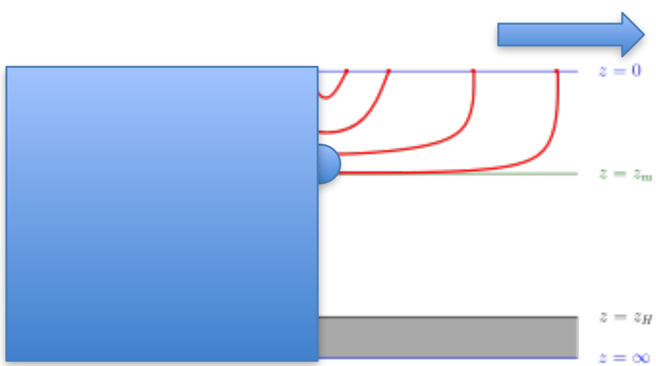

Small black hole

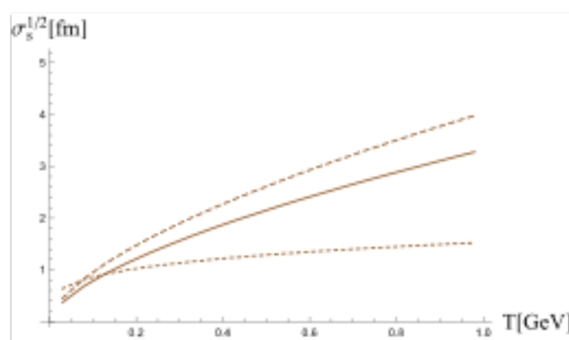

solid - Xy plane
dashed – xY plane,
dotted y_1Y_2 plane.

Ageev, IA, Golubtsova, Gourgoulhon, NPB'18

Jet quenching

The jet-quenching parameter is related with the average of the light-like Wilson loop in the adjoint representation

Kovner, Wiedemann, hep/ph 0106240

$$W_A(C) = e^{-\frac{1}{4\sqrt{2}}\hat{q}L_-\ell^2} = e^{2iS_{string}}$$

H. Liu, K. Rajagopal and Wiedemann, PRL'06

C is a rectangular contour with large extension L_- in a light-like and small extension ℓ in a transversal one

For x-light-like (x_-=t-x) direction

$$\hat{q} = -\frac{2^{\frac{2}{\nu}+2}\nu^{\frac{\nu+2}{\nu}}\pi^{\frac{2}{\nu}-\frac{1}{2}}\Gamma\left(-\frac{\nu}{2\nu+2}\right)}{(\nu+1)^{\frac{2(\nu+1)}{\nu}}\Gamma\left(1+\frac{1}{2\nu+2}\right)}T^{\frac{\nu+2}{\nu}}$$

Ageev, IA, Golubtsova, Gourgoulhon, NPB'18

Direct photons and electric conductivity

$$G^R_{\mu\nu}(k) = i \int d^4x e^{ik\cdot x} \theta(x^0) \langle [J^a_\mu(x), J^b_\nu(0)] \rangle$$

Direct photons and electric conductivity

The thermal-photon production from the QGP plays an essential role.
Photons after they are produced in HIC almost do not interact with the QGP.
Photons give us the local information on heavy ion collisions.

$$G^R_{\mu\nu}(k) = i\int d^4x e^{ik\cdot x}\theta(x^0)\langle[J^a_\mu(x), J^b_\nu(0)]\rangle$$

Direct photons and electric conductivity

The thermal-photon production from the QGP plays an essential role.
Photons after they are produced in HIC almost do not interact with the QGP.
Photons give us the local information on heavy ion collisions.

The photon-emission rate is related to the **retarded correlator** of currents in momentum space

$$G^R_{\mu\nu}(k) = i\int d^4x e^{ik\cdot x}\theta(x^0)\langle[J^a_\mu(x), J^b_\nu(0)]\rangle$$

Direct photons and electric conductivity

The thermal-photon production from the QGP plays an essential role.
Photons after they are produced in HIC almost do not interact with the QGP.
Photons give us the local information on heavy ion collisions.

The photon-emission rate is related to the **retarded correlator** of currents in momentum space

$$G^R_{\mu\nu}(k) = i\int d^4x e^{ik\cdot x}\theta(x^0)\langle[J^a_\mu(x), J^b_\nu(0)]\rangle$$

$$d\Gamma = -\frac{d^3k}{(2\pi)^3}\frac{e^2 n_b(|\mathbf{k}|)}{|\mathbf{k}|}\mathrm{Im}\left[\mathrm{tr}\left(\eta^{\mu\nu}G^{ab\,R}_{\mu\nu}\right)\right]_{k^0=|\mathbf{k}|}$$

Direct photons and electric conductivity

The thermal-photon production from the QGP plays an essential role.
Photons after they are produced in HIC almost do not interact with the QGP.
Photons give us the local information on heavy ion collisions.

The photon-emission rate is related to the **retarded correlator** of currents in momentum space

$$G^R_{\mu\nu}(k) = i\int d^4x e^{ik\cdot x}\theta(x^0)\langle[J^a_\mu(x), J^b_\nu(0)]\rangle$$

$$d\Gamma = -\frac{d^3k}{(2\pi)^3}\frac{e^2 n_b(|\mathbf{k}|)}{|\mathbf{k}|}\mathrm{Im}\left[\mathrm{tr}\left(\eta^{\mu\nu}G^{ab\,R}_{\mu\nu}\right)\right]_{k^0=|\mathbf{k}|}$$

S.I.Finazzo and R.Rougemont, PRD'16
I.Iatrakis, E.Kiritsis, C.Shen and D.L.Yang, arXiv:1609.07208

DIRECT PHOTONS

- emerge directly from a particle collison
- represent less than 10% of all detected photons

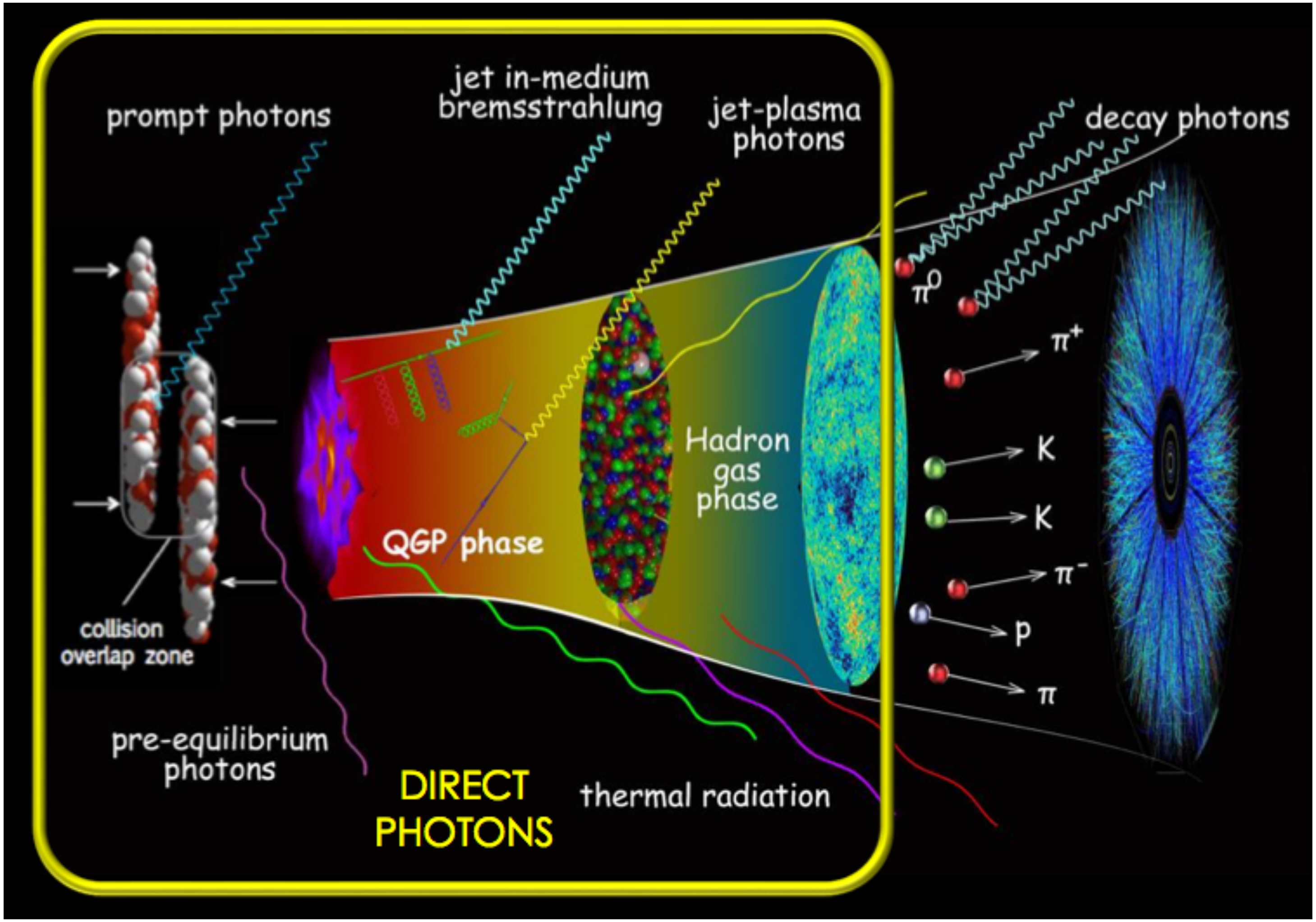

[Source: C. Shen, talk at ECT*, Trento 12/2015]

Electric conductivity

Electric conductivity

$$\sigma \approx \left(\frac{2\pi\nu}{1+\nu}\right)^{3-2/\nu} \frac{T^{3-2/\nu}}{\left(1-\left(\frac{\nu+1}{\nu}\right)^{\frac{2+3\nu}{\nu}} q^2 \left(\frac{1}{2\pi T}\right)^{\frac{2+4\nu}{\nu}}\right)^{3-2/\nu}}$$

Electric conductivity

$$\sigma \approx \left(\frac{2\pi\nu}{1+\nu}\right)^{3-2/\nu} \frac{T^{3-2/\nu}}{\left(1-\left(\frac{\nu+1}{\nu}\right)^{\frac{2+3\nu}{\nu}} q^2 \left(\frac{1}{2\pi T}\right)^{\frac{2+4\nu}{\nu}}\right)^{3-2/\nu}}$$

$$q = 0$$

Electric conductivity

$$\sigma \approx \left(\frac{2\pi\nu}{1+\nu}\right)^{3-2/\nu} \frac{T^{3-2/\nu}}{\left(1-\left(\frac{\nu+1}{\nu}\right)^{\frac{2+3\nu}{\nu}} q^2 \left(\frac{1}{2\pi T}\right)^{\frac{2+4\nu}{\nu}}\right)^{3-2/\nu}}$$

$$q = 0$$

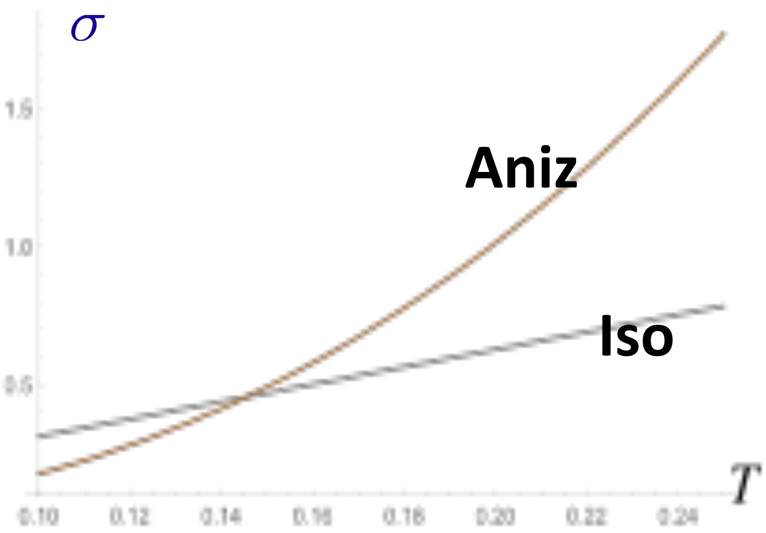

Electric conductivity

$$\sigma \approx \left(\frac{2\pi\nu}{1+\nu}\right)^{3-2/\nu} \frac{T^{3-2/\nu}}{\left(1-\left(\frac{\nu+1}{\nu}\right)^{\frac{2+3\nu}{\nu}} q^2 \left(\frac{1}{2\pi T}\right)^{\frac{2+4\nu}{\nu}}\right)^{3-2/\nu}}$$

$q = 0$

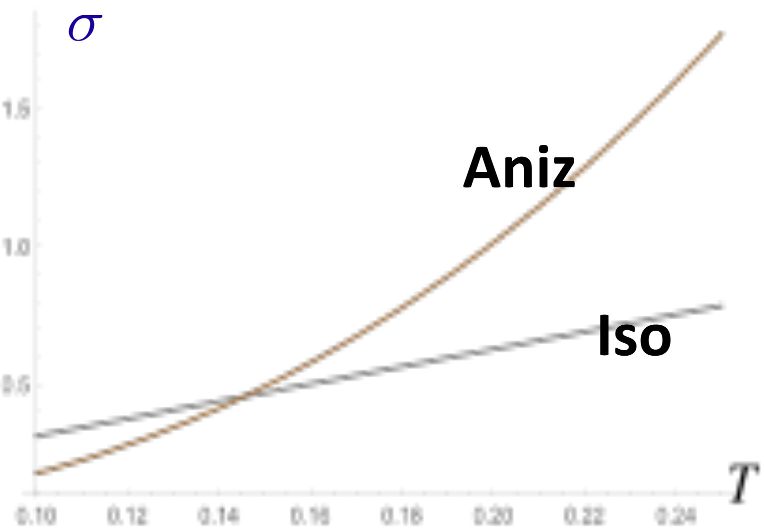

$q \neq 0$

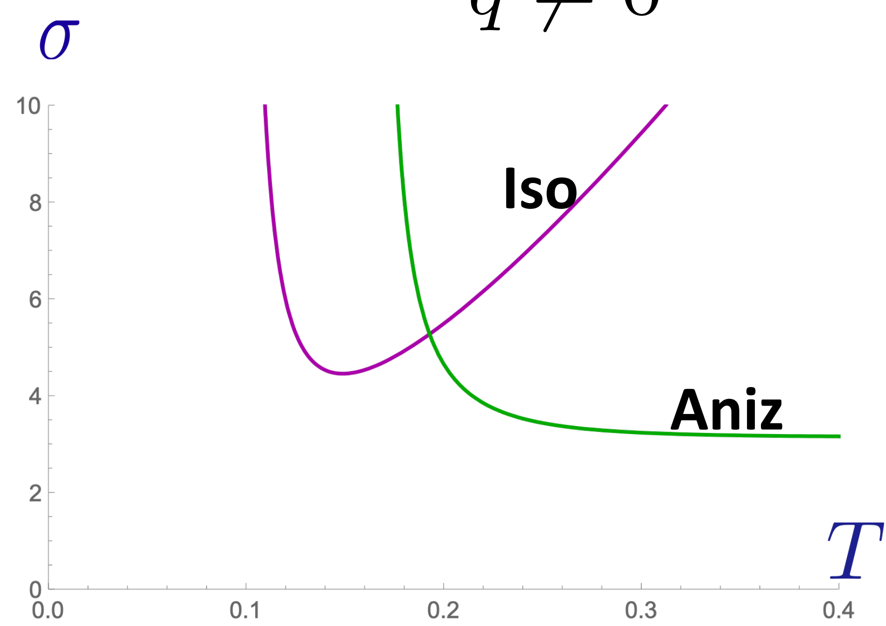

Increasing the anisotropy we increase the EC at $T>T_{cr}$, and via versa for at $T<T_{cr}$

Electric conductivity

$$\sigma \approx \left(\frac{2\pi\nu}{1+\nu}\right)^{3-2/\nu} \frac{T^{3-2/\nu}}{\left(1-\left(\frac{\nu+1}{\nu}\right)^{\frac{2+3\nu}{\nu}} q^2 \left(\frac{1}{2\pi T}\right)^{\frac{2+4\nu}{\nu}}\right)^{3-2/\nu}}$$

$q = 0$

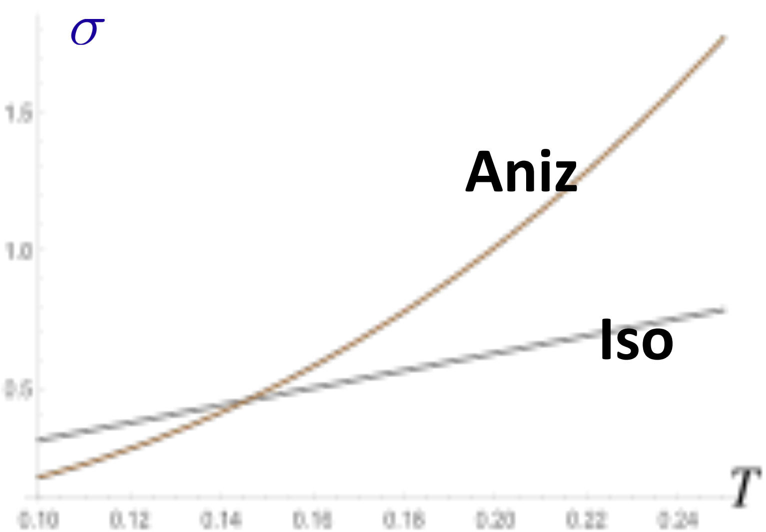

$q \neq 0$

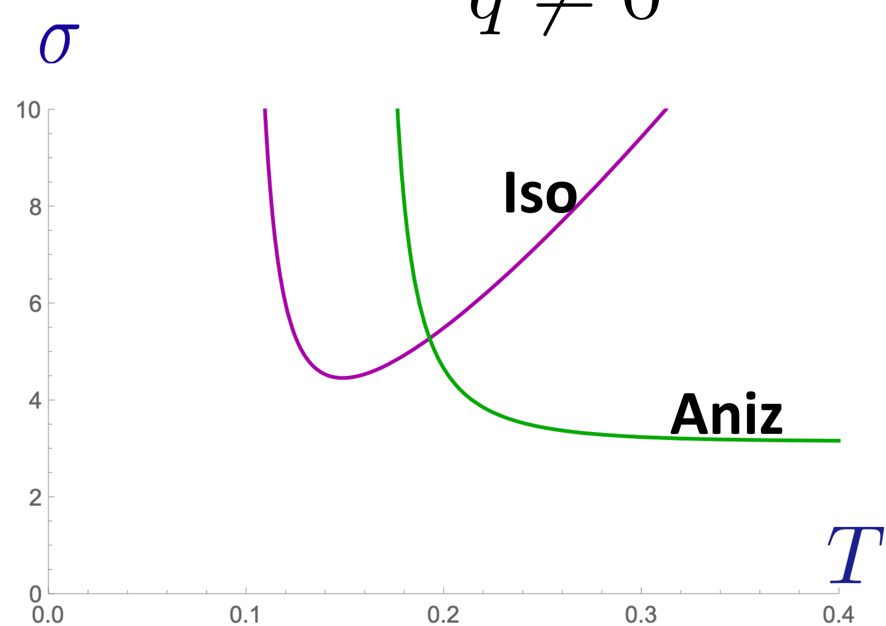

Increasing the anisotropy we increase the EC at $T>T_{cr}$, and via versa for at $T<T_{cr}$

IA, arXiv:1612.08928

Conclusion

Conclusion

Holographic models are some kind of phenomenological models with few number of parameters

Conclusion

Holographic models are some kind of phenomenological models with few number of parameters

We have considered the anizotropic model that describes:
multiplicity, quark confinement;

predicts:
crossover transition line between confinement/deconfinement phases
anizotropy in hadron spectrum (for a short time after collisions)

Conclusion

Holographic models are some kind of phenomenological models with few number of parameters

We have considered the anizotropic model that describes:
multiplicity, quark confinement;

predicts:
crossover transition line between confinement/deconfinement phases
anizotropy in hadron spectrum (for a short time after collisions)

Anisotropy drastically change standard holographic calculations, in particular,
- Wilson loops, and quark potential
- Jet quenching
- Drag forces
- shear viscosity and therefore elliptic flows
- susceptibility
- thermalization time

BACKUP SLIDES

Details: **Blackening function g(z)**

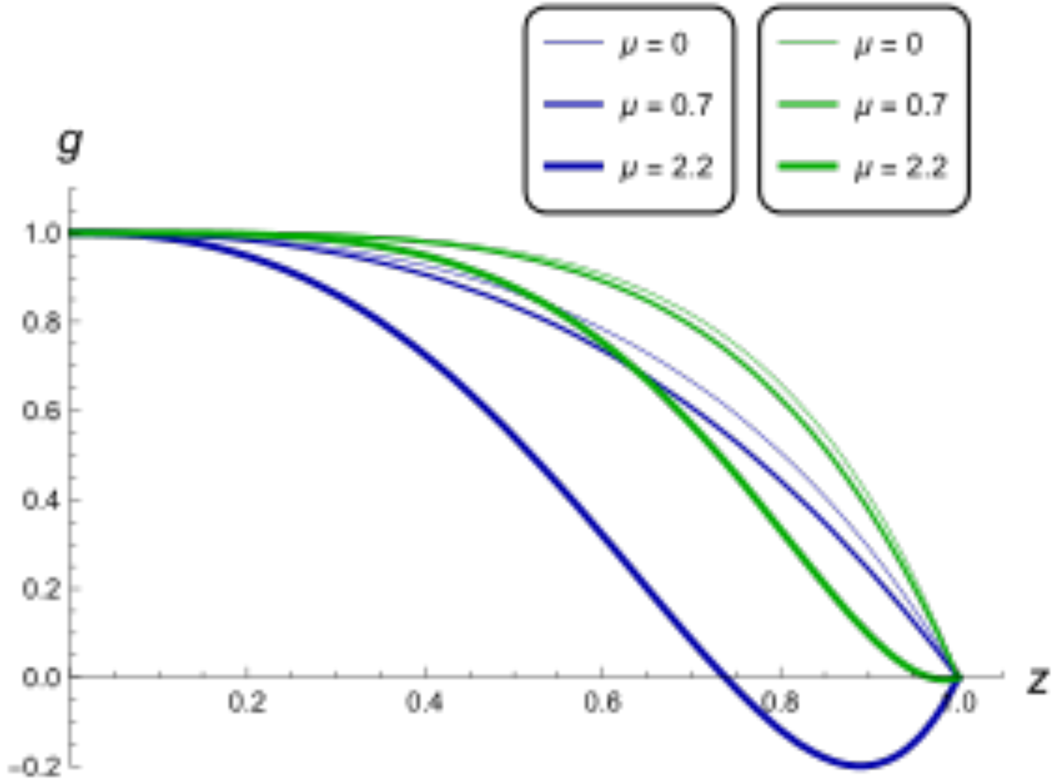

$z_h = 1,\ \nu = 4.5,\ c = -1$ (blue lines)

$\nu = 1,\ c = -1$ (green lines)

Coupling function f_2

$$f_2(z) = \frac{\nu - 1}{q^2\nu^2}\, z^{-\frac{4}{\nu}} e^{\frac{cz^2}{2}} \Bigg[4(1+\nu) - 3c\,\nu\, z^2 + 4\, \frac{z^{2+\frac{2}{\nu}}}{z_h^{2+\frac{2}{\nu}}} \Bigg\{ \frac{\nu\, e^{-\frac{3cz^2}{4}}}{\mathfrak{G}\left(\frac{3}{4}cz_h^2\right)} - (1+\nu)\, \frac{\mathfrak{G}\left(\frac{3}{4}cz^2\right)}{\mathfrak{G}\left(\frac{3}{4}cz_h^2\right)}\, \mathfrak{F}$$

$$+ \frac{\mu^2 c\,\nu\, z_h^{2+\frac{2}{\nu}} e^{-cz^2+\frac{cz_h^2}{2}}}{4\left(1 - e^{\frac{cz_h^2}{4}}\right)^2} \left(1 - e^{\frac{cz^2}{4}}\, \frac{\mathfrak{G}\left(cz_h^2\right)}{\mathfrak{G}\left(\frac{3}{4}cz_h^2\right)} \right) \Bigg\} + 3c\,\nu\, \frac{z^{4+\frac{2}{\nu}}}{z_h^{2+\frac{2}{\nu}}}\, \frac{\mathfrak{G}\left(\frac{3}{4}cz^2\right)}{\mathfrak{G}\left(\frac{3}{4}cz_h^2\right)}\, \mathfrak{F} \Bigg]$$

$$\mathfrak{F} = 1 - \frac{\mu^2 c\, z_h^{2+\frac{2}{\nu}} e^{\frac{cz_h^2}{2}}}{4\left(1 - e^{\frac{cz_h^2}{4}}\right)^2} \left(\mathfrak{G}\left(cz_h^2\right) - \mathfrak{G}\left(cz^2\right) \frac{\mathfrak{G}\left(\frac{3}{4}cz_h^2\right)}{\mathfrak{G}\left(\frac{3}{4}cz^2\right)} \right).$$

Details: Scalar Field

$$\phi' = \frac{1}{\nu z}\sqrt{\frac{3}{2}\nu^2 c^2 z^4 - 9\nu^2 c z^2 + 4\nu - 4}$$

$$\phi' = \frac{c}{z}\sqrt{\frac{3}{2}(\alpha^2 - z^2)(\beta^2 - z^2)},$$

$$\alpha = \sqrt{\frac{3}{c} - \frac{1}{c}\sqrt{9 - \frac{8(\nu-1)}{3\nu^2}}}, \qquad \beta = \sqrt{\frac{3}{c} + \frac{1}{c}\sqrt{9 - \frac{8(\nu-1)}{3\nu^2}}}.$$

c>0 instability regions

C=0

$$\phi = \frac{2\sqrt{\nu - 1}}{\nu}\ln\left(\frac{z}{z_h}\right)$$

C<0

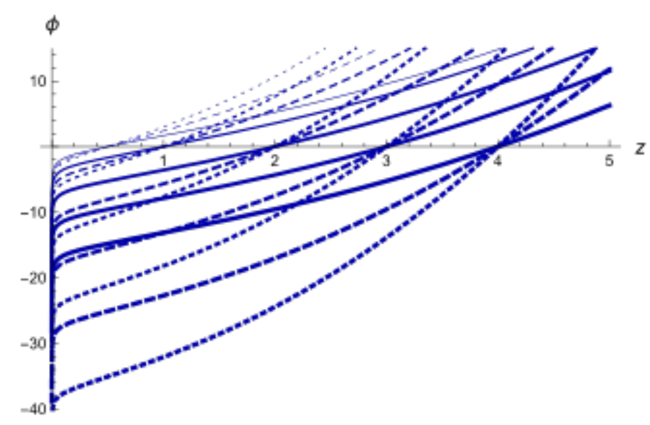

phicn2

Details: **Blackening function g(z)**

$$b(z) = e^{\frac{cz^2}{2}}$$

$$\mathfrak{G}(x) = x^{-1-\frac{1}{\nu}}\, \gamma\left(1 + \frac{1}{\nu}, x\right)$$

$$\mathfrak{G}(x) = \sum_{n=0}^{\infty} \frac{(-1)^n\, x^n}{n!(1 + n + \frac{1}{\nu}}$$

Details: Blackening function g(z)

$$b(z) = e^{\frac{cz^2}{2}}$$

$$g(z) = 1 - \frac{z^{2+\frac{2}{\nu}}}{z_h^{2+\frac{2}{\nu}}} \frac{\mathfrak{G}(\frac{3}{4}cz^2)}{\mathfrak{G}(\frac{3}{4}cz_h^2)} - \frac{\mu^2 c z^{2+\frac{2}{\nu}} e^{\frac{cz_h^2}{2}}}{4\left(1-e^{\frac{cz_h^2}{4}}\right)^2} \mathfrak{G}(cz^2) + \frac{\mu^2 c z^{2+\frac{2}{\nu}} e^{\frac{cz_h^2}{2}}}{4\left(1-e^{\frac{cz_h^2}{4}}\right)^2} \frac{\mathfrak{G}(\frac{3}{4}cz^2)}{\mathfrak{G}(\frac{3}{4}cz_h^2)} \mathfrak{G}(cz_h^2)$$

$$\mathfrak{G}(x) = x^{-1-\frac{1}{\nu}} \gamma\left(1+\frac{1}{\nu}, x\right) \qquad \mathfrak{G}(x) = \sum_{n=0}^{\infty} \frac{(-1)^n x^n}{n!(1+n+\frac{1}{\nu})}$$

Details: Blackening function g(z)

$$b(z) = e^{\frac{cz^2}{2}}$$

$$g(z) = 1 - \frac{z^{2+\frac{2}{\nu}}}{z_h^{2+\frac{2}{\nu}}} \frac{\mathfrak{G}(\frac{3}{4}cz^2)}{\mathfrak{G}(\frac{3}{4}cz_h^2)} - \frac{\mu^2 c z^{2+\frac{2}{\nu}} e^{\frac{cz_h^2}{2}}}{4\left(1 - e^{\frac{cz_h^2}{4}}\right)^2} \mathfrak{G}(cz^2) + \frac{\mu^2 c z^{2+\frac{2}{\nu}} e^{\frac{cz_h^2}{2}}}{4\left(1 - e^{\frac{cz_h^2}{4}}\right)^2} \frac{\mathfrak{G}(\frac{3}{4}cz^2)}{\mathfrak{G}(\frac{3}{4}cz_h^2)} \mathfrak{G}(cz_h^2)$$

$$\mathfrak{G}(x) = x^{-1-\frac{1}{\nu}} \gamma\left(1 + \frac{1}{\nu}, x\right)$$

$$\mathfrak{G}(x) = \sum_{n=0}^{\infty} \frac{(-1)^n x^n}{n!(1 + n + \frac{1}{\nu})}$$

$$g_{appr}(z) = 1 - \frac{z^{2+\frac{2}{\nu}}}{z_h^{2+\frac{2}{\nu}}} \left(\rho + Q z_h^2 - Q z^2\right)$$

$$\rho = \frac{4(1+2\nu) - 3cz^2(1+\nu)}{4(1+2\nu) - 3cz_h^2(1+\nu)},$$

$$Q = \frac{\mu^2 c^2 \nu\, z_h^{2+\frac{2}{\nu}} e^{\frac{cz_h^2}{2}}}{4\left(1 - e^{\frac{cz_h^2}{4}}\right)^2 \left(4(1+2\nu) - 3cz_h^2(1+\nu)\right)}.$$

Details: **Blackening function g(z)**

$$b(z) = e^{\frac{cz^2}{2}}$$

$$\mathfrak{G}(x) = x^{-1-\frac{1}{\nu}}\,\gamma\left(1+\frac{1}{\nu}, x\right)$$

$$\mathfrak{G}(x) = \sum_{n=0}^{\infty} \frac{(-1)^n\, x^n}{n!(1+n+\frac{1}{\nu})}$$

Details: Blackening function g(z)

$$b(z) = e^{\frac{cz^2}{2}}$$

$$g(z) = 1 - \frac{z^{2+\frac{2}{\nu}}}{z_h^{2+\frac{2}{\nu}}} \frac{\mathfrak{G}(\frac{3}{4}cz^2)}{\mathfrak{G}(\frac{3}{4}cz_h^2)} - \frac{\mu^2 c z^{2+\frac{2}{\nu}} e^{\frac{cz_h^2}{2}}}{4\left(1 - e^{\frac{cz_h^2}{4}}\right)^2} \mathfrak{G}(cz^2) + \frac{\mu^2 c z^{2+\frac{2}{\nu}} e^{\frac{cz_h^2}{2}}}{4\left(1 - e^{\frac{cz_h^2}{4}}\right)^2} \frac{\mathfrak{G}(\frac{3}{4}cz^2)}{\mathfrak{G}(\frac{3}{4}cz_h^2)} \mathfrak{G}(cz_h^2)$$

$$\mathfrak{G}(x) = x^{-1-\frac{1}{\nu}} \gamma\left(1 + \frac{1}{\nu}, x\right) \qquad \mathfrak{G}(x) = \sum_{n=0}^{\infty} \frac{(-1)^n x^n}{n!(1+n+\frac{1}{\nu})}$$

Details: Blackening function g(z)

$$b(z) = e^{\frac{cz^2}{2}}$$

$$g(z) = 1 - \frac{z^{2+\frac{2}{\nu}}}{z_h^{2+\frac{2}{\nu}}} \frac{\mathfrak{G}(\frac{3}{4}cz^2)}{\mathfrak{G}(\frac{3}{4}cz_h^2)} - \frac{\mu^2 c z^{2+\frac{2}{\nu}} e^{\frac{cz_h^2}{2}}}{4\left(1 - e^{\frac{cz_h^2}{4}}\right)^2} \mathfrak{G}(cz^2) + \frac{\mu^2 c z^{2+\frac{2}{\nu}} e^{\frac{cz_h^2}{2}}}{4\left(1 - e^{\frac{cz_h^2}{4}}\right)^2} \frac{\mathfrak{G}(\frac{3}{4}cz^2)}{\mathfrak{G}(\frac{3}{4}cz_h^2)} \mathfrak{G}(cz_h^2)$$

$$\mathfrak{G}(x) = x^{-1-\frac{1}{\nu}} \gamma\left(1 + \frac{1}{\nu}, x\right) \qquad \mathfrak{G}(x) = \sum_{n=0}^{\infty} \frac{(-1)^n x^n}{n!(1 + n + \frac{1}{\nu})}$$

$$g_{appr}(z) = 1 - \frac{z^{2+\frac{2}{\nu}}}{z_h^{2+\frac{2}{\nu}}} \left(\rho + Qz_h^2 - Qz^2\right)$$

$$\rho = \frac{4(1+2\nu) - 3cz^2(1+\nu)}{4(1+2\nu) - 3cz_h^2(1+\nu)},$$

$$Q = \frac{\mu^2 c^2 \nu \, z_h^{2+\frac{2}{\nu}} e^{\frac{cz_h^2}{2}}}{4\left(1 - e^{\frac{cz_h^2}{4}}\right)^2 \left(4(1+2\nu) - 3cz_h^2(1+\nu)\right)}.$$